

Titre: Performance Evaluation of Electro-Fenton for Thiosalts Treatment in
Title: Mine Effluents

Auteur: Jennifer Dubuc
Author:

Date: 2022

Type: Mémoire ou thèse / Dissertation or Thesis

Référence: Dubuc, J. (2022). Performance Evaluation of Electro-Fenton for Thiosalts
Citation: Treatment in Mine Effluents [Mémoire de maîtrise, Polytechnique Montréal].
PolyPublie. <https://publications.polymtl.ca/10311/>

 **Document en libre accès dans PolyPublie**
Open Access document in PolyPublie

URL de PolyPublie: <https://publications.polymtl.ca/10311/>
PolyPublie URL:

**Directeurs de
recherche:** Carmen Mihaela Neculita, Lucie Coudert, & Olivier P Lefebvre
Advisors:

Programme: Génie Minéral
Program:

POLYTECHNIQUE MONTRÉAL

affiliée à l'Université de Montréal

et

l'Université du Québec en Abitibi-Témiscamingue

Performance evaluation of electro-Fenton for thiosalts treatment in mine effluents

JENNIFER DUBUC

Département des génies civil, géologique et des mines

Mémoire présenté en vue de l'obtention du diplôme de *Maîtrise ès sciences appliquées*

Génie minéral

Avril 2022

POLYTECHNIQUE MONTRÉAL

affiliée à l'Université de Montréal

et

l'Université du Québec en Abitibi-Témiscamingue

Ce mémoire intitulé:

Performance evaluation of electro-Fenton for thiosalts treatment in mine effluents

présenté par **Jennifer DUBUC**

en vue de l'obtention du diplôme de *Maîtrise ès sciences appliquées*

a été dûment accepté par le jury d'examen constitué de :

Dominique CLAVEAU-MALLET, présidente

Carmen M. NECULITA, membre et directrice de recherche

Lucie COUDERT, membre et codirectrice de recherche

Olivier P. LEFEBVRE, membre et codirecteur de recherche

Patrick DROGUI, membre

DEDICATION

To my mother; my guardian angel, my strength, and my courage.

ACKNOWLEDGEMENTS

First and foremost, I would like to thank both my advisors, Carmen M. Neculita and Lucie Coudert, whose outstanding and continuous encouragements and support are what gave me the strength to pursue my studies and undertake a Master's. I will forever be grateful that they allowed me to harness the potential within myself that I never knew I had. Our collaboration in the past years will have opened many doors and brought new knowledge and skills. Thank you for the positive influence you have had in my life, for all the great memories and the baggage of new knowledge that you allow me to carry on with, in this new chapter of my life. A special mention also for my co-director, Olivier Lefebvre, for his contribution to this master's project and for sharing his expertise. I am grateful to have had the chance to work with an expert of his caliber. It was a real pleasure.

I would also like to thank, from the bottom of my heart, my former internship supervisor at the URSTM, Marc Paquin, for the positive influence he has had in my academic and professional career by passing on his passion for the chemistry of water treatment to me. He gave me my first chance on the job market, introduced me to the world of R&D and concretely showed me how to apply the best practices in the field. His confidence in my abilities and skills, during my three consecutive Internships, have allowed me to develop an autonomy and a work ethic that have greatly contributed to the execution and to the quality of the work presented in this document.

I could not thank enough all my former colleagues at the URSTM, who have, over time, become like my second family. I will forever have good memories of my time with the team and of all the laughs we've shared. I would like to make a special mention to Mélanie Bélanger, who with time, has become a very dear friend and without whom I can hardly imagine how this experience would have unfolded.

Finally, a special thanks to all my friends and family members who have supported me throughout this journey, especially to those who have stuck around through thick and thin, understanding that my academic goals were a non-negotiable priority.

RÉSUMÉ

Les thioisels sont des intermédiaires de soufre partiellement oxydés, formés lors de l'oxydation des minéraux sulfurés et sont responsables de l'acidité retardée, entraînant une toxicité aquatique dans les plans d'eau récepteurs. Les cycles de gel/dégel, induits par les changements de saison dans les régions nordiques, sont connus pour accélérer la cinétique d'oxydation du soufre, ce qui entraîne une augmentation des concentrations de thioisels dans les effluents miniers. Des concentrations aussi élevées que 15 g/L de thiosulfates ($S_2O_3^{2-}$) ont récemment été rapportées dans une étude évaluant l'effet des cycles de gel/dégel sur la stabilité des résidus miniers.

Les limites de la neutralisation chimique, en tant que pratique de gestion des thioisels actuellement privilégiée, nécessitent le développement de technologies émergentes. De plus, les stratégies de traitement d'eau dans les pays nordiques au climat froid sont principalement limitées par leur incapacité à traiter des concentrations extrêmes de thioisels. Par conséquent, une attention particulière aux technologies émergentes qui sont également adaptées au climat froid est nécessaire. Récemment, le procédé électro-Fenton (EF) a été prouvé efficace pour le traitement des thioisels présents dans des effluents miniers synthétiques, même lorsque la température de l'eau était de 4°C.

Afin de faire progresser la compréhension générale de cette approche de traitement, une évaluation de la performance du procédé a été effectuée à la fois sur des effluents miniers synthétiques et réels. Le terme « performance » a été défini comme étant l'efficacité d'enlèvement des contaminants, la toxicité résiduelle associée et les coûts d'opération, les trois composantes majeures du projet. Des essais de traitement par EF ont été réalisés à l'aide de paramètres pré-optimisés (cathode de brosse en fibre de carbone, anode de diamant dopé au bore revêtue d'un seul côté avec comme substrat le Nb, intensité de courant = 0,3 A, densité de courant = 0,006 A/cm², et $[Fe^{2+}]$ initiale = 0,2 mM). Dans cette étude, les concentrations de H_2O_2 n'ont pas été mesurées, mais la production de H_2O_2 a été prouvée, dans les travaux préliminaires d'optimisation des paramètres opératoires. L'efficacité d'enlèvement des contaminants a été évaluée sur quatre effluents miniers réels différents, sélectionnés en fonction de leur origine géographique (nord du Québec, Canada) et de leurs différentes concentrations en $S_2O_3^{2-}$ (219 ± 21 mg/L, 32 mg/L, 0 mg/L et 58 mg/L pour E1, E2, E3 et E4, respectivement). Des essais de traitabilité ont ensuite été réalisés sur des effluents synthétiques « simplifiés », correspondants aux effluents réels, avec et sans ajout d'alcalinité, afin

d'étudier les mécanismes sous-jacents. L'influence de la salinité chlorurée [liée à la présence des chlorures (Cl^-)] sur l'efficacité du procédé a également été étudiée sur l'effluent E1 à 2 et 4 g/L de CaCl_2 , à pH 3 et pH 5. Les solutions résultantes ont été traitées comme à l'habitude. Pour l'évaluation de la toxicité résiduelle, E1 et E4 ont été testés pour la toxicité aiguë sur *Daphnia magna*, à la fois avant et après le traitement par EF. Enfin, une analyse technico-économique préliminaire a été réalisée pour évaluer les coûts d'opération, en termes de consommation énergétique, de coûts des réactifs et des électrodes, pour le nord du Québec par rapport au reste du Canada et aux États-Unis.

Les résultats d'efficacité d'enlèvement des $\text{S}_2\text{O}_3^{2-}$ étaient encourageants : un enlèvement complet (> 99 %) a été obtenu en moins de 60 min pour tous les effluents testés, y compris les effluents synthétiques correspondants, avec et sans alcalinité, indépendamment de la concentration en Cl^- . Cependant, l'alcalinité a été identifiée comme étant un inhibiteur du procédé pour l'enlèvement des thiosels, ce qui a entraîné une augmentation du temps de traitement de 0.25 sec dans E2 à 12 min dans son effluent synthétique correspondant en présence d'alcalinité. En revanche, l'influence de la salinité chlorurée sur l'efficacité du procédé semble être plus complexe. Il a été observé que l'oxydation des $\text{S}_2\text{O}_3^{2-}$ était plus rapide à pH 5 qu'à pH 3, et plus rapide à 4 g/L de CaCl_2 qu'à 2 g/L de CaCl_2 , avec E1 non-modifié montrant la cinétique d'oxydation des $\text{S}_2\text{O}_3^{2-}$ la plus lente. Ces observations sont conformes à la littérature, qui semble indiquer que les Cl^- interfèrent avec le traitement des thiosels via leur interaction avec le Fe^{2+} dans la plage de pH optimal de la réaction de Fenton. De plus, les espèces oxydantes du Cl^- formées à l'anode pourraient accélérer le traitement, tandis que leur réaction avec les HO^\bullet pourrait ralentir l'oxydation des thiosels.

Les résultats de l'évaluation de la toxicité résiduelle ont révélé que la matrice initiale n'avait aucun impact sur la toxicité finale pour *D. magna*, pour ni l'un ni l'autre des effluents testés. L'effluent E1 présentait initialement une mortalité des daphnies, mais était inférieur au seuil de toxicité aiguë ($\text{CL} < 50\%$). L'oxydation complète des thiosels dans E1 a entraîné l'élimination de la mortalité de *D. magna* pour l'ensemble de la population. Le traitement de l'effluent E4, qui présentait initialement une toxicité aiguë ($\text{CL} > 50\%$) pour les daphnies, a entraîné une élimination complète de la toxicité et de la mortalité.

Les résultats de l'analyse technico-économique préliminaire ont montré que la consommation d'énergie était le principal contributeur (58–64 %) aux coûts d'opération totaux, lorsque le diesel

était la principale source d'énergie (nord du Québec), alors que les coûts des électrodes étaient largement supérieurs (76–77 %), lorsque l'hydroélectricité était utilisée (juridictions centrales du Canada et des États-Unis).

Les résultats de cette étude ont permis de mieux comprendre les mécanismes généraux régissant l'oxydation des thiosels par EF dans des eaux minières réelles. De plus, il a été démontré que, dans certains cas, le procédé ne génère aucune toxicité résiduelle et qu'il peut même réduire ou éliminer la toxicité initiale de l'effluent. Bien entendu, d'autres études en termes de toxicité associée au traitement par EF devront être faites afin d'approfondir ces nouvelles connaissances. L'analyse technico-économique préliminaire a permis de déterminer que le procédé pourrait être économiquement viable dans l'industrie minière (sauf dans le Nord où les coûts élevés de l'électricité défavorisent l'implantation de technologies de traitement des eaux électrochimiques), mais des études devront être faites pour trouver des matériaux d'électrode qui sont moins dispendieux. Globalement, au cours de l'exécution de ce projet, des informations cruciales ont été acquises, constituant un point de départ dans le domaine de la recherche appliquée pour le développement de l'EF en tant que nouvelle technologie de traitement des eaux minières efficace et écologiquement durable.

ABSTRACT

Thiosalts are partially oxidized sulfur intermediates formed during the oxidation of sulfide minerals and are responsible for delayed acidity, leading to aquatic toxicity in receiving water bodies. Freeze/thaw (F/T) cycles, induced by season changes in northern regions, are known to accelerate sulfur oxidation kinetics, which entails increased thiosalts concentrations in mine water. Concentrations as high as 15 g/L of thiosulfates ($S_2O_3^{2-}$) have recently been reported in a study evaluating the effect of F/T cycles on the stability of mine waste.

The limitations of chemical neutralization, used as the current preferred thiosalts management practice, entail the development of emerging technologies. In addition, water treatment strategies in northern countries are mainly limited by their inability to deal with extreme thiosalt contamination. A particular focus on emerging technologies that are also suitable in cold climate is necessary. Recently, the electro-Fenton (EF) process has been reported as effective for thiosalts treatment in synthetic mine water, even when the temperature of the water was as low as 4°C.

To further advance the general understanding of this approach, a performance evaluation was conducted on both synthetic and real mine effluents. The term “performance” was defined as contaminant removal efficiency, associated residual toxicity, and operating costs, the three components of the project. EF treatment tests were performed using pre-optimized parameters (carbon fiber brush cathode, single-side coated Nb/boron-doped diamond plate anode, current intensity = 0.3 A, current density = 0.006 A/cm² and initial $[Fe^{2+}] = 0.2$ mM). In this study, H_2O_2 concentrations were not measured, but H_2O_2 production was proven during the preliminary work to optimize the operating parameters. Contaminant removal efficiency was evaluated on four different real mine effluents, selected based on their geographical origin (northern Quebec, Canada) and differing $S_2O_3^{2-}$ concentrations (219 ± 21 mg/L, 32 mg/L, 0 mg/L and 58 mg/L for E1, E2, E3 and E4, respectively). Treatability tests were then performed on “simplified”, corresponding synthetic effluents, with and without addition of alkalinity, to investigate underlying mechanisms. The influence of chlorinated salinity (related to the presence of Cl^-) on the EF process performance was also studied on effluent E1 at 2 and 4 g/L $CaCl_2$, at pH 3 and pH 5. Resulting solutions were treated as per usual. For the assessment of residual toxicity, E1 and E4 were tested for acute toxicity to *Daphnia magna*, both before and after EF treatment. Finally, a preliminary techno-economic

analysis was conducted to evaluate operating costs, in terms of energy consumption, reagents and electrode costs, for northern Quebec vs the rest of Canada and the USA.

Thiosulfate removal efficiency results were encouraging. Complete removal (> 99%) was achieved under 60 min for all effluents tested, including corresponding synthetic effluents, with and without alkalinity, and independent of the Cl^- concentration. Alkalinity was identified as a process inhibitor, resulting in an increased treatment time from 0.25 sec in E2 to 12 min in its corresponding synthetic effluent when alkalinity was added. The influence of chlorinated salinity on the process performance seemed more complex. It was observed that $\text{S}_2\text{O}_3^{2-}$ removal was faster at pH 5 than pH 3, and faster at 4 g/L CaCl_2 than at 2 g/L CaCl_2 , with unmodified E1 showing the slowest $\text{S}_2\text{O}_3^{2-}$ oxidation kinetics. These observations were in accordance with the literature, which seems to indicate that Cl^- interfere with thiosalts treatment via their interaction with Fe^{2+} at the optimal pH range of the Fenton reaction. Furthermore, oxidative Cl^- species formed at the anode could accelerate the treatment, whereas their HO^\bullet -scavenging properties could slow down thiosalts oxidation.

Results of the residual toxicity assessment revealed that the initial matrix had no impact on the acute toxicity to *D. magna* for all effluents tested. Effluent E1 showed *D. magna* mortality initially but was below the acute toxicity threshold ($\text{LC} < 50\%$). Complete oxidation of thiosalts in E1 resulted in the elimination of *D. magna* mortality. EF treatment of effluent E4, which was initially acutely toxic, resulted in the elimination of toxicity to *D. magna*.

Results of the preliminary techno-economic analysis showed that energy consumption was the main contributor (58–64%) to the total operating costs, when diesel was the main power supply (northern Quebec), whereas electrode costs were highly superior (76–77%), when hydroelectricity was used (central jurisdictions of Canada and the USA).

The results of this study provided a better understanding of the general mechanisms governing the oxidation of thiosalts by EF in real mine water. In addition, it has been shown that, in some cases, the process does not generate any residual toxicity and can even reduce or eliminate the effluent's initial toxicity. Further studies in terms of toxicity associated to EF treatment will need to be done in order to deepen the acquired knowledge. The preliminary techno-economic analysis showed that the process could be economically viable in the mining industry (except in the North where the implementation of electrochemical water treatment technologies is unfavored due to high

electricity costs), but studies will need to be done to identify alternative electrode materials that are less expensive. Overall, during the execution of this project, crucial information was acquired, constituting a starting point in the field of applied research for the development of EF as a new efficient and environmentally sustainable mine water treatment technology.

TABLE OF CONTENTS

DEDICATION	iii
ACKNOWLEDGEMENTS	iv
RÉSUMÉ.....	v
ABSTRACT.....	viii
TABLE OF CONTENTS	xi
LIST OF TABLES	xiv
LIST OF FIGURES.....	xvi
LIST OF SYMBOLS AND ABBREVIATIONS.....	xviii
LIST OF APPENDICES	xx
CHAPTER 1 INTRODUCTION.....	1
1.1 Context	1
1.2 Problematic.....	2
1.3 Objectives.....	3
1.4 Content of the dissertation and impacts of the project	3
CHAPTER 2 LITERATURE REVIEW.....	7
2.1 Thiosalts	7
2.1.1 Generalities.....	7
2.1.2 Geochemical behaviour.....	7
2.1.3 Thiosalts speciation in aqueous solutions	14
2.1.4 Toxicity	14
2.2 Treatment	23
2.2.1 Current thiosalts treatment methods.....	23
2.2.2 Water treatment in northern countries.....	24

2.2.3	Advanced oxidation processes	25
2.2.4	Electrochemical advanced oxidation processes	32
2.3	Summary of main findings and research needs.....	41
2.4	Preliminary research work	44
2.4.1	Comparative efficiency of three advanced oxidation processes for thiosalts oxidation in mine-impacted water (Gervais et al., 2020).....	44
2.4.2	Electro-Fenton beyond the degradation of organics: Treatment of thiosalts in contaminated mine water (Olvera-Vargas et al., 2021)	46
CHAPTER 3	METHODOLOGY	52
3.1	Contaminant removal	52
3.1.1	Sampling of real effluents and preparation of synthetic effluents	52
3.1.2	Analysis of effluents, before and after treatment	55
3.1.3	Treatability tests	59
3.2	Preliminary techno-economic analysis.....	60
3.2.1	BDD electrode costs.....	61
CHAPTER 4	CONTAMINANT REMOVAL EFFICIENCY	63
4.1	Oxidation “boosts”	63
4.2	EF treatment of synthetic and real mine effluents.....	66
4.2.1	Initial physicochemical characterization.....	66
4.2.2	Evolution of pH and S species during treatment.....	72
4.3	Effect of alkalinity.....	76
4.4	Effect of chlorinated salinity	78
CHAPTER 5	ARTICLE 1 ELECTRO-FENTON TREATMENT OF CONTAMINATED MINE WATER TO DECREASE THIOSALTS TOXICITY TO <i>DAPHNIA MAGNA</i>	80
5.1	Introduction	82

5.2	Materials and methods	84
5.2.1	Mine effluent sampling and characterization	84
5.2.2	EF treatment	85
5.2.3	Sample preparation for toxicity tests.....	86
5.2.4	Toxicity tests	88
5.2.5	Cost calculations	89
5.3	Results and discussion.....	91
5.3.1	EF treatment of mine effluents.....	91
5.3.2	Toxicity assessment.....	98
5.3.3	Preliminary evaluation of EF operating costs	101
5.4	Conclusion.....	105
5.5	References	106
CHAPTER 6	GENERAL DISCUSSION.....	110
6.1	Impact of chlorides on the overall performance of thiosalts treatment by EF	110
6.2	Techno-economic evaluation: BBD electrode costs	111
CHAPTER 7	CONCLUSION AND RECOMMENDATIONS.....	115
REFERENCES.....		120
APPENDICES.....		128

LIST OF TABLES

Table 2.1 Influence of temperature on thiosalts generation at pH 7.5 (adapted from Negeri et al., 1999).....	8
Table 2.2 Summary of studies which evaluated the impact of F/T cycles on the hydrogeological properties, hydrogeochemical behavior and reactivity of different materials from various locations in northern regions.	12
Table 2.3 Compilation of available toxicological data of thiosalts, other S-based compounds and salinity to various aquatic organisms	16
Table 2.4 Thiosalt speciation reactions and dominant pH ranges considered in the ecological thiosalts risk assessment model.....	19
Table 2.5 Characteristics of effluents in the investigation of sporadic aquatic toxicity by Novak and Holtze (2010).....	21
Table 2.6 Current water treatment strategies at Swedish mines and their efficiencies (adapted from Wahlström et al., 2017).	25
Table 2.7 Summary of AOPs for the treatment of mine-impacted water.....	27
Table 2.8 Toxicity assessment of organic-contaminated wastewaters treated by EF.	40
Table 2.9 Energy consumption and $S_2O_3^{2-}$ removal efficiency, after 90 and 120 min of treatment by EF, at different current densities.	49
Table 2.10 Preliminary techno-economic evaluation of operating costs of thiosalt treatment in synthetic and real mine water (as presented in Olvera-Vargas et al., 2021).	50
Table 3.1 Characteristics of EF treatability tests performed including treatment duration, sampling times and analyzed parameters, before, during and after treatment, for all synthetic and real effluents.	56
Table 3.2 Initial physicochemical characteristics of real mine effluents E1, E2, E3 and E4.	59
Table 3.3 Variable values in the techno-economic model for BDD electrode cost estimations. ...	62
Table 5.1 Variable values in the techno-economic model.....	90
Table 5.2 Physicochemical parameters of untreated and treated effluents ME_{high} and ME_{low}	96

Table 5.3 Preliminary OCs evaluation for the treatment of effluents ME_{high} and ME_{low} by EF. 104

Tableau A.7.1 Paramètres à analyser pour la caractérisation des effluents avant, pendant et après traitement.....138

LIST OF FIGURES

Figure 1.1 Project structure flowchart.....	5
Figure 1.2 Framework of the project.....	6
Figure 2.1 Thiosalts exposure assessment model developed by Fahd (2014).....	20
Figure 2.2 Main steps involved in the development of EAOPs for a prospective large-scale application (adapted from Garcia-Rodriguez et al., 2020).....	38
Figure 3.1 Step-by-step methodological approach of the project.	53
Figure 3.2 Detailed approach and justifications for the “efficiency” component of the project.	54
Figure 4.1 Evolution of water parameters for HRTs of 15 min (x-axis = 0) to 7 days, following oxidation “boosts” of 1, 15 and 30 min on S0 (1 g/L S ₂ O ₃ ²⁻).	64
Figure 4.2 pH and S ₂ O ₃ ²⁻ evolution during EF treatment of (a) E1, (b) S1 and (c) S1+alk.	72
Figure 4.3 pH evolution of E2, between 0 and 15 min, during EF treatment.	74
Figure 4.4 pH and S ₂ O ₃ ²⁻ evolution during EF treatment of (a) E2, (b) S2 and (c) S2+alk.	74
Figure 4.5 pH evolution during EF treatment of (a) E3, (b) S3 and (c) S3+alk.....	76
Figure 4.6 Effect of chlorinated salinity, at 2 g/L and 4 g/L CaCl ₂ , on EF treatment in effluent E1, at pH 3 and 5. (a) S ₂ O ₃ ²⁻ removal, (b) pH evolution and (c) Cl ⁻ concentration.....	79
Fig. 5.1 Preparation of effluents for acute toxicity testing on <i>D. magna</i> . Step 1 – EF treatment (ME _{high} or ME _{low}), in triplicate. Step 2 – homogenization of triplicates to produce a composite sample. Step 3 – pH adjustment/filtration of the composite sample. Step 4 – pH adjustment/filtration of the initial effluent (ME _{high} only) and acute toxicity testing on <i>D. magna</i> using (un-)treated effluents (ME _{high} or ME _{low}).	87
Fig. 5.2 Evolution of various parameters during EF treatment of effluent ME _{low} : (a) S ₂ O ₃ ²⁻ , SO ₄ ²⁻ , pH; (b) Br ⁻ and Cl ⁻ . Evolution of these parameters during EF treatment of effluent ME _{high} are presented elsewhere (Olvera-Vargas et al., 2021).....	93
Fig. 5.3 S ₂ O ₃ ²⁻ disproportionation pathways in acidic media (adapted from Miranda-Trevino et al., 2013).....	94

Fig 5.4 Mortality evolution of *D. magna* for (un-)treated effluents (a) ME_{high} and (b) ME_{low}99

Fig 5.5 EF operating cost proportions of E_{consum} , $FeSO_4 \cdot 7H_2O$, and Na_2CO_3 for Canada, northern QC, and the USA, for effluents ME_{high} (ME_h) and ME_{low} (ME_l). 101

Figure 6.1 EF operating cost proportions of E_{consum} , $FeSO_4 \cdot 7H_2O$, Na_2CO_3 and BDD electrodes for Canada, northern QC, and the USA, for effluents E1 and E4. 112

LIST OF SYMBOLS AND ABBREVIATIONS

ACS	American Chemical Society
AMD	Acid mine drainage
AOP	Advanced oxidation process
BDD	Boron-doped diamond
BDL	Below detection limit
CCBE	Covers with capillary barrier effect
CEAEQ	Centre d'Expertise en Analyse Environnementale du Québec
CEC	Contaminant of emerging concern
CFA	Coal fly ash
CND	Contaminated neutral drainage
COD	Chemical oxygen demand
CPE	Catalytic particle electrode
D019	Directive 019 (Quebec's Environmental Guidelines on Mining Industry)
DO	Dissolved oxygen
DSA	Dimensionally stable anodes
EAOP	Electrochemical advanced oxidation process
EC	Electrical conductivity
EC50	Concentration that is estimated to produce adverse effects (immobilization or an endpoint other than lethality) to 50% of the test population
EF	Electro-Fenton
F/T	Freeze/thaw
HRT	Hydraulic retention time

IC	Ion chromatography
IC25	Concentration that is estimated to inhibit growth or reproduction in 25% of the test population
ICP-AES	Inductively coupled plasma - atomic emission spectroscopy
LC50	Concentration that is estimated to be lethal to 50% of the test population
LQE	Law on the Quality of the Environment
MBR	Membrane bioreactor
MFC	Microbial fuel cells
MMER	Metal and Diamond Mining Effluent Regulations
NUS	National University of Singapore
PPU	Price per unit
RSAC	Rice straw activated carbon
TIF	Tailing impoundment facilities
TIR	Toxic inhibition rate
TOC	Total organic carbon
UNAM	National Autonomous University of Mexico

LIST OF APPENDICES

Appendix A	Experimental protocol	128
Appendix B	Toxicity analysis certificate for effluent E1 (untreated).....	143
Appendix C	Toxicity analysis certificate for effluent E1 (treated).....	146
Appendix D	Toxicity analysis certificate for effluent E4 (untreated).....	149
Appendix E	Toxicity analysis certificate for effluent E4 (treated)	152

CHAPTER 1 INTRODUCTION

1.1 Context

The mining industry has long been a major contributor to the global economy by providing the materials needed to build infrastructures and instruments of daily use (Carvalho, 2017). A constant and accentuated exploitation of mines is required owing to the incessantly increasing demand for raw materials (Taušová et al., 2017). Mining activities cause significant environmental alterations despite the favorable economic spinoffs particularly in terms of physical space, consumption of water as well as energy and production of large quantities of solid and aqueous waste (Bussière et al., 2005).

Among the environmental issues related to the mining industry, acid mine drainage (AMD) represents a particular challenge. Acid mine drainage is the result of the circulation of water through the components of a mine site (e.g., waste rock piles, tailings storage and impoundment facilities, open pit, underground tunnels) containing sulfide minerals exposed to air, that oxidize to generate sulfuric acid (H_2SO_4) (Nordstrom et al., 2015). The chemical stability of mine waste is compromised when the interaction between the water and the solid contaminates the draining water (Bussière et al., 2005). The grinding of the ore further accelerates the oxidation by increasing the surface area of the grains available to react with the oxygen and water. When the water becomes acidic, several metal(loid)s trapped in the minerals become soluble and contribute to an increased contamination of the drainage. These contaminants, along with the acidity, are toxic to organisms in the receiving water bodies and are highly damaging to the surrounding ecosystems.

The current exploitation of low-grade and refractory sulfidic ores leads to higher amounts of tailings stored in tailing impoundment/storage facilities, higher concentrations of contaminants as well as contaminant mixing, causing the proper management of mine water to represent a growing challenge for mining companies (Olvera-Vargas et al., 2021). The large volumes of contaminated water generated, which are in the order of several thousand ML/d (Dieter et al., 2018), and the unpredictable precipitations and freeze/thaw (F/T) events amplified by climate change also contribute to water treatment challenges, making the process not only expensive, but also highly complex.

Provincial and federal laws require mine operators to have a restoration plan including safe containment measures for waste as well as measures to manage contaminated mine water. As an example, Directive 019 (D019), under the Quebec provincial law on the quality of the environment (LQE), and the Metal and Diamond Mining Effluent Regulations (MMER), under the Canadian Fisheries Act, require that the criteria of physicochemical quality and toxicity of the final effluent be met, before its release into the environment (JUS 2002; MDDELCC, 2012). These criteria include a final effluent pH 6.0-9.5 and a concentration of thiosalts, which does not represent a risk of lowering the pH below 6.0. Toxicity criteria must also be met and will be discussed in Section 2.3.

1.2 Problematic

Currently, the preferred AMD treatment method is the addition of a chemical neutralizer (such as limestone or lime) to the water retention basins. By increasing the pH, heavy metals and sulfate (SO_4^{2-}) are removed by (co)precipitation and sorption (Miranda-Trevino et al., 2013; Bejan et al., 2015; Skousen et al., 2017). This approach has some disadvantages including the oxidation of ferrous iron [Fe(II)] to ferric iron [Fe(III)] by atmospheric oxygen (or by another oxidant), leading to the precipitation of Fe(III) which generates water (H_2O). As a result, the treatment sludge contains multiple contaminants as well as large amounts of water, making treatment difficult and costly (Bejan et al., 2015). In addition, some chemical species are insensitive to treatment by chemical neutralization. For example, thiosalts remain in solution and are present in the final effluent even after treatment. Complete oxidation of thiosalts to H_2SO_4 as end-product leads to a retarded acidification of the final effluent (Miranda-Trevino et al., 2013). Precisely, a final effluent can meet all the criteria under provincial and federal laws in terms of pH, SO_4^{2-} and heavy metal(loid)s concentrations but, if it contains thiosalts, their slow and delayed oxidation will cause a drop in pH after the release of the effluent into the environment or its recirculation to the mine. Thiosalts left untreated by the addition of a chemical neutralizer can threaten aquatic life, the integrity of the ecosystems near the receiving water bodies or the proper functioning of the mine's equipment and machinery by accelerated corrosion (Kuyucak et al., 2014).

Thiosalts have been the focus of many studies with the aim of better understanding their behavior in water, their toxicity to organisms in the receiving environment and to develop/optimize efficient treatment technologies. Although research has led to major advances, thiosalts are still considered

contaminants of emerging concern (CECs) due to a rise in reported concentrations related to the exploitation of low-grade and refractory sulfidic ores (Neculita et al., 2020; Ryskie et al., 2021). In this context, thiosalts treatment methods must be further optimized to prevent the possible repercussions. Knowing that thiosalts are not treated by using chemical neutralizers, their complete oxidation to SO_4^{2-} followed by neutralization of the produced acidity seems to be the best approach (Miranda-Trevino et al., 2013).

1.3 Objectives

The main objective of this research project is to evaluate the performance of the electro-Fenton (EF) process in removing thiosalts and other oxidizable contaminants present in real mine water. With this purpose, the term “performance” was defined and subdivided into three distinct aspects, constituting the specific objectives of the project. Precisely, they are the following:

- i. Evaluate the efficiency of EF, in terms of contaminant removal, in complex mine effluents under the best operating conditions predetermined on synthetic effluents.
- ii. Assess the residual toxicity associated to EF treatment by performing acute toxicity tests on *D. magna* for 2 or 3 real mine effluents (having complex chemistries), before and after treatment.
- iii. Estimate the operating costs of EF via a preliminary techno-economic analysis.

1.4 Content of the dissertation and impacts of the project

This thesis is divided into 7 main sections, which are indicated in the project structure flowchart (**Fig. 1.1**). The three main topics correspond to a specific objective each (SO; 2nd level; **Fig. 1.1**) and each level of the project flowchart refers to the chapter number. Chapter 3 presents the general methodological approach of the project and of the unpublished results, which are presented and discussed in Chapter 4. Chapter 5 is the manuscript submitted for consideration to *Science of the Total Environment*. Chapter 6 is a general discussion of the results presented in Chapters 4 and 5, highlighting the links between the results presented in both chapters. Chapter 7 summarizes the main findings of this research project and identifies possible follow-up research perspectives.

The project presented in the scope of this dissertation is part of a larger project whose aim is to improve the current knowledge pertaining to salinity treatment technologies (including thiosalts and SO_4^{2-}) as well as their performance, and to the toxicity of mine effluents, in regions characterized by significant seasonal changes, to protect aquatic life in receiving water streams and surrounding ecosystems. **Figure 1.2** summarizes how the research projects of Foudhaili (2019), Jaidi (2020) and the present project are related to provide new knowledge and a better understanding of the sources of salinity in mine water and of the mechanisms governing the performance of technologies for the treatment of sulfated salinity and its precursors (thiosalts). The three studies also provide new, in-depth knowledge in terms of the toxicity of mine water: the impact of the salinity of mine water on the toxicity of receiving water bodies is discussed by Jaidi (2020), the residual toxicity associated to the treatment of sulfate-related salinity in gold mine effluents, by means of electrocoagulation, is discussed by Foudhaili (2020) and the toxicity of mine effluents contaminated with thiosalts, following EF treatment, is assessed herein.

The results of this Master's project specifically allowed for a better comprehension of general mechanisms governing thiosalts oxidation by EF in real mine water, whose matrix is oftentimes complex and can influence the process efficiency. Moreover, by the use of EF to treat inorganic contaminants in mine water and the evaluation of performance (not only of efficiency), this project allowed notable advancements in applied research and development of new mine water treatment technologies that are adapted to northern regions: efficient, suitable in cold water, economically viable and respectful of the environment.

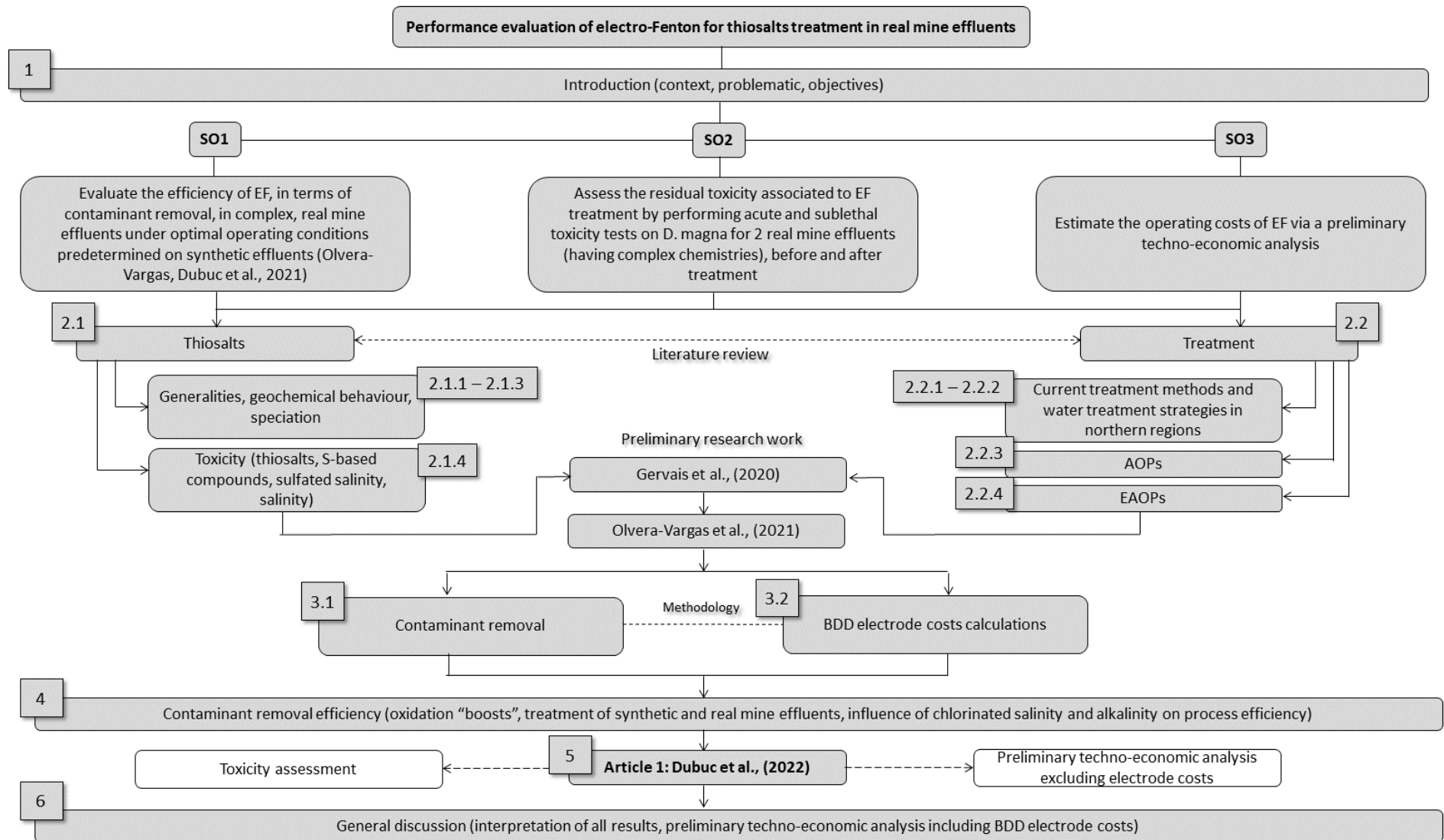


Figure 1.1 Project structure flowchart.

Foudhaili (2019) PhD

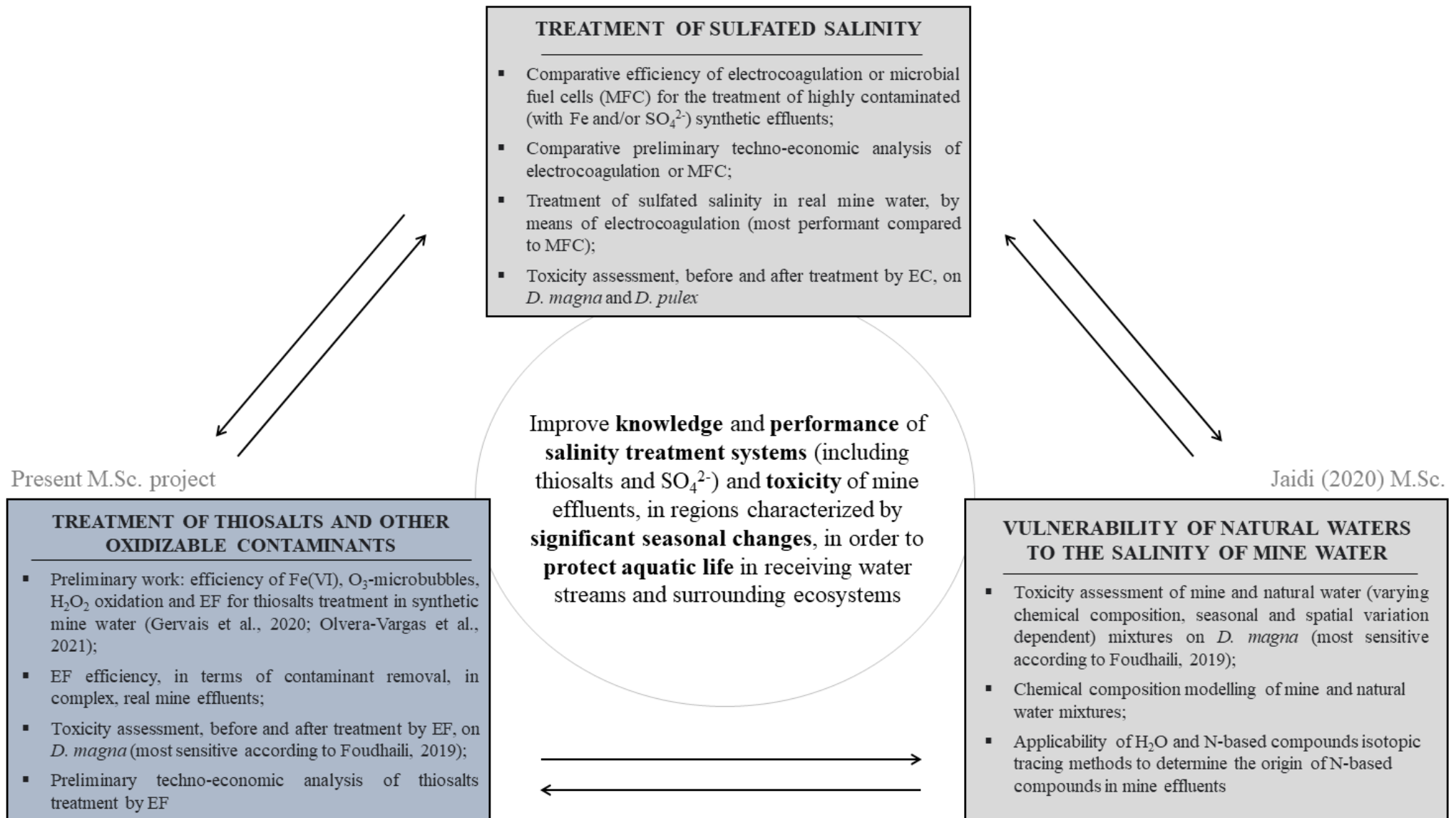


Figure 1.2 Framework of the project.

CHAPTER 2 LITERATURE REVIEW

2.1 Thiosalts

2.1.1 Generalities

The oxidation of sulfide minerals takes place in several steps. To be converted into SO_4^{2-} , the sulfur (S) atom contained in sulfide minerals must lose up to 8 electrons to pass from the oxidation state of -2 (as in pyrrhotite) or -1 (as in pyrite) to +6 (as in SO_4^{2-}) (Range and Hawboldt, 2019). The intermediate reactions that eventually lead to the formation of AMD produce metastable and partially oxidized intermediate S species, commonly referred to as thiosalts or polythionates. The main thiosalts resulting from the incomplete oxidation of sulfide minerals are thiosulfate ($\text{S}_2\text{O}_3^{2-}$), trithionate ($\text{S}_3\text{O}_6^{2-}$) and tetrathionate ($\text{S}_4\text{O}_6^{2-}$). Being the precursor of $\text{S}_3\text{O}_6^{2-}$ and $\text{S}_4\text{O}_6^{2-}$, $\text{S}_2\text{O}_3^{2-}$ is considered the major thiosalt in mine water (Miranda-Trevino et al., 2013). A recent study determined the S mass balance across 52 water samples, collected from 4 different Canadian mine sites, from 2014 to 2018. Results consistently showed, among all samples, that $\text{S}_2\text{O}_3^{2-}$ was only a minor component of total S (average $[\text{S}_2\text{O}_3^{2-}] = 4\%$). Together, all the oxidizable S species accounted for $30\% \pm 25\%$ of total S (Whaley-Martin et al., 2020). Several factors, discussed in the following section, influence thiosalts generation and resulting concentrations in mine effluents.

2.1.2 Geochemical behaviour

2.1.2.1 Thiosalts generation: influencing factors

Several intrinsic factors to mining processes contribute to the generation of thiosalts. These factors include the initial S content in the ore, grinding and flotation pH, grain size after grinding of the ore, hydraulic retention time (HRT) in the mill and the stirring speed of the pulp (Miranda-Trevino et al., 2013). Other studies reported that higher sulfide content, alkaline process waters, finer grain size, longer HRT and increased agitation rate of the pulp (which contributes, in parallel, to more dissolved oxygen (DO) in the pulp) promote the generation of thiosalts (Negeri et al., 1999). In the same study, a pyritic Cu-Zn ore from the Louvicourt mill (Quebec, Canada) and a pyrrhotitic Cu-Ni ore from the Strathcona mill (Alberta, Canada) were used to assess the influence of pulp temperature on thiosalts formation during the milling (i.e. grinding and flotation) of sulfidic

ores. **Table 2.1** presents the results obtained by the authors in terms of total thiosalts generated for a given pH, at two different temperatures and HRTs. Overall, the pyrrhotitic ore was more sensitive to pulp temperature variations than the pyritic ore. Mine operations exploiting pyrrhotite-rich ores should expect higher thiosalts concentrations. Further investigations demonstrated that even minor temperature fluctuations, which are acceptable in standard flotation tests, caused important differences in total thiosalts produced. It was estimated that a 1°C increase in pulp temperature would result in increases of 2.2 and 11.2 g/t of total thiosalts generated for the pyritic and the pyrrhotitic ores, respectively.

Table 2.1 Influence of temperature on thiosalts generation at pH 7.5 (adapted from Negeri et al., 1999).

Temperature (°C)	HRT (min)	Thiosalts generated (g/t)	
		Pyritic ore	Pyrrhotitic ore
10.0	10.0	30	59
25.0	10.0	47	160
10.0	30.0	31	90
25.0	30.0	49	267

The nature of the reagents used during the milling of sulfidic ores also influences the amount of thiosalts generated. For example, sulfur dioxide (SO₂) in operating units with a pH greater than 8 is likely to contribute to the oxidation of S to S₂O₃²⁻ (Miranda-Trevino et al., 2013). The type of neutralizing agent used to control the pH also influences the generation of thiosalts (i.e. sodium carbonate is a stronger kinetics enhancer of thiosalts generation than lime; Miranda-Trevino et al., 2013). The addition of xanthates, the most widely used collectors during flotation, also increases thiosalts concentrations in effluents via two main pathways: i) a transfer of thiosalts from the surface of mineral particles to the solution due to xanthate “collecting” characteristics and ii) increased sulfide surface of exposure accessible for oxidation (Negeri et al., 1999).

Bacteria also play an important role in thiosalts formation. *Acidithiobacillus* spp. (i.e. *A. ferrooxidans* and *A. thiooxidans*) are well known contributors of AMD generation via S oxidation, entailing the production of thiosalts (Whaley-Martin et al., 2019). A study demonstrated that the dominant microbial communities in contaminated neutral drainage (CND)

varied from those in AMD. It was found that *Halothiobacillus* spp. dominated 7 of the 9 total S oxidizing bacteria communities in 3 of the 4 CNDs studied, and *A. ferrooxidans* and *A. thiooxidans* were absent. *Halothiobacillus* spp. are a family of bacteria capable of oxidizing sulfide, S^0 , $S_2O_3^{2-}$ and $S_4O_6^{2-}$ to S, SO_3^{2-} , polythionates and SO_4^{2-} , influencing thiosalts concentrations in mine water (Whaley-Martin et al., 2019).

2.1.2.2 Effect of freeze/thaw cycles on the oxidation of sulfide minerals

Freeze/thaw cycles are known to alter the physical structure of soils by creating surface cracks eventually leading to internal breaches, which promote the infiltration of oxygen and form preferential pathways for the infiltration of water. Some particles may also be fractured, resulting in an increased surface area available to react with the water and the oxygen (Éthier, 2011).

Table 2.2 compares the results obtained mainly in terms of sulfide oxidation products (S species, thiosalts, and Fe) and neutralizing minerals dissolution products (Ca, Mn, and Mg) from several studies. The impact of F/T cycles on hydrogeological properties, hydrogeochemical behavior and reactivity of different materials was assessed. Schudel et al. (2019) evaluated the effect of F/T cycles on thiosalts concentrations where column tests were carried out with tailings mostly composed of pyrrhotite and serpentine. For columns subjected to F/T cycles, results demonstrated that $S_2O_3^{2-}$ concentrations reached 10,000 mg/L vs 7200 mg/L at ambient temperature. Additionally, $S_4O_6^{2-}$ concentrations reached 2600 mg/L in F/T columns and 2200 mg/L in columns at ambient temperature. Another study, aimed at better understanding the effect of F/T cycles on the leaching of contaminants, showed an increased reactivity of minerals (Jouini et al., 2020). In this latter study, residues originated from a tri-unit Fe-rich passive treatment system (the composition of the residues of each unit are presented in **Table 2.2**). Results showed very high cumulative SO_4^{2-} concentrations in all units after 22 cycles, as well as high cumulative Ca concentrations in units 1 and 2, indicating high material reactivity under F/T conditions.

Consistently, Éthier (2011) and Éthier et al. (2012) found that repeated F/T cycles increase the oxidation rate of sulfide minerals. The study also observed that the alternation of F/T cycles disturbs the oxidation-neutralization relations via a decrease of the neutralization (Ca+Mg)/oxidation (S) products ratio. To do so, the cumulated Ca+Mg in weathering cell leachates was plotted as a function of the cumulated S and the parameters of the regression lines were evaluated. **Table 2.2** shows the slopes of the regression lines for weathering cells at 22°C and

subjected to F/T cycles. The slopes of the regression lines for each sample studied decreased under F/T conditions, indicating an increase in cumulative S and/or a decrease in cumulative Ca+Mg. Moreover, annual S leaching rates of all the samples were increased by 1.5–2x for F/T samples compared to those at 22°C.

Consistently, Boulanger-Martel (2015) observed that O₂ fluxes in gravel-bentonite covers with capillary barrier effect (CCBEs) increased by 50x after 3 F/T cycles (<1 mol/m²/year initially to >50 mol/m²/year) for bentonite compositions of 5.0 and 8.0% (**Table 2.2**). Both covers were initially saturated (>85%) and were desaturated with F/T cycles, explaining the increased oxygen diffusion. Accordingly, it was also observed, for a bentonite composition of 6.5%, that the k_{sat} increased by 735x after 5 F/T cycles compared to its initial value. These findings indicated that repeated F/T cycles affect the hydrogeological properties and, inevitably, the performance of bentonite in CCBEs. The use of gravel-bentonite CCBEs in northern regions for progressive restoration, where temperatures are below the freezing point in winter and increase to positive values in summer, would lead to greater amounts of oxygen and water reaching the materials beneath the cover, resulting in an increased reactivity of the rock and greater leaching of contaminants.

In agreement with the laboratory studies presented above, an *on-site* study (2007-2012) within the Diavik Waste Rock project, determined the impact of F/T cycles on the geochemistry of a 15 m high waste rock pile (Sinclair et al., 2015). In 2009-2010, a decrease in pH was observed at all depths of the pile, leading to final pH of 3.5 and 4-5 at the core of the pile (2-9 m) and at all other depths, respectively, in 2012. Moreover, a near-depletion of alkalinity at all locations of the pile was observed in 2009-2010, resulting in the exhaustion of all carbonates by the end of 2012. **Table 2.2** shows the variation in Ca, Fe and SO₄²⁻ concentrations after n cycles.

Moreover, an *on-site* case study at Boliden Mineral AB (Sweden) reported the cumulative amounts of thiosalts, discharged from the mill and from the tailings' dam, from January 2008 to February 2009 (Forsberg, 2011). In Boliden, mining operations are naturally subject to the effects of F/T cycles with average minimums of -14°C in winter and average maximums of 20°C in

summer¹. **Table 2.2** presents the cumulative amounts of $S_2O_3^{2-}$ and $S_4O_6^{2-}$ discharged from the mill and in the effluent from the Gillervattnet tailings' dam during this period. A total of 640 t of thiosalts were discharged from the mill and 660 t of total thiosalts were cumulated in the effluent of the tailings' dam.

In contrast, another study revealed that a repetition of F/T cycles had no significant impact on the hydrogeological properties of desulfurized tailings used as a cover in a CCBE (Lessard, 2018). Indeed, the initial and final measurements of the saturated hydraulic conductivity (k_{sat}) in the water retention layer were in the same order of magnitude (1.1×10^{-5} initially vs. 7.2×10^{-5} after 8 F/T cycles) (**Table 2.2**). Moreover, the pH, acidity and alkalinity of the exfiltration waters remained the same overall. The unchanged properties of the studied material despite the freezing and thawing conditions could be attributable to the fine grain size of the studied material compared to other materials due to reduced physical structure alterations. A possible explanation for the difference observed with other studies could have been the variations in the freezing profiles of the material in laboratory columns compared to *on-site* test piles. The freezing profiles observed by Lessard (2018) for the column tests were the same as those reported by Sinclair et al. (2015). Indeed, when subjected to freezing temperatures, the material at the surface of the column (0.4 m) froze first. Then, the material at the bottom of the column froze (1.60 m) and the material at the center of the column froze last (0.75–0.90 m; Lessard, 2018). For *on-site* test piles, the freezing profile was the same: the top, the bottom and the outside of the pile froze first, in early fall, while the center of the pile froze last, in late fall/early winter (Sinclair et al., 2015).

In summary, all the above-mentioned studies, either conducted at laboratory or field scale, agree that the climatic conditions of northern regions, where successive F/T cycles occur naturally as a result of season changes, alter the hydrogeological properties (i.e. increased O_2 fluxes, degrees of saturation and k_{sat}), the hydrogeochemical behavior (i.e. increased contaminants' leaching in drainage water) and the reactivity (increased S oxidation and O_2 consumption rates) of materials.

¹ (<https://weatherspark.com/y/86556/Average-Weather-in-Boliden-Sweden-Year-Round>)

Table 2.2 Summary of studies which evaluated the impact of F/T cycles on the hydrogeological properties, hydrogeochemical behavior and reactivity of different materials from various locations in northern regions.

Material, composition and location	Experimental conditions	Number of F/T cycles (<i>n</i>)	Length of a cycle (days)	Measured parameters	Observations	Ref.		
Weathered tailings (3–5 years); pyrrhotite (27.9%) and serpentine (34.0%); Raglan mine site	Laboratory, column tests	10	35	O ₂ consumption (mol O ₂ /m ² /yr)	2500 (<i>n</i> = 3) to ~750 (<i>n</i> = 10)	[1]		
				pH	Circumneutral (<i>n</i> = 1) to < 4 (<i>n</i> = 10)			
				Ca (mg/L)	~500			
				Mg (mg/L)	~ 2500			
				S species (mg/L)	[S ₂ O ₃ ²⁻] _{max} = 10,000 [S ₄ O ₆ ²⁻] _{max} = 2600 [SO ₄ ²⁻] _{max} = 10,000			
Residues from an Fe-rich AMD passive tri-unit treatment system*; Lorraine mine site	Laboratory weathering cell kinetic tests	22	7	pH	7.5–8 (mean, all units)	[2]		
				Acidity (mg/L CaCO ₃)	3–5 (mean, all units)			
				Alkalinity (mg/L CaCO ₃)	~45 (mean, all units)			
					<i>Unit 1</i>		<i>Unit 2</i>	<i>Unit 3</i>
				Cumulative Ca**	~10,000		~8000	~1900
				Cumulative Fe	~20		~10	~ 10
				Cumulative Mn	~50		~ 8	~0.65
				Cumulative SO ₄ ²⁻	~25,000		~20,000	~25,000
Waste rock; 7 types***; Raglan mine site	Laboratory weathering cell kinetic tests	11	7	Regression line slope of Ca+Mg vs. S cumulation (mg/kg)	<i>Sample</i>	<i>22 °C</i>	<i>F/T</i>	[3, 4]
					1	3.36	1.70	
					2	5.69	1.48	
					3	6.45	3.57	
					4	4.33	5.33	
					5	8.37	5.55	
					6	22.08	2.21	
					7	33.23	11.60	
Gravel-Bentonite as CCBE; Raglan mine site	Laboratory column tests	5	5	Degree of saturation (%)	<i>% bentonite</i>	<i>n</i> = 0	<i>n</i> = 3	[5]
					5.0	> 85	desaturated	
					6.5	< 52	< 52	

Material, composition and location	Experimental conditions	Number of F/T cycles (n)	Length of a cycle (days)	Measured parameters	Observations	Ref.
					8.0 > 85 desaturated	
				O ₂ flux (mol/m ² /year)	5.0 < 1 > 50	
					6.5 > 100 (at all values of n)	
					8.0 < 1 > 50	
Waste rock; 0.053wt. %S; Diavik mine site	On site, test pile scale (15 m high)	6	365	pH	Pile core (2–9 m): ~3.5 All other depths: 4–5	[6]
				Alkalinity	Depleted	
				Carbonates	Depleted	
				Ca (mg/L)	500–1000 (all depths; $n = 2$) to 250–500 (all depths; $n = 6$)	
				Fe (mg/L)	< 1 ($n \leq 4$) to 1.5–2 ($n > 4$)	
				SO ₄ ²⁻ (mg/L)	1000–2000 (pile core; $n = 1$) to ~3000 (all depths; $n = 6$)	
Sulfide-rich tailings; pyrite and pyrrhotite (mainly); Boliden Mineral AB	On site, survey	1	365		<i>Discharged from mill</i> <i>Gillervattnet tailings' dam</i>	[7]
				Cumulative S ₂ O ₃ ²⁻ (t)	~ 550 ~ 525	
				Cumulative S ₄ O ₆ ²⁻ (t)	~ 90 ~ 135	
Desulfurized tailings as CCBE; Raglan mine site	Laboratory column tests	8	20		$n = 0$ $n = 8$	[8]
				pH	~ 8 ~ 8	
				Acidity (mg/L CaCO ₃)	~ 12.5 ~ 12	
				Alkalinity (mg/L CaCO ₃)	~ 140 ~ 140	
				k_{sat}	1.1×10^{-5} 7.2×10^{-5}	
				Ca (mg/L)	~ 140 ~ 500	
				Mg (mg/L)	~ 60 ~ 175	
				SO ₄ ²⁻ (mg/L)	~ 900 ~ 6000	

* Unit 1 = 50% wood ash, 50% wood chips, unit 2 = 10% sand, 40% wood chips, 20% chicken manure, 10% compost; 20% calcite, unit 3 = 50% calcite, 50% wood chips.

** All cumulative concentrations for this study are presented as mg/kg.

*** 1 = Peridotite Mine 3, 2 = Peridotite mine Kikialik, 3 = Olivine-pyroxenite Mine 3, 4 = Olivine-pyroxenite Mine 2, 5 = Gabbro Mine 2, 6 = Argillite Mine 3, 7 = Volcanic

Note: The approximate values (~) presented in this table were retrieved from graphs.

References: [1] - Schudel et al. (2019); [2] - Jouini et al. (2020); [3] - Éthier (2011); [4] – Éthier (2012); [5] - Boulanger-Martel (2015); [6] - Sinclair et al. (2015); [7] – Forsberg (2011); [8] - Lessard (2018)

The only exception observed was for fine grain material (i.e. desulfurized tailings), for which F/T cycles seem to have no apparent impact. In this context and knowing that F/T cycles can have negative impacts on the quality of mining water, it is essential to develop new water treatment methods efficient for high and mixed contamination.

2.1.3 Thiosalts speciation in aqueous solutions

Thiosalts are sensitive to the physicochemical parameters of the water. Their respective concentrations in an effluent strongly depend on the parameters of the water, particularly pH and temperature. For example, $S_2O_3^{2-}$ demonstrates greater stability in neutral to basic medium and will be found in predominant concentrations under these conditions. On the contrary, $S_3O_6^{2-}$ and $S_4O_6^{2-}$ are stable in water with an acid to neutral pH (Miranda-Trevino et al., 2013). Although their oxidation takes place naturally, the process is very slow and has been shown to stop when the water reaches a temperature of 4°C or less due to slower reaction kinetics and bacterial catalysis (Range and Hawboldt, 2019). Thiosalt speciation is presented in detail in Section 2.3.1.1 on the development of a prediction model for thiosalts toxicity assessment.

The increased stability of thiosalts in cold water poses a problem, particularly in northern regions where the water becomes cold enough in winter to completely inhibit the oxidation process. When the temperature rises in summer, the oxidation begins again and thiosalts are transformed into H_2SO_4 , resulting in a progressive drop of pH and rise of acidity in the effluent (Miranda-Trevino et al., 2013; Range and Hawboldt, 2019). In this sense, thiosalts represent a non-negligible source of environmental toxicity via the production of delayed acidity, especially with reported concentrations, which have continued to increase in recent years (Schudel et al., 2019).

2.1.4 Toxicity

The MMER requires that acute lethality of effluents be completely absent for *Oncorhynchus mykiss* and at least monitored for *Daphnia magna*. Sublethal toxicity must be monitored biannually on at least one of each of the following species: a fish, an invertebrate, a plant and an algal specie (JUS, 2002; Schwartz et al., 2006; Ryskie et al., 2021). Moreover, D019 states that the effluent toxicity should be below the level of acute lethality according to standard tests on the rainbow trout (*O. mykiss*) and *D. magna* (MDDELCC, 2012). The available data on

thiosalts toxicity is limited (Ryskie et al., 2021) and predicting the toxicity associated to thiosalts in complex aqueous solutions is challenging because the polythionates form a complex equilibrium system (Fahd, 2014). This section provides a review of the available information relative to thiosalts toxicity as well as that of other S-based compounds and other sources of salinity commonly found in mine water.

2.1.4.1 Direct and indirect toxicity of thiosalts

When released untreated, thiosalts represent a minimal risk of direct toxicity (Miranda-Trevino et al., 2013; Range and Hawboldt, 2019) relative to other contaminants, at concentrations generally found in mine water. The acute toxicity of thiosalts is most often not directly due to the presence of thiosalts, but rather indirectly due to the acidity generated by the production of H_2SO_4 as an end-product of the oxidation process (Miranda-Trevino et al., 2013). A relevant study showed that for $\text{S}_2\text{O}_3^{2-}$ concentrations up to 4100 mg/L, acute toxicity to rainbow trout was not observed, but there was toxicity when the pH of the solution dropped below 5.0 (Schwartz et al., 2006). Yet, reported thiosalts concentrations in contaminated mine water are on the rise due to the current worldwide exploitation of low-grade refractory sulfidic ores, as well as accelerated S oxidation kinetics owing to the influence of F/T cycles (Schudel et al., 2019). In this context, the direct toxicity of thiosalts to aquatic organisms could be of increasing concern.

Despite the current gaps in thiosalts toxicity data in the literature, all studies agree that $\text{S}_2\text{O}_3^{2-}$ is more toxic than all other polythionates, except for *O. mykiss*, for which $\text{S}_4\text{O}_6^{2-}$ is more toxic (Fahd, 2014). For this reason, research on the direct and indirect toxicity of thiosalts shows an absence of correlation between total thiosalts concentrations and mortality of test organisms. In a study conducting direct acute and sublethal toxicity tests on all organisms regulated by the MMER, *O. mykiss* was found to be the most tolerant specie to the presence of thiosalts, with no apparent adverse effects at all tested concentrations (Schwartz et al., 2006). Contrastingly, *C. dubia* was found to be the most sensitive organism to thiosalts with the lowest reported IC25. The data presented in **Table 2.3** indicates that $\text{S}_2\text{O}_3^{2-}$ was more toxic to all organisms than $\text{S}_4\text{O}_6^{2-}$, but results were inconclusive for the rainbow trout because the IC25 were above the highest tested concentrations (Schwartz et al., 2006). These findings prove that the toxicity of the different thiosalts is not additive, explaining the lack of correlation between total thiosalts and mortality of the species.

Table 2.3 Compilation of available toxicological data of thiosalts, other S-based compounds and salinity to various aquatic organisms

Family of toxicants	Toxicant	Test Organism	Toxicity endpoint	Test duration	Observations (mg/L)	Ref.	
Thiosalts	S ₂ O ₃ ²⁻	<i>O. mykiss</i>	IC25	96 h	> 819	[1]	
			LC50	96 h	7378	[2]	
		<i>C. dubia</i>	IC25	7 days	59	[1]	
		<i>L. minor</i>			498		
		<i>P. promelas</i> (juvenile)			665		
		<i>S. capricornutum</i>	EC50		~ 2000	[1]	
	<i>D. magna</i>	LC50	48 h	1012	[2]		
	S ₄ O ₆ ²⁻	<i>O. mykiss</i>	IC25	96 h	> 800	[1]	
					<i>C. dubia</i>		562
					<i>L. minor</i>		> 901
					<i>P. promelas</i> (juvenile)		> 891
<i>S. capricornutum</i>			EC50		~ 2000		
<i>D. magna</i>		LC50	48 h	~ 750	[2]		
Xanthates	Sodium ethyl xanthate	<i>O. mykiss</i>	LC50	N/A	13	[3]	
		<i>D. magna</i>	EC50		0.35		
		<i>L. minor</i>			< 10		
	Na-isopropyl xanthate	<i>P. subcapitata</i>			EC50		0.5
		<i>C. dubia</i>	3				
		<i>D. magna</i>	3.7				
	Na-isobutyl xanthate	<i>D. magna</i>	EC50		3.6		
		<i>L. minor</i>			< 10		
	Na-isopentyl	<i>L. minor</i>	EC50		< 10		
	K-amyl xanthate	<i>P. subcapitata</i>	EC50		0.5		
		<i>C. dubia</i>			3		
<i>D. magna</i>		3.67					
K-pentyl xanthate	<i>D. magna</i>	EC50	3				
Salinity	Sulfated salinity*	<i>D. magna</i>	EC50	48 h	E1 (untreated)	No effect	[4]
					E1 (treated)	No effect	
					E2 (untreated)	> 100**	
					E2 (treated)	32	
		<i>D. pulex</i>			E1 (untreated)	> 100	

Family of toxicants	Toxicant	Test Organism	Toxicity endpoint	Test duration	Observations (mg/L)	Ref.		
	Sulfated salinity (cont.)	<i>D. pulex</i>	EC50	48 h	E1 (treated)	> 100		
					E2 (untreated)	41		
					E2 (treated)	19		
		<i>D. magna</i>	LC50		E1 (untreated)	Not lethal		
					E1 (treated)	Not lethal		
					E2 (untreated)	> 100		
		E2 (treated)			36			
		<i>D. pulex</i>			LC50	E1 (untreated)		> 100
						E1 (treated)		> 100
	E2 (untreated)		63					
	E2 (treated)	31						
	Salinity (mainly Ca ⁺ and Na ⁺)	<i>D. magna</i>	EC50	S#2***		~ 75**		[5]
				S#3		>100		
			S#4	>100				
LC50			S#2	>100				
			S#3	>100				
			S#4	>100				

* Before and after treatment by electrocoagulation. Toxicity tests carried out using reconstituted hardwater as dilution water only, are presented.

** All concentrations for this study are presented in % (v/v).

*** Site of the dilution water used for the toxicity test.

References: [1]- Schwartz et al. (2006); [2]- Novak and Holtze; [3]- Bach et al. (2016); [4]- Foudhaili et al. (2019); [5]- Jaidi (2020)

Indirectly, the sublethal toxicity of thiosalts for all organisms was high when the pH of the solution decreased below 5, except for *L. minor*, for which no mortality was observed at pH as low as 3.1. This exception is most likely due to the higher tolerance of *L. minor* to acidic environments, whose culture media pH is of 4.8 (Schwartz et al., 2006).

2.1.4.2 Cooperative toxic effect of thiosalts with other metals

The interactions between contaminants resulting from mixed contamination in real mine water entails further complexity (Ryskie et al., 2021). For example, confirmed toxicity at a pH near neutrality could be an indicator of the presence of other contaminants, such as Cu and Se, adding to thiosalts toxicity (Schwartz et al., 2006). In contrast, $S_2O_3^{2-}$ can act as protection agent against the harmful effects of Ag on fish through its ability to form complexes with trace metals, such as Ag. The chelation of Ag by $S_2O_3^{2-}$ results in a diminished toxicity compared to Ag alone (Schwartz et al., 2006). The synergetic toxic effect of $S_2O_3^{2-}$ with several heavy metals present in a real mine effluent was studied. Copper (Cu) and $S_2O_3^{2-}$, individually, did not correlate with the toxicity to *C. dubia* (Schwartz et al., 2006). When Cu toxic units (Eq. 2.1 shows how toxic units were calculated) were added to $S_2O_3^{2-}$ toxic units, a significant correlation ($r^2 = 0.8802$, $P < 0.0001$) was observed. The same significant correlation ($r^2 = 0.9951$, $P < 0.0001$) was seen when Se toxic units were added to Cu and $S_2O_3^{2-}$ toxic units. Then, Zn toxic units were added to Cu and $S_2O_3^{2-}$ toxic units, but the relationship was lost ($r^2 = 0.2084$, $P > 0.05$).

$$\text{Toxic unit} = \frac{\text{Concentration of toxicant in solution}}{\text{IC}_{25} \text{ of toxicant}} \quad (\text{Eq. 2.1})$$

These findings suggest that concentrations of Cu and $S_2O_3^{2-}$ or Cu, $S_2O_3^{2-}$ and Se together could potentially be used to predict toxicity to *C. dubia* in real mine water. As mentioned in a recent review, the summation of toxic units may help predict aquatic toxicity (with confidence levels $\leq 89\%$) (Ryskie et al., 2021). High concentrations of Fe (due to amorphous Fe precipitates) and of dissolved organic carbon (because of its role in metal complexation) can reduce the accuracy of toxicity estimations.

2.1.4.3 Ecological thiosalts risk assessment model

In line with the missing data relative to thiosalts toxicity to aquatic life, a study by Fahd (2014) was conducted with the aim to develop a thiosalts exposure assessment model, which considers both the risk associated to thiosalts concentration and the risk associated to pH depression resulting from complete oxidation to SO_4^{2-} . The model was used to predict thiosalts toxicity in a contaminated mine effluent from the Kidd Metallurgical site. The thiosalt concentrations measured downstream of the discharge river and considered for the case study were of 25, 40 and 60 mg/L for $\text{S}_2\text{O}_3^{2-}$, $\text{S}_3\text{O}_6^{2-}$ and $\text{S}_4\text{O}_6^{2-}$ respectively. The initial pH of the river water, downstream, was of 9.2 (Fahd, 2014). The risk associated to pH depression is considered by the model by selecting the reactions occurring at the initial pH of the water. At a pH of 9.2, reactions from Eqs. 2.2 and 2.3 are dominant and are the ones governing thiosalt speciation until the pH decreases to 7. At a pH of 7, the chemical reaction presented in Eq. 2.2, i.e. $\text{S}_3\text{O}_6^{2-}$ hydrolysis, is still occurring but at a rate $\sim 7.5x$ faster than for pH 7–9.2 (Fahd, 2014). At a pH of 5.6, the reaction presented in Eq. 2.4 contributes to thiosalt speciation, along with Eq. 2.2 (until the pH drops below 4). The thiosalt speciation reactions to be considered in the model are shown in **Table 2.4**.

Table 2.4 Thiosalt speciation reactions and dominant pH ranges considered in the ecological thiosalts risk assessment model.

Equation no.	Reaction	Dominant pH range
2.2	$\text{S}_3\text{O}_6^{2-} + \text{H}_2\text{O} \rightarrow \text{S}_2\text{O}_3^{2-} + \text{SO}_4^{2-} + 2 \text{H}^+$	7.0–9.2, at reaction rate = $1.9 \times 10^{-3}/\text{h}$ 4.0–7.0, at reaction rate = $14.6 \times 10^{-3}/\text{h}$
2.3	$\text{S}_4\text{O}_6^{2-} + \text{SO}_3^{2-} \rightarrow \text{S}_2\text{O}_3^{2-} + \text{S}_3\text{O}_6^{2-}$	7.0–9.2
2.4	$2 \text{S}_2\text{O}_3^{2-} + \text{H}^+ \rightarrow \text{HSO}_3^- + \text{SO}_3^{2-} + 2 \text{S}$	2.9–5.6

The moles of H^+ released from each reaction participating in the different pH-decreasing steps were calculated. Using the reaction rates and stoichiometry of the reactions, final thiosalts concentrations and water pH were estimated. Overall, 60 h would be necessary for $\text{S}_2\text{O}_3^{2-}$ to completely be oxidized and for $\text{S}_3\text{O}_6^{2-}$ and $\text{S}_4\text{O}_6^{2-}$ concentrations to reach 18.7 and 5.9 mg/L, respectively. Finally, the model predicted a final pH of 4 and final $\text{S}_3\text{O}_6^{2-}$ and $\text{S}_4\text{O}_6^{2-}$ concentrations of 13.04 and 5.9 mg/L, respectively, after 77 h (Fahd, 2014). **Figure 2.1** summarizes the main steps involved in the prediction of the final pH and thiosalts concentrations.

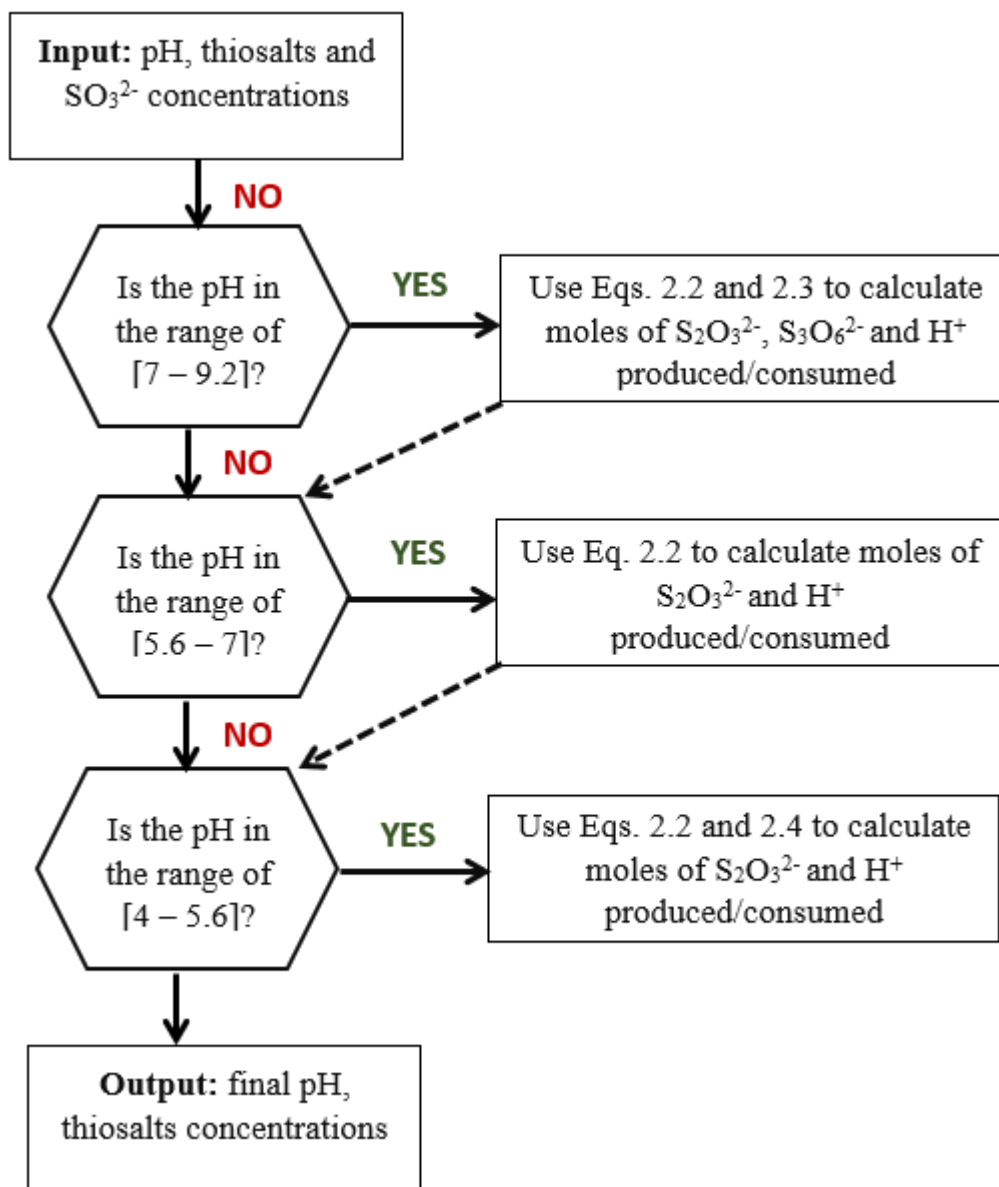


Figure 2.1 Thiosalts exposure assessment model developed by Fahd (2014).

The model assumes that: 1) the pH of the receiving water body is slightly basic, 2) the effluent is undiluted in the receiving water stream, which inherently assumes a worst-case scenario and 3) metals and all forms of catalysts including bacteria are absent (Fahd, 2014). Two main problems arise from assumption 3. Information presented in Section 2.3.1.2 explains how thiosalts interaction with heavy metals can alter the toxicity of thiosalts, decreasing the reliability of the

predictions. In addition, bacteria and UV rays are well known catalysts that actively participate in thiosalts speciation and oxidation reactions (Miranda-Trevino et al., 2013; Range and Hawboldt, 2019) and are nearly always present in nature. Assuming the complete absence of naturally occurring catalysts also diminishes the reliability of the predictions.

2.1.4.4 Xanthates' toxicity: A case study

Xanthates are among the most widely used collectors in the flotation process, a popular ore-processing technique in the mining industry used to separate base metals-bearing minerals from gangue minerals present in the ore. Xanthates play the role of “collectors”, which are organic molecules that contain a polar group, binding the metal-bearing mineral, and a non-polar group allowing the collector to attach to the air bubbles and be transported to the foam phase, at the surface (Bach et al., 2016). The effective concentration of xanthates during the flotation process depends on pulp temperature. As a result, xanthates dosage must be adjusted in accordance with seasonal temperatures and the residual xanthates concentrations in the flotation tailings vary. In general, 1 t of ore requires 300–500 g of xanthates for efficient metal separation (Sun and Forsling, 1997).

An investigation, on effluents from four different mining operations experiencing sporadic toxicity, was carried out to determine the cause of toxicity (Novak and Holtze, 2010). All the effluents contained similar contaminants and the mortality trends were comparable (**Table 2.5**).

Table 2.5 Characteristics of effluents in the investigation of sporadic aquatic toxicity by Novak and Holtze (2010).

	#1	#2	#3	#4
Organism	Rainbow trout and <i>D. magna</i>	Rainbow trout	Rainbow trout	Rainbow trout
Time to 100% mortality (h)	72–96	72–96	24	72–96
Annual period of mortality	May + August to October	Summer	May to October	March to April
Total thiosalts (mostly $S_2O_3^{2-}$) (mg/L)	8–140	300–600	128–1700	< 10–1000
Xanthates (mg/L)	< 5–13	0.1–2	Unknown, but used	< 5–24

The study reported an absence of correlation between total thiosalts and mortality, consistent with other studies (Schwartz et al., 2006; Fahd, 2014). Other samples were tested with the same thiosalt concentrations, but the pH decrease resulting from thiosalts oxidation to SO_4^{2-} was not enough to cause mortality. Subsequently, one of the four effluents ([total thiosalts] = 400 mg/L, rainbow trout mortality after 96 h = 100%) was treated using a variety of methods (i.e. anion exchange, boiling, adjustment of effluent pH to 3, chlorination, Fenton-like). The mortality to rainbow trout after 96 h exposure was of 0% after all treatments, even though thiosalts were still present in the effluent at concentrations varying from < 10 to 318 mg/L.

The same effluent was treated by elution on a C18 column, which can remove non-polar organic molecules. In other words, the result of this treatment is the absence of an effect on thiosalts and a retainment of organic molecules on the resin of the column. Results showed that despite the presence of thiosalts in the treated effluent, it was non-toxic, indicating that the toxicant was attached to the resin. Finally, a methanol extraction from the C18 resin and analysis of the concentrate by gas chromatography coupled to mass spectrometry revealed the presence of xanthates and their role in the toxicity for the four effluents (Novak and Holtze, 2010).

The pH decrease of effluents could cause other contaminants to be even more toxic. In acidic conditions, xanthates are highly toxic to aquatic organisms because they degrade very rapidly to ethanol, carbon disulfide (CS_2) and caustic soda (Novak and Holtze, 2010; Bach et al., 2016). **Table 2.3** shows the toxicity of various xanthates to different freshwater species (Bach et al., 2016). The low EC50 and LC50 values for all xanthates, presented therein, mirror their highly toxic nature for aquatic species, especially when compared to the high EC50 and LC50 values of thiosalts.

2.1.4.5 Sulfated salinity and other sources of salinity

The *D. magna* is widely used in research as a representative indicator of acute toxicity because of its higher sensitivity. However, *D. pulex* is abundant and commonly found in Canadian lakes and water streams (Ryskie et al., 2021) so assessing the toxicity of mine effluents on *D. pulex* is of primordial importance for Canadian mines. Recently, a comparative study of the sensitivity of *D. magna* and *D. pulex* for neutral mine water highly contaminated with sulfated salinity, before and after treatment by electrocoagulation, was conducted (Foudhaili et al., 2019). Acute lethality and immobilization tests were carried out on two real mine effluents (E1 and E2, $[\text{SO}_4^{2-}] = 2870$

and 1280 mg/L, respectively), using five dilution waters (reconstituted hardwater synthesized in laboratory and four surface waters from mine sites of different lithologies). In summary, the results of all the tests demonstrated a higher toxicity to *D. pulex* as compared to *D. magna* (**Table 2.3**).

The vulnerability of natural watercourses to the salinity of mine water was studied by Jaidi (2020). Part of the investigation aimed to assess the toxicity of mixtures of mine water with three natural waters originating from different geological contexts, in varying proportions (0–100%), on *D. magna*. All mixtures were submitted to short duration acute toxicity tests, and no mortality was observed for all dilutions. Then, salinity was added to the mine water as NaCl and CaCl₂•2H₂O at concentrations of 1.58 and 4.1 g/L, respectively. When the mine water was diluted with the natural water sampled at site #2, 25% of the *D. magna* population was immobilized at a concentration of 56% (v/v) and 85% was immobilized when the mine water was not diluted. Yet, when the natural dilution water from site #3 was used, the immobility of the *D. magna* population did not exceed 15% (Jaidi, 2020). Test results were different depending on the natural dilution water used, indicating that the vulnerability of natural waters to the salinity of mine water in terms of toxicity towards *D. magna* is dependent of the initial composition of the natural water. The EC₅₀ and LC₅₀ values obtained for *D. magna* in the scope of the study are presented in **Table 2.3**.

2.2 Treatment

2.2.1 Current thiosalts treatment methods

The most employed method for preventing a pH decrease of the receiving water body caused by the latent acidity generated, when thiosalts oxidation is complete, is the addition of neutralizing agents, such as lime or carbonates (Kuyucak, 2014). This increases the buffering capacity of the effluent and hinders the pH from decreasing, temporarily. Lime neutralization is the preferred approach because of its simplicity and relatively low cost (Kuyucak, 2014). The main issues with this approach are related to the complexity of quantifying the appropriate dosage since there is no correlation between the total thiosalts concentration and the amount of generated delayed acidity. As an example, three mine sites, which reported total thiosalts concentrations of 440, 500 and 1900 mg/L, all observed pH depressions of approximately 5 units (Miranda-Trevino et al., 2013). Furthermore, the large volumes of sludge produced, high water content and multiple

contaminant content as well as their long-term chemical stability also constitute limitations to treatment by chemical neutralization (Wahlstrom et al., 2017).

2.2.2 Water treatment in northern countries

A report aimed at developing a water treatment concept in northern countries regrouped operating mines from Finland, Sweden and Norway (Wahlström et al., 2017). The quantity and quality of waters to be treated by each mine were reported along with the current treatment operations in each country. **Table 2.6** presents the water treatment strategies at Swedish mines for which initial and final effluent qualities were documented. It is worthy of note that insufficient data was available to calculate removal efficiencies at Finnish mines and that mine effluents at Norwegian mines are discharged in the environment without treatment.

Although the water treatment technologies implemented at Swedish metal mines (**Table 2.6**) are suitable for current needs, most technologies are not applicable in the case of CECs such as thiosalts and As in large concentrations. For example, the As concentrations to be treated at the Garbenberg, Kankberg, Maurliden and Renström mines are of 40, 15, 40 and 20 $\mu\text{g/L}$, respectively. The worldwide depletion in available native and high-grade deposits requires an accentuated exploitation of low-grade and refractory sulfidic ores during which aggressive extraction processes are used for Au recovery. These processes inherently generate large quantities of thiosalts in the process waters, with F/T further amplifying the problem (Schudel et al, 2019). Massive leaching of As can also result, because Au is most often lodged within As-bearing minerals (Clary et al., 2018). A record concentration of 137 g/L As in mine water has already been reported (Majzlan et al., 2014). The current water treatment practices of metal mines in Sweden would be insufficient to meet effluent discharge criteria if faced with such high concentrations of CECs and the instability of formed sludges would be a cause for concern.

Several water treatment technologies are limited in cold climate owing, in part, to slowed reaction kinetics and inhibited biological activity (i.e. ion exchange and certain biological methods; Wahlström et al., 2017). Yet, mining activities in the climatic conditions of northern regions require efficient water treatment technologies adapted to huge water flows and very cold water. In this context, further research is imperative. Electrochemical methods have been reported as efficient for contaminants removal, even in cold water (Wahlström et al., 2017).

Electrochemical technologies are an interesting avenue to exploit to develop treatment technologies suitable for cold water, provide a viable year-round solution and to facilitate the removal of CECs such as thiosalts (oxidation to SO_4^{2-}) and As (oxidation of more mobile and more toxic As(III) to As(V)) prior to liming (Miranda-Trevino et al., 2013; Wang et al., 2014).

Table 2.6 Current water treatment strategies at Swedish mines and their efficiencies (adapted from Wahlström et al., 2017).

Mine	Water treatment strategy	Removal efficiency
Garpenberg	Fenton process combined with liming for thiosalts oxidation and metal precipitation, Moving Bed Biofilm Reactor (MBBR) technology for nitrogen compounds' removal	80% As 83% Cd 84% Cu 92% Pb 89% Zn 98.5% thiosalts 87% nitrogen
Kankberg	pH raised to 9.5 with slaked lime, metal precipitation as sludge	As and Pb > 90% Cd, Cu and Zn > 95%
Kiirunavaara	Clarification pond with addition of H_2SO_4 for pH adjustment and reduction of ammonia	Soluble sulfur reduced to [24–5.4 mg/L]
Maurliden	pH is raised to 10 with slaked lime in treatment plant, metal precipitation in lamella thickeners and centrifugal thickeners, flocculants are added before the thickeners	Cd and Pb > 99.5% As, Cu and Zn > 99.9%
Renström	pH is raised to 9.5 with slaked lime, metal precipitation in lamella thickeners. Flocculant is added to the water before the thickener and the water is sent to sand filters.	Cd > 87% As > 92% Cu > 90% Zn > 84%

2.2.3 Advanced oxidation processes

Previous findings have demonstrated that advanced oxidation processes (AOPs) are a promising alternative (Miranda-Trevino et al., 2013; Kuyucak, 2014). The AOPs are, by definition, processes in which highly reactive oxidants are used to react, non-selectively, with oxidizable contaminants present in the solution, at ambient temperature (Nair et al., 2021). This section provides an overview of the advancements of AOPs developments in research concerning the treatment of AMD, with emphasis on thiosalts. **Table 2.7** summarizes the experimental conditions, reported efficiencies, advantages and disadvantages of the different AOPs presented in this section, for contaminants typically found in AMD.

2.2.3.1 Oxidation by hydrogen peroxide

The efficiency of hydrogen peroxide (H_2O_2) for thiosalts oxidation in AMD (pH = 3.08) was evaluated, before and after the lime neutralization process (Kuyucak, 2014). The AMD contained 172 mg/L of thiosalts (as $\text{S}_2\text{O}_3^{2-}$, $\text{S}_3\text{O}_6^{2-}$ and $\text{S}_4\text{O}_6^{2-}$) as well as other species, which were expected to consume additional H_2O_2 , such as Fe^{2+} (1 mole of H_2O_2 per 2 moles of Fe) and Mn^{2+} (1 mole of H_2O_2 per 1 mole of Mn). The tested $\text{H}_2\text{O}_2:\text{S}_2\text{O}_3^{2-}$ molar ratios selected were 0.5, 1 and 1.5x the stoichiometric requirement for the theoretical complete removal of $\text{S}_2\text{O}_3^{2-}$. **Table 2.7** summarizes the results obtained for all $\text{H}_2\text{O}_2:\text{S}_2\text{O}_3^{2-}$ molar ratios, in acid and lime-neutralized water. Results showed that H_2O_2 could effectively remove $\text{S}_2\text{O}_3^{2-}$ from acid mine water, but operating costs could be an obstacle for mining operations and long treatment times were required, especially in cold water (Kuyucak, 2014).

The freeze concentration effect, known to accelerate the rate of several reactions, is described as the following: When the freezing process begins and crystals of ice start growing, solutes are expelled from the ice phase resulting in a difference of electric potential between the expanding ice and the solution. Ions accumulate at the ice-solution interface due to the electrostatic force generated. The created potential is then neutralized by an exchange of OH^- and H_3O^+ between the ice and the solution causing the pH to vary (Takenaka et al., 1996). The same study, which evaluated the freeze concentration effect on the oxidation of nitrite (NO_2^-) to nitrate (NO_3^-), found that the accelerated reaction rates are induced by the confinement of the reactants in the boundaries of ice crystals.

In a subsequent study, Sato et al. (2002) evaluated the impact of the freeze concentration effect on thiosalts oxidation using a $\text{S}_2\text{O}_3^{2-}/\text{H}_2\text{O}_2$ solution. It was found that the rate of the freezing reaction was 20x faster than that of the reaction at room temperature. To do so, a $100 \mu\text{mol}/\text{dm}^3$ solution of $\text{Na}_2\text{S}_2\text{O}_3$ was mixed with a $2.00 \text{ mmol}/\text{dm}^3$ solution of H_2O_2 . The mixture was frozen at -15°C , then thawed in a hot water bath. Results showed that most of the $\text{S}_2\text{O}_3^{2-}$ were consumed after 60 min of freezing according to Eq. 2.5 (Sato et al., 2002). Although all other intermediate S species (sulfides, thiosalts, sulfite) were completely oxidized, the majority of $\text{S}_4\text{O}_6^{2-}$ were not transformed into SO_4^{2-} , even when the solution was refrozen. These findings suggest that $\text{S}_4\text{O}_6^{2-}$ could be preserved in ice. As crystals begin to grow and thiosalts are gradually expelled, the solution becomes negatively charged. Knowing that H_3O^+ will be exchanged between the ice and

Table 2.7 Summary of AOPs for the treatment of mine-impacted water.

Treatment process	Contaminant and concentration	Experimental conditions	Reported efficiencies (%)	Advantages	Disadvantages	Ref.							
Oxidation by H ₂ O ₂	S ₂ O ₃ ²⁻ , 172 mg/L	Real mine water, laboratory scale, pH 3	<i>r</i> *	T°C	Simple operations, treatment kinetics can be accelerated by freezing	Efficiency influenced by T°C, long reaction time, instability/degradation of H ₂ O ₂ over time	[1, 2]						
			0.5	20				69					
			1	20				84					
			1	4				85					
		Real mine water, laboratory scale, pH 10	2	20				98					
			0.5	20				44					
			1	20				72					
			1	4				71					
2	20	97											
Fenton	S ₂ O ₃ ²⁻ , unknown concentration	Real mine water, field scale	98.5	Excellent efficiency, fast reaction (14 orders of magnitude faster than H ₂ O ₂ alone), already applied at industrial scale	Possibility of residual H ₂ O ₂ , limited chain reaction lifetime, large amounts of sludge	[3]							
Fe(VI)	As, 100 mg/L	Synthetic mine water, laboratory scale, [Fe(VI)] = 0.5 g/L, pH = 6.6	> 99				Good efficiency, high reaction rate constant with thiosalts, removal of metals/metalloids by oxidation/sorption/ precipitation	Fe(VI) must be synthesized on site, addition of salinity, need for final pH adjustment, mixed contamination requires greater doses, less efficient N-NH ₃ removal if SCN ⁻ is present	[4]				
				N-NH ₃ (mg/L)	SCN ⁻ (mg/L)	CN ⁻ (mg/L)					N-NH ₃	SCN ⁻	CN ⁻
			S1	45	-	-				S1	99	-	-
			S2	-	118	-				S2	-	99	-
			S3	37	116	-				S3	30	99	-
			E1	62	470	19.7				E1	-	97	99
E2	22	-	1.7	E2	99	-	59						
O ₃ microbubbles	N-NH ₃ , ~ 50 mg/L	Synthetic mine water, pilot- scale	pH 7		8.4	Excellent efficiency, fast reaction, limitation of residual salinity	Continuous pH adjustment required, possible interference if presence of O ₃ -consuming compounds, additional polishing step required for colour removal	[6]					
			pH 9		92.6								
			pH 11		86								
			pH 11**		74								
	N-NH ₃ , from 22.9 to 43.4 mg/L	Real mine water, pilot-scale, batch mode for effluents R, G, C and H, continuous flow at 1.11 L/min for effluent M	R		~ 30***								
			G		~ 40								
			C		~ 85								
			H		~ 80								
M		99.3											

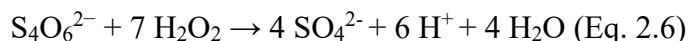
* $r = \text{H}_2\text{O}_2 : \text{S}_2\text{O}_3^{2-}$ molar ratio

**The pH was non-maintained throughout the treatment

** Approximate efficiencies (~) were retrieved from graphs

References: [1]-Kuyucak (2014); [2]- Vongporm (2008); [3]- Wahlstrom et al. (2017); [4]- Prucek et al. (2013); [5]- Gonzalez-Merchan et al. (2018); [6]- Ryskie et al. (2020)

the solution during freezing to neutralize the electric potential, an acidic pH is induced (Takenaka et al., 1996). Since $S_4O_6^{2-}$ are more stable in acidic conditions (Miranda-Trevino et al., 2013), their oxidation in frozen solutions, as shown in Eq. 2.6, is not favored and requires more H_2O_2 (Sato et al., 2002).

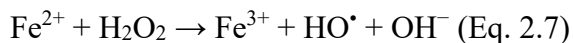


Sato et al. (2002) also evaluated the impact of the freeze concentration effect for thiosalts oxidation in alkaline conditions. They observed that at an initial pH of 10, no $S_3O_6^{2-}$ or $S_4O_6^{2-}$ were formed and all S species were oxidized to SO_4^{2-} . This observation could be explained by the acidity being buffered following H_3O^+ exchange into the solution, preventing a decrease in pH and promoting the oxidation of $S_3O_6^{2-}$ and $S_4O_6^{2-}$.

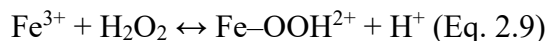
The freeze concentration effect on thiosalts was also studied by Vongporm (2008). They evaluated the effect of F/T cycles on thiosalts speciation at acidic (2, 4), neutral (7) and basic (9) pH, using a fast-freeze process and a normal-freeze process. Results demonstrated that the normal-freeze process was more effective at oxidizing thiosalts into SO_4^{2-} , and that pH 9 was more effective than all other pH values tested. The fast-freeze process enhanced the stability of thiosalts. These findings agree with those of Sato et al. (2002), proving that thiosalts oxidation by the freeze concentration effect is more efficient in alkaline conditions.

2.2.3.2 Fenton

In the Fenton reaction, the H_2O_2 , activated by an Fe(II) catalyst, generates hydroxyl radicals (HO^\bullet) which are highly unstable. The radicals are then available to react with any potentially oxidizable contaminant in a non-selective manner, particularly in mixed contamination, as shown in Eqs. 2.7 and 2.8 (Neyens et al., 2003).



Ferrous iron (Fe^{2+}) is then regenerated by the reduction of Fe^{3+} with H_2O_2 , as indicated by Eq. 2.9 (Neyens et al., 2003).

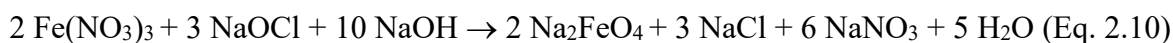


As presented in **Table 2.6** of Section 2.2.2, Fenton was applied at industrial scale, combined with liming for thiosalts oxidation and metal precipitation at the Garpenberg mine in Sweden (property of Boliden Mineral AB), resulting in almost complete removal of thiosalts (98.5%), although their initial concentration is not reported. Prior to treatment, the pH and alkalinity of tailings' slurry is decreased with the addition of H_2SO_4 , which decreases the amount of thiosalts generated and costs associated to Fenton reagents (Forsberg, 2011; Wahlström et al., 2017).

The Fenton process has demonstrated impressive efficiencies for thiosalts removal even for industrial scale applications. The difficulties associated with chemical Fenton treatment include the formation of high amounts of Fe-hydroxide sludge in the neutralization step and high consumption of Fe^{2+} by HO^\bullet at a rate greater than that of its regeneration by H_2O_2 , reducing the lifespan of the chain reaction (De Luna et al., 2012). The limitations of treatment by conventional Fenton also include its narrow optimal working pH range [2–4] as well as the risks associated to handling, transportation, and storage of H_2O_2 (Olvera-Vargas et al., 2021; Nair et al., 2021). In addition, the Fenton reaction can result in residual H_2O_2 in the treated water if its initial concentration is not optimal (Zhang et al., 2005).

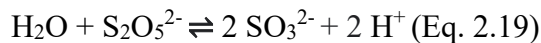
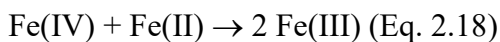
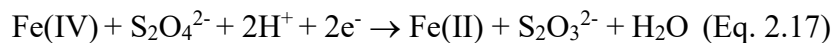
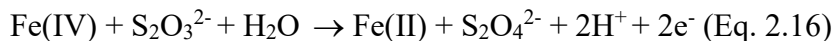
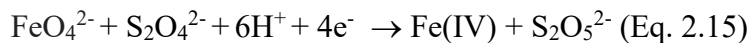
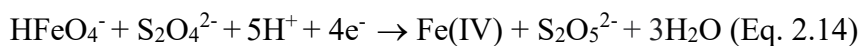
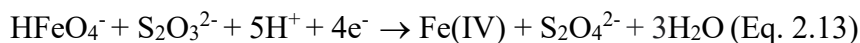
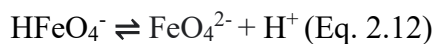
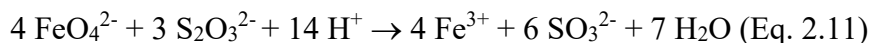
2.2.3.3 Ferrates

Ferrates(VI) can be used for water treatment in solid form or in liquid form. Liquid Fe(VI) are synthesized from Fe^{3+} under very alkaline conditions in the presence of a strong oxidant according to Eq. 2.10 (Gonzalez-Merchan et al., 2016).



The Fe(VI)-based treatment can be explained by redox reactions (Gonzalez-Merchan et al., 2016a). Fe(VI) are high oxidation state (+6) of Fe, making them highly unstable and readily reactive with oxidizable contaminants. When they are present at the same time, Fe(VI) react by fixing the electrons of these contaminants to find their more stable forms as Fe²⁺ or Fe³⁺. Simultaneously, oxidizable contaminants are oxidized and the Fe is reduced (Read et al., 2001; Gonzalez-Merchan et al., 2016).

In a series of three studies evaluating the mechanisms and kinetics of the oxidation of S compounds by Fe(VI), the high reaction rate constant of Fe(VI) with thiosalts (Eq. 2.11) was reported as one of the advantages of the technology (Read et al., 2001; Read et al., 2005a, 2005b). Various S₂O₃²⁻:Fe(VI) molar ratios (1:1 to 10:1 and 3:4) were tested, in alkaline conditions, to determine the rate constant of the reaction between S₂O₃²⁻ and Fe(VI) (Eq. 11). Results showed that the average rate constant for all tested S₂O₃²⁻:Fe(VI) molar ratios was of 8 x 10¹¹ M⁻²s⁻¹ (Read et al., 2001). The mechanism of S₂O₃²⁻ oxidation by Fe(VI) proposed by Read et al. (2001) is shown in Eqs. 2.12 to 2.19, with Eq. 2.13 being the rate-determining step (lowest rate constant).



Once the Fe is reduced, the Fe-oxyhydroxide precipitates (formed at $\text{pH} > 3.5$) can also remove other co-contaminants in solution by acting as a coagulant-flocculant (Prucek et al., 2013). A study focusing on arsenite and arsenate removal from synthetic effluents found that Fe(VI) have the ability to trap contaminants *in situ* in the tetrahedral sites of the crystal network of Fe-oxyhydroxides (Prucek et al., 2013). Using a Fe(VI) concentration of 0.5 g/L and an initial As concentration of 100 mg/L at pH 6.6, the authors reported achieving a final As concentration below the detection limit of the device used for analysis, indicating complete removal of the contaminant.

Fe(VI) have also shown potential for thiocyanates (SCN^- , generated as a result of the cyanidation process employed for the extraction of refractory gold in sulfidic ores) oxidation, in three synthetic and two real gold mine effluents, containing or in the absence of ammonia nitrogen (N-NH_3) and cyanide (CN^-), using various Fe(VI) doses (Gonzalez-Merchan et al., 2016). Efficient SCN^- oxidation to cyanates (OCN^-) and SO_4^{2-} was observed, regardless of whether N-NH_3 was present or absent in the solution (see S3 and E1; **Table 2.7**). Required Fe(VI) doses for efficient SCN^- removal increased by roughly three times when initial concentrations were low. The tendencies for N-NH_3 oxidation were different than that of SCN^- oxidation. When SCN^- were absent, N-NH_3 was efficiently removed, but when SCN^- were present, either the removal of N-NH_3 was less efficient (**Table 2.7**) or its concentration even increased ($\leq 50\%$) and the 1 h reaction time was insufficient, despite increased Fe(VI) doses. The oxidation of CN^- was efficient when SCN^- was present, but the efficiency decreased by 40% when N-NH_3 was present (see E1 and E2; **Table 2.7**). These findings allowed the authors to suggest that when treated with Fe(VI), SCN^- are completely oxidized before N-NH_3 degradation. Mixed contamination appears to interfere with treatment, reducing removal efficiencies and possibly resulting in longer treatment times and/or increased Fe(VI) doses. Moreover, the effective Fe(VI) dosage must be adjusted according to contaminant concentrations and extreme contamination could result in higher salinity of the effluent post-treatment (Gonzalez-Merchan et al., 2016).

2.2.3.4 Ozone microbubbles

Recently, the removal of N-NH_3 from synthetic and five real mine effluents (R, G, C, H and M) using O_3 microbubbles, at pilot-scale, was investigated (Ryskie et al., 2020). Initially, the optimal working pH was determined on synthetic effluents. At pH values of 9 and 11, N-NH_3 removal efficiencies of 92.6% and 86%, respectively, were obtained, whereas only 8.4% was

removed at pH 7. When the initial pH was set at 11, and not maintained throughout the treatment process, only 74% of N-NH₃ was removed (**Table 2.7**; Ryskie et al., 2020).

Results of treatability testing (1.11 L/min) on real effluents showed that the highest N-NH₃ removal efficiency (99.3%; **Table 2.7**) was obtained in effluent M, after 570 min of treatment, but the process efficiency was dependent of the initial quality of the effluent. In agreement with previous findings (Gonzalez-Merchan et al., 2016), the authors also found that when present, cyanide compounds (i.e. CN⁻, SCN⁻, OCN⁻) were completely oxidized prior to N-NH₃ treatment. It was suggested that the absence of cyanide compounds in effluent M could explain why the highest removal efficiency was obtained for this effluent, because less O₃-consuming compounds were present to compete with N-NH₃ oxidation. In this sense, mixed contamination could interfere with treatment and result in longer treatment times. Additionally, a colour change from clear to turquoise was observed in one of the real effluents, owing to dissolved Cu requiring precipitation, requiring an additional polishing step, after treatment.

2.2.4 Electrochemical advanced oxidation processes

Electrochemical advanced oxidation processes (EAOPs) seem promising for mine water treatment due to their versatility and environmental compatibility. EAOPs are considered environmentally friendly because oxidants are generated via electron production by an electrical current. Inherently, EAOPs avoid the use and handling of hazardous materials employed in non-electrochemical AOPs and nearly generate no secondary waste that require post-treatment management (Garcia-Rodriguez et al., 2020; Oturan, 2021). The following section will provide an overview of advancements in research concerning EAOPs for water treatment.

2.2.4.1 Electrochemical and bio-electrochemical ion exchange

In a study comparing the efficiency of a two-chamber flow-through bio-electrochemical and abiotic electrochemical ion exchange system, simultaneous removal of Cu and S₄O₆²⁻ in highly acidic (pH = 2) synthetic mine water was achieved (Sulonen et al., 2018). The initial Cu and S₄O₆²⁻ concentrations were of 1 and 2 g/L, respectively, in both systems. Results showed that the degradation of S₄O₆²⁻ for the bio-electrochemical treatment proceeds via the generation of S and S₂O₃²⁻, which are formed as intermediates during the biological treatment of thiosalts. On the other hand, S₄O₆²⁻ were directly transformed to SO₄²⁻ with the abiotic electrochemical system.

After 9 days of treatment, both systems allowed for complete removal of Cu (> 99%). Final Cu and $\text{S}_4\text{O}_6^{2-}$ concentrations reached < 0.3 mg/L and < 0.5 g/L, respectively. These findings are particularly interesting for the mining industry considering that contaminated mine water originating from sulfide mineral processing often contains a variety of heavy metals and thiosalts.

2.2.4.2 Electro-Fenton

Electro-Fenton (EF) is classified as one of the most powerful EAOPs (Oturán, 2021). During EF treatment, a method derived from the chemical Fenton reaction, H_2O_2 is generated *in-situ*, in the electrochemical cell. Its formation involves a $2e^-$ reduction of O_2 at the cathode. To induce the Fenton reaction, Fe^{2+} must be added, in catalytic amount, but the use of sacrificial Fe-based anodes can replace the use of Fe-based salts. The disadvantages of Fe-based anodes include the production of sludge, which is difficult to manage afterwards. Then, the Fe^{2+} is constantly regenerated at the cathode via the reduction of Fe^{3+} (García-Rodríguez et al., 2020; Nair et al., 2021).

The efficiency of EF has been widely studied for the treatment of organic compounds and showed significant contaminant removal. As an example, a study evaluated the efficiency of EF in continuous mode for decontamination of wastewater containing synthetic dyes namely Lissamine Green B, Methyl Orange, Reactive Black 5 and Fuchsin Acid. Removal efficiencies for all dyes varied between 60–80% after 21 h of treatment. In a test aimed at evaluating the efficiency of EF process for decoloration of a mixture of all four dyes, a 43% efficiency was obtained after 21 h of residence time (Rosales et al., 2009). The mineralization of picloram, a common herbicide, using EF process was also studied. Its removal was followed by total organic carbon (TOC) analysis, 95% of which was removed after 8 h of reaction time (Özcan et al., 2008). The EF oxidation of a widely employed colorant by the food and drugs industries, namely, Sunset Yellow FCF, was also investigated using a reticulated vitreous carbon cathode and platinum gauze anode. It was found that 2 h of treatment was sufficient for almost complete degradation (97%) of the dye (Ghoneim et al., 2011).

Electro-Fenton is an interesting AMD treatment technology because it provides solutions to the limitations of the conventional Fenton process including a lower quantity of sludge produced and a more efficient propagation of the chain reaction due to constant regeneration of Fe^{2+} and *in-*

situ generation of H₂O₂ (Brillas et al., 2009; De Luna et al., 2012). This way, the risks associated to handling, transportation, and storage of H₂O₂ are eliminated (Nair et al. 2021).

2.2.4.2.1 *Electro-Fenton for the treatment of inorganic contaminants*

Very few studies have focused on EF treatment of water contaminated with inorganic, oxidizable micropollutants such as the ones present in mine-impacted water. A study investigated the oxidation of mobile and highly toxic As(III) to As(V), at an initial concentration of 1 mg/L, using a biologically modified EF process (bio-EF) under neutral conditions. The electrodes consisted of a carbon felt anode and carbon felt covered with γ -FeOOH as cathode for microbial iron source (Wang et al., 2014). The EF process was operated in a dual-chamber microbial fuel cell (MFC) (separated by a cation exchange membrane) without external energy supply. In the bio-EF process, electrons are released from biological reactions in the anodic compartment and are transported to the cathodic compartment via an external load circuit. Then, like abiotic EF, H₂O₂ and Fe²⁺ are continuously regenerated at the cathode. Results showed that, within 12 h of treatment, As(III) depletion efficiency reached > 85% at a γ -FeOOH concentration of 2 g/L whereas 96% of As(III) was removed within 72 h of treatment (Wang et al., 2014). Although bio-EF seems promising for the oxidation of As(III) to As(V), the As concentrations treated (1 mg/L) in the scope of this work are considerably lower than those that can be encountered in mine water (Majzlan et al., 2014; Clary et al., 2018). Furthermore, treatment times are long and would result in the need for excessively large reactors in a mining context considering that the volume of contaminated water on a mine site can reach several thousand ML/d (Dieter et al., 2018).

Recently, the simultaneous removal of Fe²⁺ and Mn²⁺ in AMD by EF was studied (Chai et al., 2020). This study is particularly interesting because the removal of Mn²⁺ is especially problematic in AMD with high concentrations of Fe, owing to the inhibition of Mn²⁺ at Fe/Mn molar ratios > 4/1 (Neculita and Rosa, 2019; Skousen et al., 2017). The study aimed to optimize the main parameters affecting the efficiency of the process, namely, current intensity (200 mA), inter-electrode distance (1.5 cm), initial pH of the water to be treated (4.0) and aeration rate (100 mL/min). These parameters were optimized on synthetic mine effluents, using a ruthenium oxide-covered titanium anode (RuO₂/Ti) anode and an activated carbon felt cathode, and were subsequently applied to treat real mine water. The initial concentrations of Fe²⁺ and Mn²⁺ were 200 and 20 mg/L, respectively, and their removal efficiencies reached 96.5% and 86.5%,

respectively. Then, the study aimed to evaluate the cost of EF process for the simultaneous removal of both contaminants. The authors were able to demonstrate that EF was cheaper when compared to liming and electrocoagulation (\$0.56/kg for EF vs. \$2.67/kg and \$2.14/kg for liming and electrocoagulation, respectively) (Chai et al., 2020).

2.2.4.2.2 *EF configurations and electrode material*

In EF, electrode material influences the efficiency of the process, via, mainly, the *in-situ* generation rate of H_2O_2 (Oturán, 2021). Electrode material is also a key parameter that governs the degradation mechanisms (García-Rodríguez et al., 2020). Depending on the type of electrode material, the EF process has 2 different configurations: (1) Fe^{2+} is added from outside the cell, H_2O_2 is added to the reactor from outside the cell or electrochemically generated and inert electrodes with high catalytic activity are used as anode material; (2) only H_2O_2 is added from outside and Fe^{2+} is provided from sacrificial cast iron anodes (Nidheesh et Gandhimathi, 2012).

In configuration (1), the most effective anode materials for contaminant removal are those with high O_2 evolution overpotentials for supplementary HO^\bullet generation (Drogué et al., 2007). These anodes have the capacity to produce surface-absorbed HO^\bullet that contribute to the oxidation of contaminants (García-Rodríguez et al., 2020; Nair et al., 2021). Boron-doped diamond (BDD) electrodes have been classified as the most effective anodes due to their exceptional properties including their high O_2 evolution overpotential, wide potential window, low background current, chemical inertness, long term stability and durability in aggressive media as well as weak adsorption on their surface (García-Rodríguez et al., 2020; Oturán, 2021). Platinum (Pt) anodes are also commonly employed, but studies have demonstrated that $\text{Pt}(\text{HO}^\bullet)$ are produced in much lower quantities than $\text{BDD}(\text{HO}^\bullet)$, resulting in lower degradation rates (Brillas et al., 2009). Contrary to active anodes, such as Pt or dimensionally stable anodes (DSA), where HO^\bullet are chemically absorbed, $\text{BDD}(\text{HO}^\bullet)$ are physically absorbed on a thin layer close to the electrode surface and are more easily available to oxidize contaminants. The BDD film can be deposited on different substrates, such as silicon (Si), titanium (Ti), niobium (Nb) and tungsten (W) (Oturán, 2021). A study, which compared the efficiency of Si/BDD and Nb/BDD, found that Si/BDD electrodes yielded better results, but the Nb/BDD electrode resulted in lower energy consumption due to its better conductivity (Brito et al., 2018). Another study evaluated the influence of the diamond/graphite ratio within the BDD film, which played a key role in the electrochemical

properties of the electrode, according to the results. A lower diamond/graphite ratio resulted in higher conversion of Rhodamine B dye (intermediates were adsorbed on the graphite) and a higher diamond/graphite ratio resulted in greater mineralization of the solution (Medeiros et al., 2014). Greater diamond content in the BDD film could result in greater contaminant removal.

In this version of configuration (1), the H_2O_2 can either be added externally or generated inside the cell (Nidheesh et Gandhimathi, 2012). When the H_2O_2 is added externally, the BDD electrode surface acts as the electrocatalyst, meaning it participates in the electrochemical reaction through the electrolysis of H_2O . The result of this version of configuration (1) is the oxidation of contaminants through an amalgam of the classical Fenton reaction and electrooxidation, specifically anodic oxidation at the BDD electrode surface. When the H_2O_2 is generated inside the cell, the result is a mix of EF (electrochemical generation of H_2O_2) and electrooxidation (Drogui et al., 2007).

In configuration (1), anodes with low O_2 evolution overpotentials can also be used. Among these, DSA electrodes are a good example, especially when only partial decontamination of the water is required in the case of EF as part of a sequential treatment process (Garcia-Rodriguez et al., 2020). In this version of configuration (1), EF is the main mechanism through which $\cdot\text{OH}$ are produced because anodes with low O_2 evolution overpotentials do not promote the formation of surface-adsorbed $\cdot\text{OH}$. These types of anodes can oxidize Cl^- into more reactive chlorine species, which contribute to contaminant oxidation. The formation of sulfate radicals ($\text{SO}_4^{\cdot-}$), which are powerful oxidants, is also possible (Oturán, 2021).

In configuration (2), H_2O_2 is added from outside and Fe^{2+} is provided from sacrificial cast iron anodes (Nidheesh et Gandhimathi, 2012). In recent years, many publications have demonstrated the potential of natural Fe minerals including hematite, goethite, magnetite and chalcopyrite to catalyse H_2O_2 decomposition to $\cdot\text{OH}$ (Meijide et al., 2021). According to the results, certain transition metals such as Cu, Cr, Co and Mn could favor H_2O_2 decomposition into $\cdot\text{OH}$ through Fenton-like pathways, although the classical-Fenton reaction is based on the use of Fe^{2+} as the catalyst. The common consensus was that the use of natural Fe-based minerals as anode material are a promising alternative catalyst due to high contaminant removal efficiencies attained, negligible metal leaching and high metal stability within the network structure when transition metals are present (Meijide et al., 2021).

Cathode material also plays an important role in EAOPs. Effective cathode materials have a high overvoltage for H^+ evolution reaction, low capacity for H_2O_2 degradation, high stability and high conductivity (Nair et al., 2021). Some cathode materials produce H_2O_2 via a reaction involving a $2e^-$ reduction of O_2 . These cathodes are the best option for Fenton-based reactions, such as EF (Garcia-Rodriguez et al., 2020). In this sense, carbonaceous cathode materials are particularly interesting owing to their high H_2O_2 production rate, low cost, durability and low toxicity (Garcia-Rodriguez et al., 2020; Oturan, 2021). Among these, activated carbon fibers arise as one of the best options due to their high effective surface area (2D planar structure of the fibers), adsorption, conductivity and catalytic properties. For the mineralization of persistent organic pollutants, carbon felts have also been classified as an interesting option. Their hydrophobicity and low redox reaction kinetics limit their utilization (Nair et al., 2021). Carbon nanotubes and carbon aerogels also have interesting properties as cathode material for EF treatment. Factors responsible for the high performance of carbon aerogels include large specific surface area, abundant pore size, low density, good corrosion resistance and modifiable surface chemistry (Nair et al., 2021). Studies that have explored the possibility of using BDD electrodes as cathodes agree that this avenue is less interesting because similar results can be achieved with more cost-effective cathode materials, such as carbon-based materials (Oturan, 2021).

2.2.4.2.3 *Up-scaling*

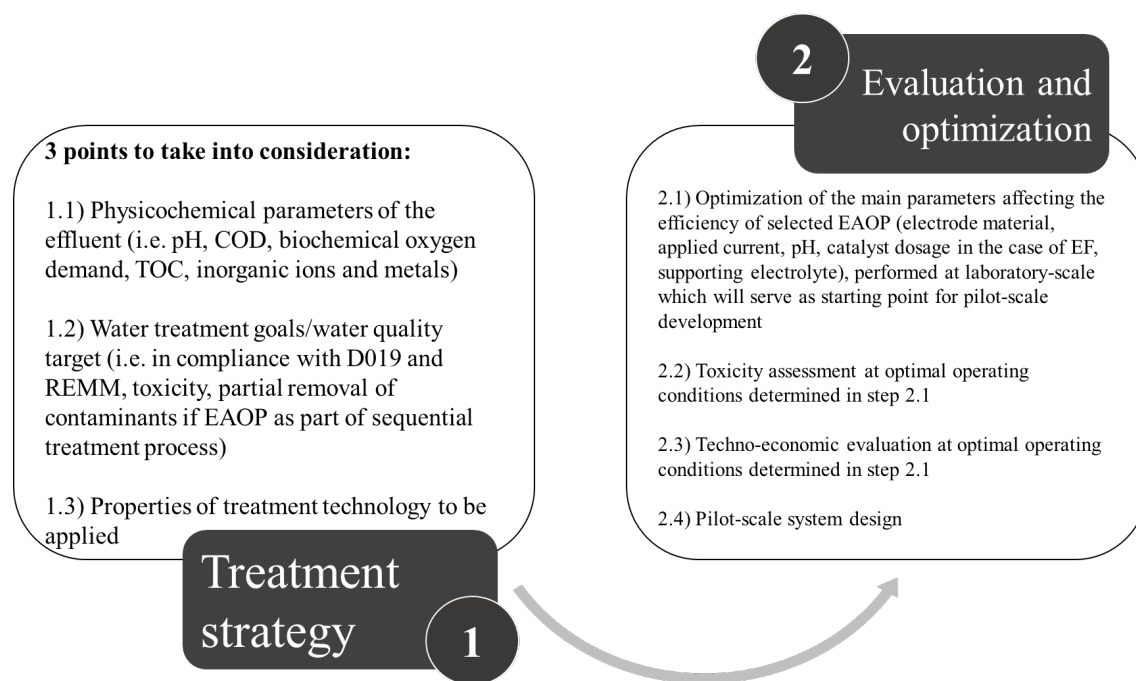
Several studies focusing on the development of EAOPs have been conducted at laboratory scale on synthetic wastewaters. The use of hand-made solutions avoids the wastewaters' conditions in reality (i.e. mixed contamination and buffer solutions at equilibrium and with complex chemistries) because they govern preferential degradation pathways and EAOPs removal efficiencies. In this sense, it is crucial to use real conditions when developing EAOPs for eventual large-scale applications (Garcia-Rodriguez et al., 2020).

The main stages involved in the development of a pilot-scale system for an EAOP are depicted in **Figure 2.2** (adapted from Garcia-Rodriguez et al., 2020). Based on the findings detailed in a recent review on the toxicity assessment of wastewaters following treatment by several AOPs (Rueda-Marquez et al., 2020), a supplementary step (step 2.2; **Fig. 2.2**) was added to improve the suitability of the processes for their application to the treatment of mine-impacted

water. The details of this review and the importance of conducting toxicity bioassays prior to designing pilot-scale systems are presented in Section 2.2.4.2.4.

When designing the pilot-scale system, two engineering parameters are crucial to ensure successful upscaling of electrochemical processes, namely reactor design in terms of mass transfer and the area of the electrode per unit of volume, as well as current density. Coherently, studies agree that the mass transfer and the area of the electrode per unit of volume should be as high as possible, to design a reactor as compact as possible. Electrochemical treatment processes are driven by electricity, making energy consumption the leading expense. Hence, optimal applied current density is also imperative (Garcia-Rodriguez et al., 2020).

Figure 2.2 Main steps involved in the development of EAOPs for a prospective large-scale application (adapted from Garcia-Rodriguez et al., 2020).



The engineering of an appropriate electrochemical reactor configuration is of maximal importance to reduce costs and optimize efficiencies when considering the upscaling of EAOPs (Nair et al., 2021). A pilot-scale EF treatment plant was installed and run under continuous mode for five months in Gyeonggi-do (South Korea) to treat organic pollutants [reduction of chemical

oxygen demand (COD)] using Ti mesh cathodes. The system was able to treat 40 m³/day of water with COD removal efficiencies of 86%. The electrode stacks consisted of alternative layers of twenty-one Ti mesh cathodes and twenty iridium oxide and ruthenium oxide coated Ti (Ti/IrO₂+RuO₂) mesh anodes. A techno-economic evaluation of the pilot scale EF system was conducted, which showed that the operational costs associated to reagents and energy consumption were of \$2.26/kg of COD removed (Nair et al., 2021). Similarly, a pilot-scale EF system was installed in India for the treatment of real textile industry wastewater, where Al cathodes and Ti/RuO₂ anodes were employed. A cost analysis was performed, which concluded that total costs added up to \$5.76/kg of COD removed, \$0.10/kg of which were associated to electrical energy (Nair et al., 2021). These findings show the importance of selecting appropriate electrodes to avoid electrode deterioration, reduce the cost of EF and maximize removal efficiencies.

2.2.4.2.4 Associated toxicity

Fenton-based AOPs often lead to the generation of toxic by-products associated to potential environmental risks. The literature states that some by-products can even be more toxic than initial compounds to be treated and that the final toxicity of effluents strongly depends on the nature of treated effluents (Rueda-Marquez et al., 2020; Nair et al., 2021).

Up until now, a total of four studies have reported results on the toxicity associated to treatment by EF (**Table 2.8**), all of which were carried out on organic-contaminated wastewaters (i.e. textile industry wastewater, biologically treated coking wastewater and wastewater containing azo dyes). The treatment of textile industry wastewater revealed that complete removal of toxicity for *Aplocheilus panchax*, a common freshwater fish, was achieved after treatment by EF (Kaur et al., 2018). Two studies which evaluated the associated toxicity of EF treatment of biologically pretreated coking wastewaters observed different tendencies. The treatment of the coking wastewater pretreated using an anoxic-aerobic-aerobic biofilm system resulted in a decrease of the inhibition ratio for *Vibrio qinghaiensis*, a luminescent freshwater bacterium (Li et al., 2011). The treatment of the coking wastewater pretreated with a membrane bioreactor (MBR) entailed a 57% increase in mortality for *Oryzias latipes* (Japanese rice fish), after treatment (Zhu et al., 2013). Finally, for the study which focused on the treatment of azo-dyes' contaminated wastewater, the toxicity assessment was carried out using four EF scenarios: 1) 2D-EF; 2) 3D-EF with coal fly ash (CFA) as catalytic particle electrode (CPE); 3) 3D-EF with waste rice straw activated carbon

Table 2.8 Toxicity assessment of organic-contaminated wastewaters treated by EF.

Effluent type	EF experimental conditions	Test organism	Measured parameter	Toxicity assessment		Ref.
				Untreated	Treated	
Textile industry wastewater	Anode: Ti/RuO ₂ (2x) Cathode: Aluminum (2x) Current intensity: 1.10 A [Fe]: 0.55 mM Continuous aeration with air diffusers Reaction time: 137 min	<i>Aplocheilus panchax</i>	Mortality (%)	Untreated	Treated	[1]
				100 (1 min exposure)	0 (96 h exposure)	
Anoxic-aerobic-aerobic biofilm system pre-treated coking wastewater	Anode: Graphite felt Cathode: 2-ethyl anthraquinone-modified graphite felt (2x) Fe-zeolite Y catalyst Inter-electrode distance: 2 cm Current density: 10 A/m ² Cathodic potential: -0.7 V Aeration rate: 0.5 L/min pH: neutral Reaction time: 60 min	<i>Vibrio qinghaiensis</i>	Inhibition ratio (triplicate average)	Untreated	Treated	[2]
				0.36	0.14	
Wastewater containing azo dyes*	Anode: Boron-doped diamond Cathode: Activated carbon fibers Inter-electrode distance: 6 cm Current density: 10 mA/cm ² Aeration rate: 5 L/min pH: 6.5 Temperature: 25 °C Reaction time: 120 min	<i>Daphnia magna</i>	TIR (%)	CPE material	Treated**	[3]
				2D	~ 42.5	
				CFA-3D	45	
				CFA/RSAC-3D	~ 27.5	
				RSAC-3D	50	
MBR pre-treated coking wastewater	N/A	<i>Oryzias latipes</i> (embryos and larvae)	Mortality after 96 h exposure (%)	Untreated	Treated	[4]
				43	100	

* Samples were boiled for 1 h following treatment to remove residual H₂O₂.

** TIR of untreated wastewater = 60%

Note: The approximate values (~) presented in this table were retrieved from graphs.

References: 1 – Kaur et al. (2018); 2 – Li et al. (2011); 3 – Zhuang et al. (2017); 4 – Zhu et al. (2013)

(RSAC) as CPE and 4) 3D-EF with CFA/RSAC composite as CPE. The results showed that all scenarios allowed for a decrease in the toxic inhibition rate (TIR) for *D. magna*.

Despite increasing amounts of studies aimed at assessing EF efficiency for the removal of inorganic contaminants (Chai et al., 2020; Wang et al., 2014), those evaluating the residual toxicity following EF treatment of inorganic-contaminated water, such as mine water, are absent from the literature. Yet, the lack of knowledge and incoherent tendencies observed concerning the toxicity and potential adverse effects of by-products resulting from EF treatment indicate that contaminant removal is not the best and only criteria to consider in assessing EF efficiency. In this context, a toxicity assessment of the final effluent is essential.

2.3 Summary of main findings and research needs

Mining activities produce large volumes of aqueous waste containing a variety of environmentally harmful compounds that threaten aquatic life and biodiversity. Responsible management of contaminated mine water is required. Currently, the main approach for the treatment of AMD is the addition of chemical neutralizers, which increase the pH of the effluent and simultaneously allow the removal of metal(loid)s and SO_4^{2-} by coprecipitation and sorption. The outcome of the treatment is low density sludge, with high water content and various contaminants, resulting in complex and costly management. Thiosalts, which are metastable, partially oxidized sulfur intermediates formed during the oxidation of sulfide minerals, cannot be removed by chemical precipitation. They are responsible for delayed acidification of natural water streams, leading to aquatic toxicity and to the deterioration of the flora and fauna of water body.

Increased thiosalts generation is promoted when the initial S content of the ore is high, grinding and flotation pH is alkaline, granulometry of particles after grinding of the ore is fine, HRT in the mill is long and agitation speed of the pulp is high. Higher temperatures and the nature of reagents used during the milling of the ores have also demonstrated influence in thiosalts generation. Successive F/T cycles can generate highly contaminated mine water, containing extreme thiosalt concentrations, by increasing the reactivity of sulfide minerals. Thiosalts are sensitive to water physicochemical parameters. Water temperatures lower than 4°C can stop the oxidation process.

Thiosalts are not regulated by Canadian nor Quebec legislation, but acute and sublethal requirements must be met. Directly, thiosalts are less likely to pose a problem, but they are likely

to have harmful adverse effects, indirectly, via the delayed acidity produced when the oxidation process is completed. The toxicity of thiosalts is not additive: $S_2O_3^{2-}$ is more toxic than $S_4O_6^{2-}$ to all regulated organisms (the opposite is only true for *O. mykiss*) and thiosalts toxicity is altered in the presence of certain heavy metals such as Cu and Se. There is no correlation between total thiosalts and mortality of test organisms. A thiosalts exposure assessment model was developed to predict thiosalts toxicity in receiving water bodies. The model considers both the risks associated to thiosalts concentrations and the risks entailed by the pH depression. The model assumes that catalysts (i.e. UV rays and bacteria) are absent, but it is a well-known fact that they actively influence thiosalts speciation and oxidation reactions.

Xanthates, “collector” molecules used during the flotation process, are rapidly degraded to CS_2 , ethanol and caustic soda in acidic conditions. Xanthates are likely to cause toxicity when thiosalts are present (the probability is high because thiosalts are mostly generated during flotation), are oxidized to SO_4^{2-} and produce acidity, resulting in xanthate degradation. The salinity of mine waters can also be a cause of toxicity. *D. pulex* was found to be more sensitive than *D. magna* to sulfated salinity, before and after treatment by electrocoagulation. Salinity, in the form of Ca and Na, is less toxic to *D. magna* than the compounds previously mentioned.

The most common approach for thiosalts management is the lime neutralization process to increase the buffering capacity of the effluent and temporarily hinder pH decrease when thiosalts are oxidized in the receiving water body. The neutralizing agent is difficult to dose because there is no correlation between total thiosalts and generated acidity when the water is released to the environment. The current water treatment strategies in northern regions are limited (slowed reaction kinetics and inhibited biological activity in cold water) and not suitable for high contamination with CECs (i.e. thiosalts and As). The AOPs seem to be a promising solution for thiosalts removal. Peroxide (H_2O_2) oxidation proved to be efficient for thiosalts treatment in real mine water, but treatment times are long, especially in cold water (in the order of several days). Reaction kinetics could be accelerated by freezing via the freeze-concentration effect. Fenton was applied at industrial scale, combined with liming, at a Swedish metal mine (Garpenberg), and thiosalts oxidation as well as metal precipitation were successful. The Fenton process produces large quantities of Fe-hydroxide sludge, has a narrow optimal working pH range and can result in residual H_2O_2 in the treated water. The kinetics and mechanisms of thiosalt oxidation by Fe(VI) were studied and reaction rate constants are high. Fe(VI) were successful in As, SCN^- , CN^- and N-

NH₃ removal. It was observed that SCN⁻ can be oxidized regardless of whether N-NH₃ is present or absent, but N-NH₃ oxidation is influenced by the presence of SCN⁻. Mixed contamination interferes with treatment by Fe(VI) and increasing the doses would result in higher residual salinity in the treated effluent. The removal of N-NH₃ by O₃-microbubbles from synthetic and real mine effluents was fast and efficient, but the post-treatment effluent may require an additional polishing step for color removal.

The EAOPs have gained interest in recent years because they require no use or handling of dangerous reactants and secondary waste production requiring post-treatment management is non-existent. The EF provides solutions to the conventional Fenton process. For instance, no sludge is produced following treatment since the Fe²⁺ catalyst is constantly regenerated by the electrochemical reduction of Fe³⁺ and the process avoids the use and handling of H₂O₂ because it is generated inside the electrochemical cell (Olvera-Vargas et al., 2021). The degradation/mineralization of organics by EF is efficient and has been widely studied. Yet, very few studies have focused on the removal of inorganic contaminants and thiosalts oxidation in mine water has been scarcely reported. Electrode material is a key factor influencing degradation pathways. Selecting the most suitable electrode materials, case by case, can help improve their durability over time, optimize costs (material and energy consumption) and removal efficiencies when considering up-scaling.

Finally, the toxicity of effluents, before and after treatment by EF, strongly depends on their nature. The toxicity associated to EF treatment is poorly documented, with only a few EF studies on the treatment of industrial wastewaters that have incorporated toxicity assessments.

The current review aims to shed light on the main factors influencing the formation of thiosalts, the available information on thiosalts toxicity and advancements in research regarding their treatment and management in contaminated mine water. This review allowed to highlight the research needs in terms of thiosalts toxicity and treatment. To overcome these scientific gaps, future research efforts should, in a first instant, focus on developing a thiosalts risk assessment model that considers the presence of catalysts, especially bacteria, as they play an important role in the fate of thiosalts and aquatic toxicity. In addition, studies focusing on the cooperative toxic effect of thiosalts with heavy metals, especially in mine water, are required. Upcoming work should also aim to develop economically viable treatment technologies adapted to mining activities

in northern regions, with emphasis on AOPs and EAOPs. These processes should be adequate for huge water flows, be efficient for extreme and mixed contamination that F/T events can entail and finally, be efficient in very cold-water temperatures. Considering that EF showed remarkable efficiency for the treatment of organic-contaminated wastewaters, its efficiency should be assessed for the treatment of synthetic and real mine water.

2.4 Preliminary research work

In the scope of the preceding literature review, preliminary work in terms of thiosalts treatment in contaminated mine water using three different AOPs and EF has been carried out, at the University of Quebec in Abitibi-Témiscamingue (UQAT). The following sections provide summaries of the two preliminary studies of this research project.

2.4.1 Comparative efficiency of three advanced oxidation processes for thiosalts oxidation in mine-impacted water (Gervais et al., 2020)

Mélinda Gervais, **Jennifer Dubuc**, Marc Paquin, Carolina Gonzalez-Merchan, Thomas Genty and Carmen M. Neculita

This article was published in March **2020** in *Minerals Engineering*. 150: 106349.

(<https://doi.org/10.1016/j.mineng.2020.106349>)

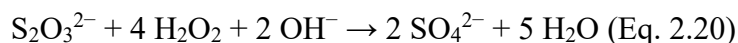
This chapter provides a summary of the paper. The aim of the study is stated, and the main results are presented herein. The student's contribution to the paper was the following: methodology, formal analysis, visualization, writing – review & editing.

2.4.1.1 Aim of the study

The aim of the study was to compare the efficiency of H₂O₂ oxidation, O₃-microbubbles and wet Fe(VI) for thiosalts oxidation in synthetic mine water. The efficiency of H₂O₂ was also assessed on real mine water, at 8°C and 22°C.

2.4.1.2 Peroxide oxidation

Thiosalts oxidation by H_2O_2 was evaluated using a $\text{H}_2\text{O}_2:\text{S}_2\text{O}_3^{2-}$ molar ratio of 2:1 (optimal according to Kuyucak, 2014). Results showed that H_2O_2 was able to remove 99% of $\text{S}_2\text{O}_3^{2-}$ in 1 h at 22°C according to Eq. 2.20. Discrepancies in the balance of S compounds showed that $\text{S}_2\text{O}_3^{2-}$ were only partially oxidized, even after 14 days of treatment. Treatment at 8°C required a reaction time of 7 days to remove 96% of $\text{S}_2\text{O}_3^{2-}$, and only 48% of initial S was recovered. In this sense, these findings not only elucidate the crucial role that temperature plays in the treatment of thiosalts by H_2O_2 , but also show its inefficacy at oxidizing thiosalt species other than $\text{S}_2\text{O}_3^{2-}$. The treatment time using H_2O_2 was the longest (7 d), when compared to the treatment times using O_3 microbubbles (2 h) and wet Fe(VI) (2 h).



2.4.1.3 Ozone microbubbles

Ozone microbubbles demonstrated great potential as a treatment technology for thiosalts oxidation to SO_4^{2-} according to Eq. 2.21. For an initial $\text{S}_2\text{O}_3^{2-}$ concentration of 290 mg/L and an ozone sparging rate of 75 g/h, 99% of $\text{S}_2\text{O}_3^{2-}$ were removed in 2 h. Of all three AOPs studied, O_3 microbubbles showed the greatest removal efficiency (99% vs. 82% and 98% for Fe(VI) and H_2O_2 , respectively) in the shortest amount of time (2 h vs. 2h for Fe(VI) and 7 d for H_2O_2).



The post-treatment pH was very acidic (~ 2.5), requiring an additional polishing step. The study of Ryskie et al. (2020) showed that the process efficiency could be higher at alkaline pH owing to increased HO^\bullet formation. The complete oxidation of thiosalts is known to generate acidity, entailing a rapid pH decrease at the beginning of the treatment. Continuous pH adjustment may be necessary to obtain optimal efficiencies when treating thiosalts with O_3 microbubbles.

2.4.1.4 Ferrates (VI)

The Fe(VI) used in this study were in liquid form and synthesized according to the method employed by Gonzalez-Merchan et al. (2016). Results showed that $S_2O_3^{2-}$ degradation was efficient, yielding a removal efficiency of 82% after 2 h of treatment for a Fe(VI) dosage of 65 mg/L. The post-treatment pH was very alkaline (> 12), which was the opposite with O_3 -microbubbles. Yet, an additional polishing step for pH adjustment is still necessary.

2.4.1.5 Originality of the study

The efficiency of H_2O_2 for thiosalts oxidation in mine water was studied by Kuyucak (2014), but was not compared to other, emerging AOPs used for the treatment of AMD. O_3 -microbubbles were used for the treatment of N-NH₃ in synthetic and real mine water in the study of Ryskie et al. (2020), but their efficiency to remove thiosalts was not documented. The mechanism and kinetics of $S_2O_3^{2-}$ by Fe(VI) was evaluated a long time ago (Read et al., 2001; Read et al., 2005a, 2005b). Additionally, Fe(VI) showed excellent efficiency for the treatment of synthetic and real gold mine effluents containing N-NH₃, SCN⁻ and CN⁻ (Gonzalez-Merchan et al., 2016), but the removal of thiosalts from mine water was not evaluated. In this context, the study in reference compares the efficiency of the above-mentioned technologies for their efficiency in thiosalts oxidation, in mine water, for the first time.

2.4.2 Electro-Fenton beyond the degradation of organics: Treatment of thiosalts in contaminated mine water (Olvera-Vargas et al., 2021)

Hugo Olvera-Vargas, **Jennifer Dubuc**, Zuxin Wang, Lucie Coudert, Carmen Mihaela Neculita, and Olivier Lefebvre

This article was published in January 2021 in *Environmental Science & Technology*. 55(4): 2564–2574.

<https://dx.doi.org/10.1021/acs.est.0c06006>

This chapter provides a summary of a recently published paper, resulting from a collaboration between the National University of Singapore (NUS), the National Autonomous University of

Mexico (UNAM) and the UQAT. The aim of the study is stated, and the main results are presented herein. The student's contribution to the paper was the following: methodology, formal analysis, writing – review & editing.

2.4.2.1 Aim of the study

The aim of the study was to optimize the main parameters affecting the EF process (i.e. current density, temperature, $S_2O_3^{2-}$ concentration) and to elucidate the principal mechanisms governing thiosalts treatment by EF.

2.4.2.2 $S_2O_3^{2-}$ removal efficiency

EF showed a remarkable efficiency for thiosalts removal in synthetic mine water (> 99% $S_2O_3^{2-}$ removal in 2 h at an initial concentration of 1 g/L) using a carbon brush cathode and BDD anode. The process efficiency was not diminished when treatability tests were performed on water with a temperature of 4°C.

2.4.2.3 Effect of current density

The current density was found to play a crucial role in the EF process. Increased current density, up to 6.25 mA/cm², resulted in accelerated $S_2O_3^{2-}$ degradation, but higher values were suspected to increase the rate of parasitic reactions, reducing EF efficiency. Current density also plays a key role in preferential degradation pathways. During anodic oxidation tests (in the absence of Fe^{2+}), the reaction of $S_2O_3^{2-}$ with BDD(HO^*) was dominant at high current values, whereas direct oxidation via electron transfer at the anode surface mainly controlled $S_2O_3^{2-}$ degradation at lower current values.

In terms of energy consumption, a current density of 6.25 mA/cm² was found to be the best compromise for optimal $S_2O_3^{2-}$ removal and operating costs associated to electricity consumption, compared to other tested current densities.

2.4.2.4 Effect of initial thiosalts concentration

The concentration of thiosalts in mine water is dependent of a variety of factors including the nature of the ore, operating parameters of ore processing techniques (i.e. pH of the pulp, grain

size, HRT, stirring speed) (Negeri et al., 1999; Miranda-Trevino et al., 2013). Furthermore, seasonal variations in northern countries, which entail accelerated S oxidation kinetics via F/T cycles, also influence the concentration of thiosalts in mine water (Éthier, 2011; Sinclair et al., 2015; Schudel et al., 2019).

In this context, the effect of initial thiosalt concentration on EF process efficiency was also evaluated in the referred study. Evidently, results demonstrated that higher thiosalt concentrations decreased the rate of removal. The authors attribute this observation to an increase in generated species during treatment that consume HO[•], while the HO[•] concentrations in solution remain the same when initial thiosalt concentrations are lower.

2.4.2.5 Degradation pathways

The study proved that the Fenton reaction dominates the oxidation of thiosalts during EF treatment. Several other degradation processes occur in the electrochemical cell that contribute to thiosalts removal. During the first few minutes of electrolysis, before the addition of Fe²⁺, thiosalts are degraded via three main pathways including: i) the direct electrochemical oxidation of S₂O₃²⁻ at the anode, ii) the reaction of S₂O₃²⁻ with H₂O₂ generated at the cathode and iii) a series of disproportionation reactions.

Boron-doped diamond electrodes are known for their capacity to produce HO[•] adhered at their surface (BDD(HO[•])). In a series of tests aimed at investigating the reactions taking place at the anode, in which no Fe²⁺ was added to exclude the Fenton reaction, it was found that S₂O₃²⁻ were oxidized directly at the surface of the anode and indirectly via their reaction with BDD(HO[•]).

It is suggested, by the authors, that the reaction between the HO[•] (produced by the reaction between Fenton reagents or BDD(HO[•])) and the S atom with the lowest oxidation state contained in S₂O₃²⁻ (one S atom is bonded with 3 oxygen atoms and is at an oxidation state of +6 while the other S atom is at an oxidation state of -2) is responsible for initiating HO[•]-mediated S₂O₃²⁻ oxidation, forming the HOS₂O₃⁻ intermediate. The reaction then proceeds via S₄O₆²⁻ formation before complete oxidation to SO₄²⁻.

In summary, the main reactions involved in thiosalts treatment by EF are those with HO[•] and BDD(HO[•]), which are equally efficient. Disproportionation reactions contribute to a lesser extent owing to slower reaction kinetics than HO[•]-mediated oxidation. Direct electron transfer at

the surface of the anode is current density dependent, only contributing significantly at low current values and negligibly at high current values.

2.4.2.6 Operational costs

Current density plays an important role in operational costs associated to electricity. **Table 2.9** depicts the $S_2O_3^{2-}$ removal efficiencies obtained and energy consumptions for treatment times of 90 and 120 min, at different current densities. The higher the current density is, the higher the energy consumption is, entailing higher operating costs. Increasing the current density above 6.25 mA/cm² would entail higher treatment costs for minimal increase in $S_2O_3^{2-}$ removal.

Table 2.9 Energy consumption and $S_2O_3^{2-}$ removal efficiency, after 90 and 120 min of treatment by EF, at different current densities.

Current density (mA/cm ²)	Energy consumption (kWh/g $S_2O_3^{2-}$)		$S_2O_3^{2-}$ removal (%)	
	90 min	120 min	90 min	120 min
2.08	~ 0.0025	~ 0.0025	~ 52	~ 53
6.25	~ 0.0060	0.0081	85	95
10.42	~ 0.0120	0.0169	95	95
15.63	0.0301	~ 0.0400	> 99	> 99

Note: Approximate values (~) were retrieved from graphs.

When EF was compared to other AOPs (i.e. H_2O_2 oxidation, Fe(VI), O_3 -microbubbles and conventional Fenton) for thiosalts treatment in synthetic and real mine water in terms of operating costs in a preliminary techno-economic evaluation, estimated treatment costs were considerably lower (**Table 10**).

For instance, when EF was used to treat a real mine effluent containing 210 mg/L of $S_2O_3^{2-}$, thiosalts were completely removed in 90 min and operating costs were estimated to be of CAD\$0.74/kg of thiosalts treated. In contrast, when H_2O_2 was used to treat 172 mg/L of $S_2O_3^{2-}$ in a real mine effluent, 7 days of storage post-treatment (10–15 min) were required to achieve 82.6% $S_2O_3^{2-}$ removal and operating costs were estimated at CAD\$2.01/kg of thiosalts removed. In synthetic effluents, Fe(VI) proved to be the most expensive treatment technology with estimated operating costs of CAD\$11.87/kg thiosalts compared to CAD\$1.18/kg thiosalts and CAD\$1.01/kg thiosalts for treatment with O_3 -microbubbles and H_2O_2 , respectively.

Table 2.10 Preliminary techno-economic evaluation of operating costs of thiosalt treatment in synthetic and real mine water (as presented in Olvera-Vargas et al., 2021).

Wastewater characteristics		Treatment process	Operating conditions	Degradation efficiency	Operating costs: US\$ (CAD\$)			Ref.
					m ⁻³ order ⁻¹	kg thiosalts ⁻¹	m ⁻³	
Mine water S ₂ O ₃ ²⁻ = 219 ± 21 mg/L, S ₄ O ₆ ²⁻ = 6 ± 10 mg/L, pH = 2.8 ± 0.05, SO ₄ ²⁻ = 738 ± 17 mg/L		EF	V = 0.5 L, i = 0.3 A, t = 90 min, at room temperature, BDD anode and carbon brush cathode	Total removal of thiosalts	0.10 (0.05)	1.50 (0.74)	0.35 (0.17)	1
Mine water Thiosalts (S ₂ O ₃ ²⁻ , S ₃ O ₆ ²⁻ and S ₄ O ₆ ²⁻) = 172 mg/L pH = 3.08 SO ₄ ²⁻ = 2.5 g/L		H ₂ O ₂ oxidation	V = 1 L 1.2 g of H ₂ O ₂ per g of S ₂ O ₃ ²⁻ t = 10-15 min, followed by 7 days of storage in TIF	82.6% of thiosalts removal	0.29 (0.39)	1.50 (2.01)	0.22 (0.29)	2*
S ₂ O ₃ ²⁻ solutions	S ₂ O ₃ ²⁻ = 100 mg/L	Fe(VI) oxidation	V = 0.3 L Fe(VI) = 65 mg/L, alkaline pH t = 2 h, T = 22 °C	82% S ₂ O ₃ ²⁻ removal	0.96 (1.31)	8.73 (11.87)	0.72 (0.97)	3**
	S ₂ O ₃ ²⁻ = 290 mg/L	Ozonation	V = 0.3 L O ₃ = 75 g/h, natural pH, t = 2 h, T = 22 °C	99% S ₂ O ₃ ²⁻ removal	0.36 (0.17)	2.49 (1.18)	0.71 (0.34)	
	Mine water S ₂ O ₃ ²⁻ = 638 mg/L, SO ₄ ²⁻ = 297 mg/L	H ₂ O ₂ oxidation	V = 0.3 L H ₂ O ₂ :S ₂ O ₃ ²⁻ molar ratio of 2:1 t = 1 h, followed by 7 days of storage in TIF, T = 22 °C	96% S ₂ O ₃ ²⁻ removal	0.33 (0.44)	0.74 (1.01)	0.45 (0.72)	
Mine water (industrial scale application at Garbenberg Mine, Sweden) Thiosalts (S ₂ O ₃ ²⁻ , S ₃ O ₆ ²⁻ and S ₄ O ₆ ²⁻)		Fenton	Addition of H ₂ O ₂ , FeSO ₄ and lime in tailing ponds***	98.5% of thiosalts removal	NR	NR	NR	4

* Operating costs in US\$ m⁻³ order⁻¹ and US\$ (kg thiosalts)⁻¹ were calculated based on the data reported by the authors.

** Costs were determined in a preliminary techno-economic analysis based on the findings of Gervais et al. (2020). Detailed calculations are available in Section S1 of Supplementary Material in Olvera-Vargas et al. (2021).

*** Details of the operating conditions were not reported (NR).

References: 1 – Olvera-Vargas et al. (2021); 2 – Kuyucak (2014); 3 – Gervais et al. (2020); 4 – Wahlstrom et al. (2017).

2.4.2.7 Originality of the study

The use of EF has been widely studied for the degradation/mineralization of organic compounds (i.e. dyes, pharmaceutical compounds, herbicides), but the treatment of water containing inorganic compounds, such as mine water, has been particularly disregarded. Recently, Chai et al. (2020) have investigated the simultaneous removal of Fe^{2+} and Mn^{2+} from AMD, but EF application to thiosalts treatment in mine water (at room temperature and at 4°C) had not yet been reported in the literature. In addition, this study presents a comparison of operational costs between EF, H_2O_2 oxidation, Fe(VI) and ozonation, for the first time, providing essential information for prospective large-scale application of the technologies. These findings could be of particular interest to mine operations in northern regions, were the development of efficient and rapid thiosalts treatment methods in cold water is required.

CHAPTER 3 METHODOLOGY

This chapter presents the strategy adopted to evaluate the performance of the EF process for thiosalts treatment in mine water in terms of contaminant removal, residual toxicity and treatment costs. The details of the experimental setup, the sampling and analytical methods of effluents before, during and after treatment, and the treatability tests performed are discussed herein. The methods employed for the aquatic toxicity and techno-economic components are also presented. Extensive detail relative to the preliminary work is presented in Chapter 2. A simplified version of the followed methodological approach is provided in **Figure 3.1**.

3.1 Contaminant removal

This section is dedicated to the efficiency component, which refers to the efficiency of the EF process in terms of contaminant removal. The detailed steps, in the exact order that they were performed, are presented in **Figure 3.2**, along with their justifications.

3.1.1 Sampling of real effluents and preparation of synthetic effluents

Effluents were selected based on their geographical origin (northern Quebec, Canada). Effluent E1, collected from a flotation process plant, was received, and first characterized in 2018. Up until EF treatability tests began (at the beginning of 2020), it has been preserved at 4°C. Results showed that, despite a noticeable evolution of the effluent after two years of preservation, $S_2O_3^{2-}$ are still present in the range of 200 mg/L, highlighting the slow and incomplete oxidation of thiosalts at low temperature. Effluents E2, E3 (received in summer 2020) and E4 (received last, in summer 2021), were final effluents at the mine site where they were collected, which explains their lower contamination compared to E1. Effluent E3 was treated, despite the absence of thiosalts, to depict underlying mechanisms that govern the EF process. E1 and E4 are referred to as ME_{high} and ME_{low} , respectively, in **Chapter 5**.

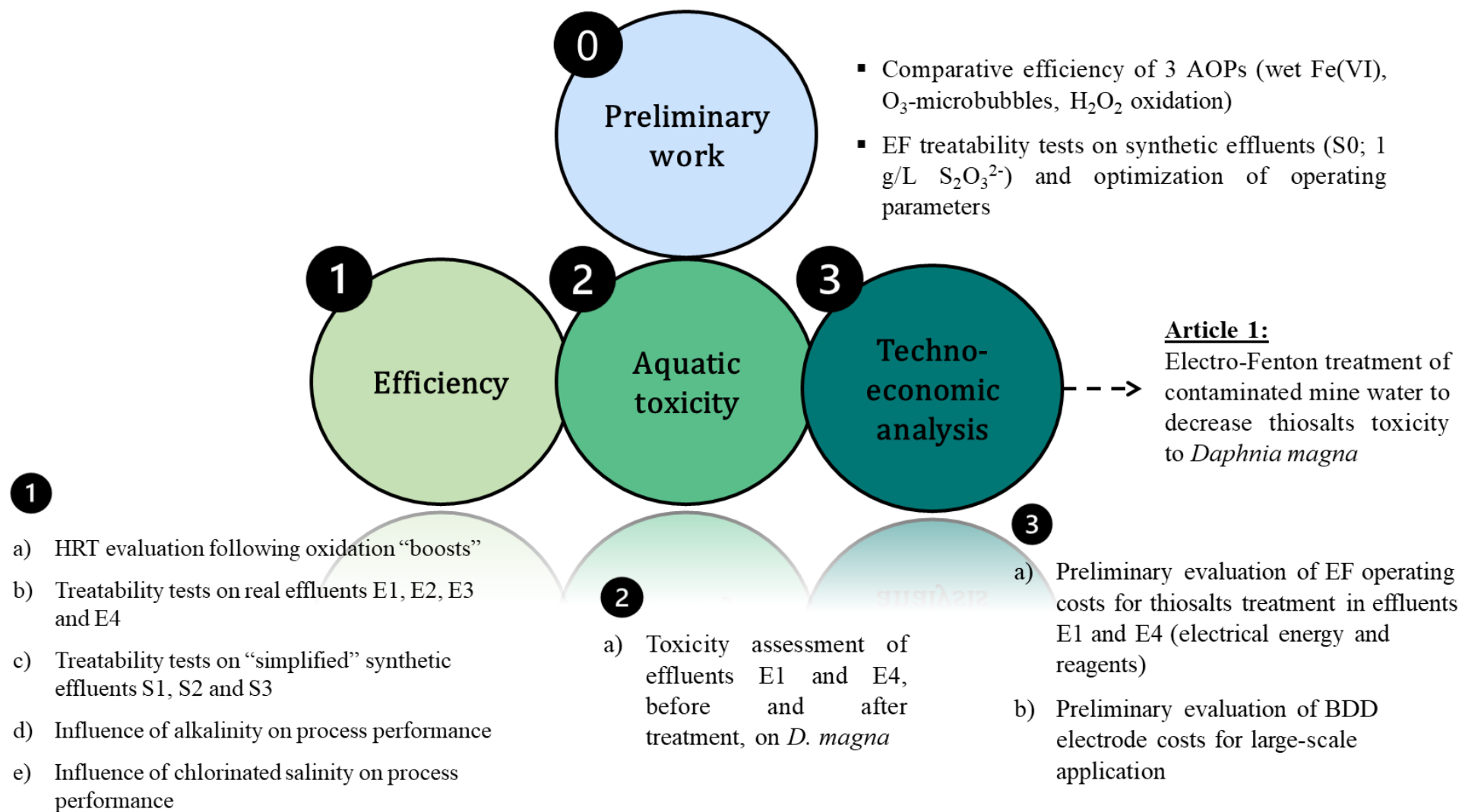


Figure 3.1 Step-by-step methodological approach of the project.

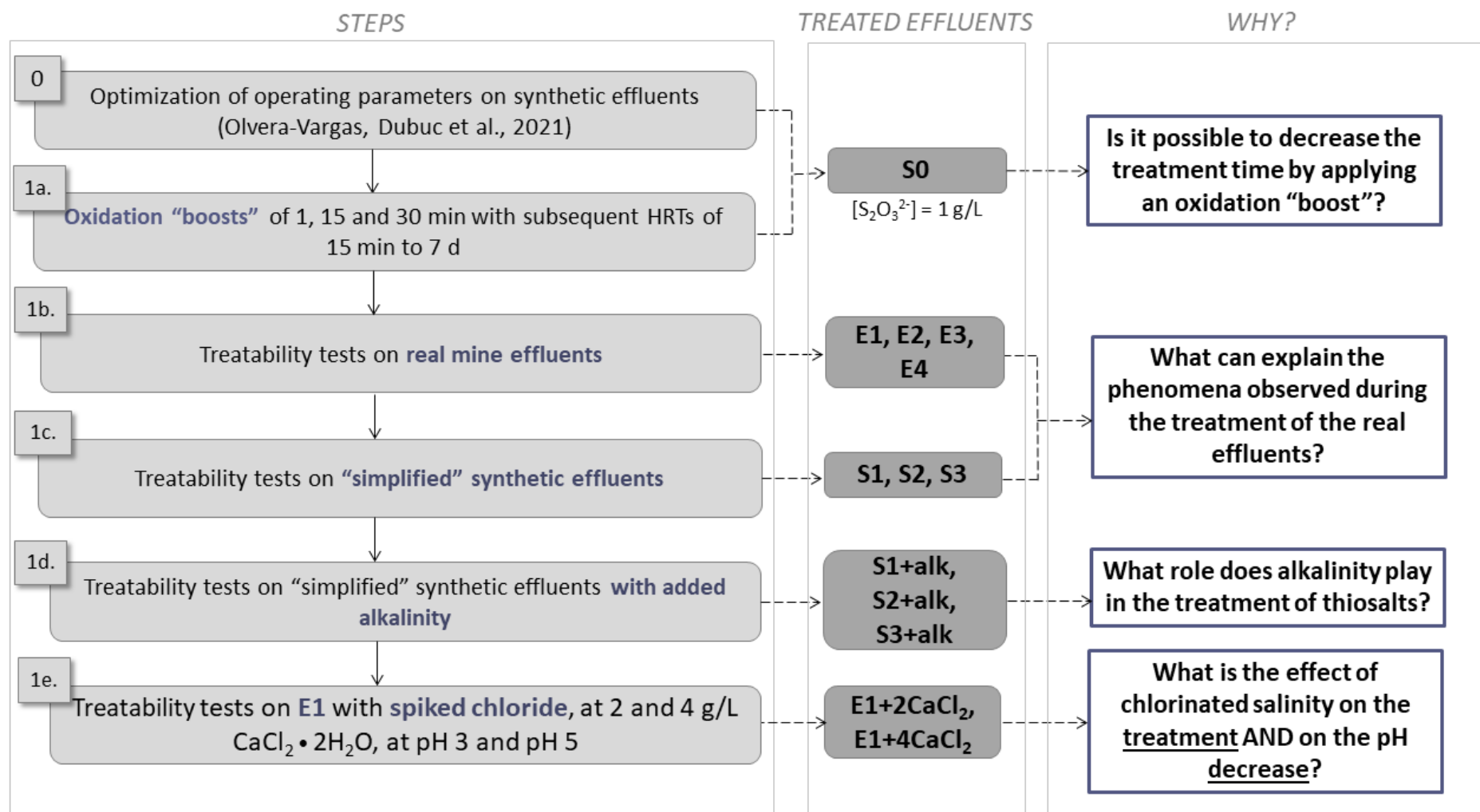


Figure 3.2 Detailed approach and justifications for the "efficiency" component of the project.

Synthetic effluents S1, S2 and S3, with or without alkalinity, were prepared according to the steps detailed in Appendix A. $S_2O_3^{2-}$ concentrations in the effluents were selected to match those of the real effluents. If the ionic strength of the solution was too low to allow a current to be generated during EF treatment (which was the case for S3 and S3 with alkalinity), sodium chloride (NaCl; Culinary grade, Sifto, Canada) was added so that the conductivity of the synthetic effluent would match that of the real effluent. Sodium chloride was selected as the supporting electrolyte because of its natural abundance due to the salinity of mine water in northern regions (Neculita et al., 2019). To evaluate the influence of alkalinity on the process efficiency, alkalinity was added to S1, S2 and S3 to match that of E1, E2 and E3.

3.1.2 Analysis of effluents, before and after treatment

A list of parameters, analyzed according to the treatability test performed, is provided in **Table 3.1**. The physicochemical characteristics of E1, E2 and E3 are presented in **Table 3.2**. Effluent E4 is discussed extensively in **Chapter 5**. The pH was measured with an Orion GD9156BNWP double junction Ag/AgCl electrode (Thermo Fisher Scientific, Canada), connected to the VWR® Symphony® multi-meter. The pH probe was calibrated with buffer solutions of pH 4, 7 and 10 (BDH, Canada). Initially, all tests were performed with sampling times of 0, 15, 30, 60, 90 and 120 min (Olvera-Vargas et al., 2021), in small sampling tubes, and the pH was measured at all sampling times, directly in the electrochemical cell. During the treatment of E2, an unexpected pH drop occurred, so a condensed treatability test was performed on E2, with additional sampling times and pH measurements (using pH paper), in between sampling times (**Table 3.1**). It was found that a drastic pH drop occurs within the first 15 seconds of treatment. Thereafter, the amount of sampling times was increased to ensure a more descriptive portrait of the phenomena occurring at the beginning of the reaction. Sampling was then done in large tubes (in which the pH electrode can be inserted) to allow pH measurements to be taken directly in the tubes, at the end of the test. Treatment duration for the treatability tests on synthetic effluents was reduced to 60 min, following the treatability tests on real effluents, which indicated the time required for complete thiosalts oxidation.

The Eh (corrected to Standard Hydrogen Electrode) was measured with a VWR® double junction Ag/AgCl electrode equipped with a platinum sensor and calibrated with a 228 mV

Table 3.1 Characteristics of EF treatability tests performed including treatment duration, sampling times and analyzed parameters, before, during and after treatment, for all synthetic and real effluents.

Type of water	Effluent code	Test performed	Treatment duration (min)	Sampling times (min)	Analyzed parameters
Real effluent	E1	Treatment – no modification (triplicates)	120	0, 15, 30, 60, 90, 120	Before and after: Eh, EC At all sampling times: pH, SO ₄ ²⁻ , S ₂ O ₃ ²⁻ , S ₄ O ₆ ²⁻ , Cl ⁻ , Br ⁻
		Addition of CaCl ₂ •2H ₂ O (2 and 4 g/L, at acidic and circumneutral pH)	60	0, 0.25, 3, 6, 9, 12, 15, 30, 60	Before and after: Eh, EC, DO, acidity, alkalinity, Ca At all sampling times: pH, SO ₄ ²⁻ , S ₂ O ₃ ²⁻ , S ₄ O ₆ ²⁻ , Cl ⁻ , Br ⁻
	E2	Treatment – no modification	120	0, 15, 30, 60, 90, 120	Before and after: Eh, EC At all sampling times: pH, SO ₄ ²⁻ , S ₂ O ₃ ²⁻ , S ₄ O ₆ ²⁻ , Cl ⁻ , Br ⁻
		Treatment - condensed	30	0, 3, 6, 9, 12, 15, 30	Before and after: Eh, EC At all sampling times: pH, SO ₄ ²⁻ , S ₂ O ₃ ²⁻ , S ₄ O ₆ ²⁻ , Cl ⁻ , Br ⁻ 0, 0.25, 1, 2, 4, 6, 8, 10, 12, 14, 16, 20, 25, 30: pH (with pH paper)
	E3	Treatment – no modification	120	0, 15, 30, 60, 90, 120	Before and after: Eh, EC At all sampling times: pH, SO ₄ ²⁻ , Cl ⁻ , Br ⁻
	E4	Treatment – no modification (triplicates)	60	0, 0.25, 3, 6, 9, 12, 15, 30, 60	Before and after: pH, Eh, EC, DO, Ca, N-NH ₃ At all sampling times: pH, SO ₄ ²⁻ , S ₂ O ₃ ²⁻ , S ₄ O ₆ ²⁻ , Cl ⁻ , Br ⁻
Synthetic effluent	S0	Treatment – no modification (duplicates)	120	0, 15, 30, 60, 90, 120	Before and after: Eh, EC At all sampling times: pH, SO ₄ ²⁻ , S ₂ O ₃ ²⁻ , S ₄ O ₆ ²⁻
		Application of oxidation “boosts” and evaluation of HRT	1, 15, 30*	0, boost duration, HRTs (15 min and 1 to 7 days)	At all sampling times: pH, Eh, EC, DO, SO ₄ ²⁻ , S ₂ O ₃ ²⁻ , S ₄ O ₆ ²⁻
	S1	Treatment – no modification	60	0, 0.25, 3, 6, 9, 12, 15, 30, 60	Before and after: Eh, EC At all sampling times: pH, SO ₄ ²⁻ , S ₂ O ₃ ²⁻ , S ₄ O ₆ ²⁻ , Cl ⁻ , Br ⁻
		Addition of alkalinity**	60	0, 0.25, 3, 6, 9, 12, 15, 30, 60	Before and after: Eh, EC, alkalinity At all sampling times: pH, SO ₄ ²⁻ , S ₂ O ₃ ²⁻ , S ₄ O ₆ ²⁻ , Cl ⁻ , Br ⁻
	S2	Treatment – no modification	60	0, 0.25, 3, 6, 9, 12, 15, 30, 60	Before and after: Eh, EC At all sampling times: pH, SO ₄ ²⁻ , S ₂ O ₃ ²⁻ , S ₄ O ₆ ²⁻ , Cl ⁻ , Br ⁻
		Addition of alkalinity	60	0, 0.25, 3, 6, 9, 12, 15, 30, 60	Before and after: Eh, EC, alkalinity At all sampling times: pH, SO ₄ ²⁻ , S ₂ O ₃ ²⁻ , S ₄ O ₆ ²⁻ , Cl ⁻ , Br ⁻

Type of water	Effluent code	Test performed	Treatment duration (min)	Sampling times (min)	Analyzed parameters
	S3	Treatment – no modification	60	0, 0.25, 3, 6, 9, 12, 15, 30, 60	Before and after: Eh, EC At all sampling times: pH, SO ₄ ²⁻ , Cl ⁻ , Br ⁻
		Addition of alkalinity	60	0, 0.25, 3, 6, 9, 12, 15, 30, 60	Before and after: Eh, EC, alkalinity At all sampling times: pH, SO ₄ ²⁻ , Cl ⁻ , Br ⁻

* In this case, treatment duration refers to the duration of the oxidation “boost”.

** Due to the evolution of E1 from 2018 (upon reception) to 2020 (time of treatability test), and the absence of alkalinity in the aged effluent, the alkalinity of S1 was adjusted to that of E1 in 2018.

standard solution (Orion 96791, Thermo Fisher Scientific, Canada). The electrical conductivity (EC) was measured with a VWR® Traceable® Expanded Range Conductivity Meter equipped with an epoxy probe and calibrated with a 1413 $\mu\text{S}/\text{cm}$ standard solution (Anachemia, Canada). The DO was measured with a HQ40D portable multimeter equipped with an IntelliCA® LDO101 luminescence probe (Hach, Canada). Acidity and alkalinity were measured by titration using the 848 Titrino Plus titrator (Metrohm, Canada). In the case of E4, N-NH_3 was measured with the Orion 9512HPBNWP ion selective electrode (Thermo Fisher Scientific, Canada), according to the standard method (ASTM D1426-15, 2015).

Metal concentrations for the initial characterization of the real effluents were measured by Inductively Coupled Plasma - Atomic Emission Spectroscopy (ICP-AES; Perkin Elmer OPTIMA 3100 RL). Validation of the calibration curve was carried out using two reference materials: river water provided by the Centre d'Expertise en analyse Environnementale du Québec (CEAEQ) and ES-H (SCP Science, Canada). Samples were filtered with 0.45 μm nylon filters and acidified (2% HNO_3) prior to analysis. When calcium chloride ($\text{CaCl}_2 \cdot 2\text{H}_2\text{O}$) was added to E1 to evaluate the influence of chlorinated salinity, Ca concentrations were measured, before and after treatment, to evaluate the possibility of gypsum precipitation, if the S mass balance were to have discrepancies.

Ion Chromatography (IC) was used for the analysis and quantification of all anionic species with the 940 Professional IC Vario instrument (Metrohm, Canada) equipped with two injection, elution, and separation systems ($2 \times \text{Supp 5}$ columns; 250×4.0 mm). $\text{S}_4\text{O}_6^{2-}$ was quantified using UV-vis detection (944 Professional UV-vis detector Vario, Metrohm, Canada) and all other anions were detected by conductimetry (945 Professional Detector Vario, Metrohm, Canada). The mobile phase in the UV-vis detection system was composed of 10 mM NaClO_4 and 1 mM NaOH . The detection of all other anions was achieved by applying an eluent gradient (eluent A: 3.2 mM Na_2CO_3 , 1 mM NaHCO_3 , and CH_3N (15% v/v); eluent B: 16 mM Na_2CO_3 , 5 mM NaHCO_3 , and CH_3N (15% v/v)) to reduce total analysis time. The eluent flow rate for both systems was set at 0.7 mL/min. The device was calibrated using three calibration standards with a concentration of 1000 ppm, namely, a multi anion standard, a nitrite standard and a thiosulfate standard (AccuSpec, SCP Science, Canada). The device was calibrated with dilutions of 1, 2, 5, 10, 25, 50 and 100 ppm, containing all three standards with deionized water. All samples were filtered with 0.45 μm nylon

filters, diluted by a factor of 10 using a carbonate buffer (0.032 M Na₂CO₃; 0.01 M NaHCO₃) and preserved at 4°C, prior to analysis.

Table 3.2 Initial physicochemical characteristics of real mine effluents E1, E2, E3 and E4.

	E1	E2	E3
pH	2.84 ± 0.05	8.43	8.15
Eh (mV)	417 ± 43	444	453
EC (µS/cm)	4053 ± 353	1580	535
Acidity (mg CaCO₃/L)	111	N/A	N/A
Alkalinity (mg CaCO₃/L)	N/A	26	45
Cl⁻ (mg/L)	497 ± 23.8	215	57.7
Br⁻ (mg/L)	14.1 ± 4.2	8.0	< 0.7
NO₃⁻ (mg/L)	73.7 ± 7.9	41.1	13.3
SO₄²⁻ (mg/L)	738 ± 17	497	110
S₂O₃²⁻ (mg/L)	219 ± 21	32	< 1
S₄O₆²⁻ (mg/L)	< 1	< 1	< 1

Legend: N/A = not applicable.

3.1.3 Treatability tests

3.1.3.1 Experimental setup

The experimental setup and operating parameters, optimized during the preliminary work on synthetic effluents (Olvera-Vargas et al., 2021), are presented in detail in **Chapter 5**. The detailed protocol is provided in Appendix A.

3.1.3.2 Oxidation “boosts”

The EF oxidation “boosts” were applied to S0. The strategy consisted in adding the Fe²⁺ (as usual), applying an external current for 1, 15 and 30 min, stopping the reaction and then allowing the effluent to rest, under mild agitation (~100 rpm). Beakers were covered with a watch glass to avoid water evaporation during the HRTs, which ranged from 15 min to 7 days. These tests were carried out to determine if the time of the electrochemical reaction could be reduced (and costs of electrical energy), and still allow for complete thiosalts removal if the effluent was given time to react with the oxidative species produced during the electrochemical reaction.

3.1.3.3 Chlorinated salinity

A recent study showed that the pH-dependent interference of Cl^- on the photo-Fenton process is more important in acidic media. Precisely, contaminant removal was slightly accelerated in the presence of 1 g/L NaCl at pH 5 compared to pH 2.8 (Vallès et al., 2021). Consistently, following the treatment of E3 and its corresponding synthetic effluents (S3, with and without alkalinity), in which thiosalts are absent and the dominant contaminant is Cl^- , the influence of chlorinated salinity on the performance of the EF process was evaluated in terms of contaminant removal and pH decrease during treatment, at acidic and circumneutral pH.

To do so, $\text{CaCl}_2 \cdot 2\text{H}_2\text{O}$ (grade ACS, Laboratoire Mat, Canada) was added to E1 at concentrations of 4.3 and 2 g/L. In a first series of tests, the pH of E1 remained unmodified (**Table 3.1**), and for another series of tests, the pH was adjusted to 5.0 using 1 N NaOH (Thermo Fisher Scientific, Canada). Effluent E1 was selected because of the absence of thiosalts in the other effluents (initially absent in E3 and completely oxidized in E2).

To spike the Cl^- concentration in E1, $\text{CaCl}_2 \cdot 2\text{H}_2\text{O}$ was selected to mimic the salinity of mine water in real conditions. Indeed, CaCl_2 is commonly used during winter, as a de-icing agent, to prevent the freezing of water in pipes, which is required for mining activities in northern climate (Kaushal et al., 2005). The tested concentrations were selected according to the toxicity threshold of daphnia, which is of 3.25 g/L CaCl_2 (equivalent to 4.3 g/L $\text{CaCl}_2 \cdot 2\text{H}_2\text{O}$; Mount et al., 1997).

3.2 Preliminary techno-economic analysis

Operating costs (OCs) were estimated in terms of energy consumption (E_{consum}), reagents ($\text{FeSO}_4 \cdot 7\text{H}_2\text{O}$ and Na_2CO_3) and BDD electrode, for effluents E1 and E4. Although BDD electrodes are not consumables, they were incorporated as operating costs for the purpose of this preliminary techno-economic study, by amortizing their investment cost over the duration of their estimated lifetime. Assumptions made in the model and calculations pertaining to E_{consum} and reagents are presented in **Chapter 5**. Hypotheses and calculations for BDD electrode costs are presented in **Section 3.2.1**.

3.2.1 BDD electrode costs

Several hypotheses were made to estimate the costs associated to the purchase of a BDD electrode to operate a treatment plant with an influent flow rate of 100 m³/day, for E1 and E4 (Table 3.3). The electrode surface area required was calculated according to Eq 3.1. The purchase price (PP) of the electrode was calculated according to Eq 3.2. Costs associated to the purchase of a BDD electrode were calculated for 2 scenarios using Eq 3.3. In scenario 1, an efficiency factor of 90% was considered to account for maintenance interruptions. In scenario 2, the frost season in cold climate regions was considered in the annual operating period of the treatment plant. For the simulation, it was assumed that the free water flow period was of 6 months. The service life of the electrode, estimated according to previous work (Serrano et al., 2015), was set at 10 years for scenario 1, and doubled for scenario 2, considering the electrode would be in operation for half the year, and stored the other half.

$$A_{plant} = A_{lab} * Q * HRT / V \quad (3.1)$$

$$PP (\$) = PP_{0.5} * A_{plant} / 0.5 \quad (3.2)$$

$$\text{Electrode cost } (\$/m^3) = PP / V_s \quad (3.3)$$

where A_{plant} is the electrode surface area in the treatment plant in m², A_{lab} is the electrode surface area used for the present experiments in m², Q is the influent flow rate in m³/h, HRT is the hydraulic retention time in h, V is the treated volume in m³, V_s is the treated volume for the entire service life of the electrode in m³ and $PP_{0.5}$ is the purchase price of a 0.5 m² electrode (largest available on the market with identical characteristics: Condias, Germany).

Results were expressed in \$ per m³ of treated effluent (\$/m³). Total OCs were also expressed in \$ per kg of thiosalts removed (\$/kg-thiosalts, Eq 3.4), to facilitate the comparison of OCs for effluents containing different initial thiosalts concentrations, and per order of magnitude of thiosalts removed (Eq 3.5).

$$\text{Total OCs (\$/kg-thiosalts)} = \frac{(E_{\text{consum}} \text{ cost in } \$/\text{m}^3 + \text{Reagent cost in } \$/\text{m}^3 + \text{Electrode cost in } \$/\text{m}^3)}{\Delta C_{\text{thiosalts}}} * 1000 \quad (3.4)$$

where $\Delta C_{\text{thiosalts}}$ is the amount of thiosalts removed in mg/L.

$$\text{Total OCs (\$/m}^3\text{/order)} = \frac{(E_{\text{consum}} \text{ cost in } \$/\text{m}^3 + \text{Reagent cost in } \$/\text{m}^3 + \text{Electrode cost in } \$/\text{m}^3)}{\log(C_i/C_f)} \quad (3.5)$$

where C_i and C_f are the initial and final thiosalts concentrations (expressed in mg/L), respectively.

Table 3.3 Variable values in the techno-economic model for BDD electrode cost estimations.

Variable	Value	
<i>Fixed variables</i>		
A_{lab} (m ²)	0.0005	
$PP_{0.5}$ (CAD\$)	27 030	
<i>Scenario-dependent variables</i>		
	<i>Scenario 1</i>	<i>Scenario 2</i>
Security factor (%)	90	N/A
Free water flow period (days)	N/A*	182
Annual operating period (days/year)	365	183
Daily operating period (hour/day)	24	24
Electrode service life (years)	10	20
Volume treated in 1 year (m ³)	32 850	18 300
V_s (m ³)	328 500	366 000

* N/A: not applicable

CHAPTER 4 CONTAMINANT REMOVAL EFFICIENCY

This chapter presents the results obtained for all EF treatment tests performed. Firstly, the efficiency of oxidation “boosts” to reduce treatment time and remove thiosalts, after the electrochemical reaction is stopped, is discussed. Then, the physicochemical characterization of effluents E1, E2 and E3, as well as their corresponding synthetic effluents (S1, S2, S3), are presented, followed by a discussion of the evolution of S species during treatment. In this chapter, E1 is only discussed briefly as a basis of comparison for the treatment of S1. Effluents E1 and E4 are discussed extensively in **Chapter 5**, where they are referred to as ME_{high} and ME_{low}, respectively, based on their differing S₂O₃²⁻ concentrations. The effects of alkalinity and chlorinated salinity on the EF process efficiency are also presented and discussed herein.

4.1 Oxidation “boosts”

Oxidation “boosts” of 1, 15 and 30 minutes were applied to S0 (S₂O₃²⁻ = 1 g/L) to determine if the electrochemical reaction time could be reduced, without compromising thiosalts removal efficiency.

During the electrochemical reaction, the pH and S₂O₃²⁻ concentrations decreased for all oxidation “boost” times tested, consistent with increasing SO₄²⁻ concentrations, indicating that thiosalts oxidation was occurring. As expected, variations in pH and S₂O₃²⁻, S₄O₆²⁻ and SO₄²⁻ concentrations were more pronounced as the oxidation “boost” time increased. (**Table 5.1**). After oxidation “boosts” of 1 and 15 min, the formed S₄O₆²⁻ (18 and 40 mg/L, respectively) were completely converted to another S species after HRTs of 6 and 7 days, respectively. Although the pH following the “boosts” (4.11, 3.39 and 3.26 for 1, 15 and 30 min “boosts”, respectively) favored S₄O₆²⁻ stability (Miranda-Trevino et al., 2013), DO saturation in the solution after an HRT of 1 day (**Fig. 5.1, Table 5.1**) could have contributed to slow S₄O₆²⁻ oxidation. Contrastingly, after an oxidation “boost” of 30 min, an HRT of 7 days was insufficient for complete removal of S₄O₆²⁻, indicating that the solution, after the “boost”, was not oxidative enough to convert the entirety of the formed S₄O₆²⁻ into another S species.

Results of the characterization, at HRTs of 15 min, and 1 to 7 days (**Fig. 5.1**), showed that all parameters remained constant – or only varied slightly – shortly after the electrochemical reaction was stopped, indicating that all oxidation “boost” times tested were insufficient for

complete thiosalts oxidation. Slight parameter variations could be attributed to the natural oxidation process of thiosalts, due to their metastable nature in aqueous solutions (Miranda-Trevino et al., 2013; Range and Hawboldt, 2019), and to DO saturation after an HRT of 1 day. These findings suggest that, in the presence of thiosalts only, EF does not generate enough residual oxidative species to allow for complete thiosalts removal. Inappropriate dosing of H_2O_2 , during chemical Fenton treatment, can result in residual H_2O_2 after treatment (Zhang et al., 2005). The results of the oxidation “boosts” experiments show that the likelihood of EF generating excess H_2O_2 is little, since residual H_2O_2 in the solution would have reacted with $\text{S}_2\text{O}_3^{2-}$, resulting in decreased $\text{S}_2\text{O}_3^{2-}$ concentrations, even after the electrochemical reaction was stopped.

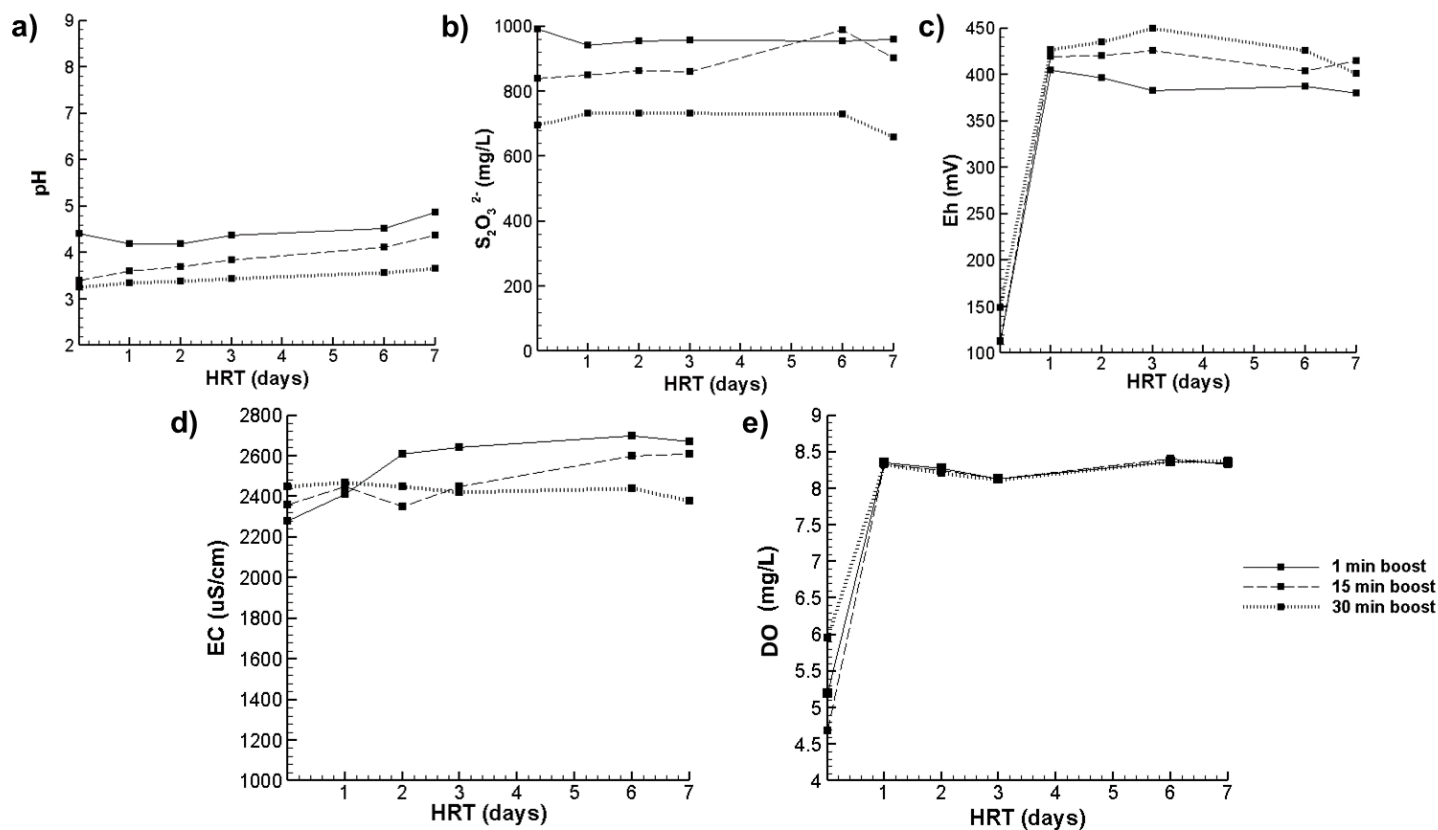


Figure 4.1 Evolution of water parameters for HRTs of 15 min (x-axis = 0) to 7 days, following oxidation “boosts” of 1, 15 and 30 min on S0 (1 g/L $\text{S}_2\text{O}_3^{2-}$).

Table 4.1 Values of all water parameters for oxidation “boosts” of 1, 15 and 30 min on S0, with subsequent HRTs from 15 min (x-axis = 0) to 7 days.

Time of “boost” (min)	Time	pH	Eh (mV)	EC ($\mu\text{S/cm}$)	DO (mg/L)	SO_4^{2-} (mg/L)	$\text{S}_2\text{O}_3^{2-}$ (mg/L)	$\text{S}_4\text{O}_6^{2-}$ (mg/L)
1	0 min	8.92	559	2220	8.62	<1	1002	<1
	After “boost”	4.11	54	2270	3.59	72	992	18
	HRT 15 min	4.40	112	2280	5.20	73	992	17
	HRT 1 day	4.19	405	2410	8.35	70	940	23
	HRT 2 days	4.19	396	2610	8.28	71	953	23
	HRT 3 days	4.37	383	2640	8.13	73	958	24
	HRT 6 days	4.52	387	2700	8.36	67	955	<1
HRT 7 days	4.86	380	2670	8.35	69	959	<1	
15	0 min	8.92	559	2220	8.62	<1	1057	<1
	After “boost”	3.39	80	2370	2.93	218	844	40
	HRT 15 min	3.41	113	2360	4.68	218	840	40
	HRT 1 day	3.61	419	2450	8.32	214	849	21
	HRT 2 days	3.70	420	2350	8.25	219	863	20
	HRT 3 days	3.84	426	2450	8.13	226	859	67
	HRT 6 days	4.11	404	2600	8.40	251	988	17
HRT 7 days	4.37	415	2610	8.33	248	903	<1	
30	0 min	8.92	559	2220	8.62	<1	1044	<1
	After “boost”	3.26	126	2450	4.46	379	696	62
	HRT 15 min	3.26	149	2450	5.96	378	694	60
	HRT 1 day	3.35	427	2470	8.32	382	732	14
	HRT 2 days	3.38	435	2450	8.21	385	731	<1
	HRT 3 days	3.43	450	2420	8.12	390	732	10
	HRT 6 days	3.56	426	2440	8.36	396	730	10
HRT 7 days	3.66	401	2380	8.38	386	659	24	

These findings suggest that the electrochemical reaction time cannot be reduced, without compromising thiosalts removal efficiency, in synthetic effluents, in the sole presence of thiosalts. Oxidation “boosts” on complex, real mine effluents could show different results. For example, oxidative Cl^- species (HClO , ClO^- , ClO_3^- and/or ClO_4^-) formed via Cl^- oxidation at the BDD anode, could allow for thiosalts oxidation, even after the electrochemical reaction is stopped. Further explanations with this focus are provided in **Chapter 5**.

The freeze concentration effect, described in detail in **Chapter 2**, could also allow for thiosalts removal following oxidation “boosts”. It was found that the rate of the freezing reaction between $\text{S}_2\text{O}_3^{2-}$ and H_2O_2 was 20x faster than that of the reaction at room temperature, due to the confinement of the reactants in the boundaries of ice crystals during freezing (Takenaka et al., 1996; Sato et al., 2002). Further testing to evaluate the impact of the freeze concentration effect on thiosalts removal after oxidation “boosts” are required to evaluate the possibility of reducing treatment time and operating costs.

4.2 EF treatment of synthetic and real mine effluents

4.2.1 Initial physicochemical characterization

4.2.1.1 Real effluents E2 and E3

Results of the physicochemical characterization of real effluents E2 and E3 showed that E2 was more contaminated than E3 (**Table 4.2**). The pH of both effluents only differed slightly (0.28 units), but E2 contained 100%, 78%, 73%, 100% and 68% more $\text{S}_2\text{O}_3^{2-}$, SO_4^{2-} , Cl^- , Br^- and NO_3^- , than E3, respectively (**Table 4.2**). Despite the absence of $\text{S}_2\text{O}_3^{2-}$ in E3, treatability tests were performed on the effluent and its corresponding synthetic effluent with the aim to further investigate EF treatment mechanisms. Both effluents contained negligible concentrations of metals, including acidogenic metals and are not presented in **Table 4.2**. Fluoride, NO_2^- , PO_4^{3-} , CNO^- and SCN^- concentrations decreased below the detection limit of the analysis method for all effluents and were also excluded for simplification purposes.

4.2.1.2 Synthetic effluents

Synthetic effluent S1 was prepared to have the same $S_2O_3^{2-}$ concentration and pH as effluent E1. The target $S_2O_3^{2-}$ concentration in S1 was 219 mg/L, and the target pH was 2.84. Results of the characterization at $t = 0$ min showed that the synthetic effluent contained 228 mg/L $S_2O_3^{2-}$ and the pH of the solution was of 3.12 (**Table 4.2**). The Cl^- concentration of both solutions differed by 94% (497 ± 23.8 mg/L for E1 vs. 29.1 mg/L for S1) since Cl^- were not considered as constituents of the matrix taking part in the EF process at the time. Results from further investigations showed that the presence of Cl^- greatly influences $S_2O_3^{2-}$ oxidation mechanisms and kinetics during EF treatment (**Section 4.4**).

Effluent E2 contained 32 mg/L $S_2O_3^{2-}$ and showed an initial pH of 8.43. Initially, synthetic effluent S2 was prepared to match both the $S_2O_3^{2-}$ concentration and pH of E2, but the EC of S2 was too low (resistivity too high) and a current could not be generated. Then, NaCl was added to the solution until the EC matched that of E2. Synthetic effluent S2, which contained 26 mg/L $S_2O_3^{2-}$ and showed an initial pH of 7.62, had an EC similar to that of E2 (1580 $\mu S/cm$ vs 1647 $\mu S/cm$ for E2 and S2, respectively), but contained 57% more Cl^- than E2 (**Table 4.2**).

Considering that $S_2O_3^{2-}$ were absent from E3, synthetic effluent S3 was prepared to have a pH and an EC matching that of E3, which were of 8.15 and 535 $\mu S/cm$, respectively (**Table 4.2**). First, NaOH was added to S3 to increase the pH of the solution, without increasing the buffering capacity of the effluent. Then, NaCl was added to the solution to match the EC of E3, resulting in a solution with a pH of 8.37 and an EC of 596 $\mu S/cm$ (**Table 4.2**). The Cl^- concentration of S3 was 69% higher than that of E3 (**Table 4.2**), attributable to the addition of NaCl.

In some cases, $S_4O_6^{2-}$ was not monitored, due to the unavailability of the measuring device when the treatability tests were performed (**Table 4.2**). Moreover, as seen during the treatment of E1 and E2, and consistent with the literature, $S_4O_6^{2-}$ was either absent during treatment, or only present negligibly, relative to $S_2O_3^{2-}$, for a brief period (Forsberg, 2011; Miranda-Trevino et al., 2013; Range and Hawboldt, 2019; Olvera-Vargas et al., 2021). In the case of S3 and S3+alk, $S_2O_3^{2-}$ and $S_4O_6^{2-}$ were not measured due to their absence from the initial solution (**Table 4.2**).

Table 4.2 Physicochemical parameters of real and synthetic effluents before, during and after treatment

Step (refer to Fig. 3.2)	Effluent code	Sampling time (min)	pH	Eh (mV)	EC ($\mu\text{S/cm}$)	Acidity (mg CaCO_3/L)	Alkalinity (mg CaCO_3/L)	Cl ⁻ (mg/L)	Br ⁻ (mg/L)	NO ₃ ⁻ (mg/L)	SO ₄ ²⁻ (mg/L)	S ₂ O ₃ ²⁻ (mg/L)	S ₄ O ₆ ²⁻ (mg/L)
1b	E1	0	2.84 ± 0.05	417 ± 43	4053 ± 353	111**	N/A	497 ± 23.8	14.1 ± 4.2	73.7 ± 7.9	738 ± 17	219 ± 21	<1
		15	2.61 ± 0.04	n/a	n/a	n/a	N/A	490 ± 8.2	23.6 ± 3.3	72.5 ± 2.9	904 ± 22	149 ± 22	<1
		30	2.61 ± 0.11	n/a	n/a	n/a	N/A	471 ± 9.7	33.3 ± 2.8	71.4 ± 1.9	966 ± 44	80 ± 22	<1
		60	2.44 ± 0.11	n/a	n/a	n/a	N/A	469 ± 9.7	64.1 ± 2.7	74.5 ± 2.0	1150 ± 39	9 ± 16	<1
		90	2.39 ± 0.11	n/a	n/a	n/a	N/A	435 ± 20.4	99.2 ± 7.3	73.2 ± 3.9	1156 ± 61	<1	<1
		120	2.42 ± 0.10	736 ± 24	4667 ± 586	n/a	N/A	409 ± 20.9	138 ± 7.4	70.4 ± 4.7	1152 ± 53	<1	<1
	E2	0	8.43	444	1580	N/A	26	215	8.0	41.1	497	32	<1
		15	3.29	n/a	n/a	n/a	N/A	205	38.9	44.0	602	<1	<1
		30	3.01	n/a	n/a	n/a	N/A	187	58.9	43.4	599	<1	<1
		60	3.02	n/a	n/a	n/a	N/A	167	100.3	42.4	614	<1	<1
		90	3.01	n/a	n/a	n/a	N/A	143	138.9	40.9	617	<1	<1
		120	3.03	623	1780	n/a	N/A	119	165.6	39.4	611	<1	<1
	E3	0	8.15	453	535	N/A	45	57.7	<0.7	13.3	110	<1	<1
		15	7.36	n/a	n/a	n/a	n/a	44.8	21.9	13.0	140	<1	<1
		30	7.36	n/a	n/a	n/a	n/a	36.5	29.2	13.0	130	<1	<1
		60	5.00	n/a	n/a	n/a	n/a	25.4	36.1	13.0	130	<1	<1
		90	4.30	n/a	n/a	n/a	N/A	16.7	36.6	13.0	130	<1	<1
		120	4.36	496	530	n/a	N/A	12.0	33.3	13.0	140	<1	<1
1c	S1	0	3.12	515	745	n/a	N/A	29.1	<0.7	N/A	5	228	<1
		0.25	3.28	n/a	n/a	n/a	N/A	25.9	<0.7	N/A	64	183	<1
		3	3.22	n/a	n/a	n/a	N/A	25.7	<0.7	N/A	84	173	<1
		6	3.16	n/a	n/a	n/a	N/A	25.5	<0.7	N/A	105	153	<1
		9	3.11	n/a	n/a	n/a	N/A	24.9	<0.7	N/A	125	143	<1
		12	3.05	n/a	n/a	n/a	N/A	27.6	<0.7	N/A	146	132	<1
		15	3.02	n/a	n/a	n/a	N/A	23.5	<0.7	N/A	165	117	<1
		30	2.79	n/a	n/a	n/a	N/A	21.8	<0.7	N/A	265	50	<1
	60	2.61	731	1586	n/a	N/A	19.4	19.5	N/A	381	<1	<1	
	S2	0	7.62	359	1647	n/a	N/A	502	<0.7	N/A	<1	26	<1
		0.25	3.93	n/a	n/a	n/a	N/A	502	14.0	N/A	41	<1	<1
		3	3.48	n/a	n/a	n/a	N/A	487	18.2	N/A	47	<1	<1
		6	3.35	n/a	n/a	n/a	N/A	481	23.4	N/A	53	<1	<1
		9	3.29	n/a	n/a	n/a	N/A	486	28.9	N/A	59	<1	<1
		12	3.23	n/a	n/a	n/a	N/A	478	34.3	N/A	62	<1	<1
		15	3.18	n/a	n/a	n/a	N/A	464	40.0	N/A	65	<1	<1

Step (refer to Fig. 3.2)	Effluent code	Sampling time (min)	pH	Eh (mV)	EC ($\mu\text{S}/\text{cm}$)	Acidity (mg CaCO_3/L)	Alkalinity (mg CaCO_3/L)	Cl^- (mg/L)	Br^- (mg/L)	NO_3^- (mg/L)	SO_4^{2-} (mg/L)	$\text{S}_2\text{O}_3^{2-}$ (mg/L)	$\text{S}_4\text{O}_6^{2-}$ (mg/L)
1c (cont.)	S2 (cont.)	30	3.23	n/a	n/a	n/a	N/A	453	69.7	N/A	70	<1	<1
		60	3.23	-83	1883	n/a	N/A	452	69.5	N/A	71	<1	<1
	S3	0	8.37	513	596	N/A	n/a	187	<0.7	N/A	<1	N/A	N/A
		0.25	4.80	n/a	n/a	n/a	N/A	205	<0.7	N/A	25.9	N/A	N/A
		3	3.57	n/a	n/a	n/a	N/A	180	10.9	N/A	26.8	N/A	N/A
		6	3.54	n/a	n/a	n/a	N/A	199	16.8	N/A	25.0	N/A	N/A
		9	3.44	n/a	n/a	n/a	N/A	196	21.7	N/A	25.5	N/A	N/A
		12	3.55	n/a	n/a	n/a	N/A	193	27.2	N/A	25.5	N/A	N/A
		15	3.45	n/a	n/a	n/a	N/A	191	33.0	N/A	24.5	N/A	N/A
		30	3.52	n/a	n/a	n/a	N/A	158	55.9	N/A	22.7	N/A	N/A
60	3.64	435	700	n/a	N/A	128	104.6	N/A	22.9	N/A	N/A		
1d	S1+alk	0	7.84	518	617	n/a	42	50.2	<0.7	N/A	<1	206	<1
		0.25	6.76	n/a	n/a	n/a	n/a	34.8	<0.7	N/A	47	188	<1
		3	6.04	n/a	n/a	n/a	n/a	31.4	<0.7	N/A	63	183	<1
		6	4.50	n/a	n/a	n/a	N/A	36.9	<0.7	N/A	76	175	<1
		9	3.89	n/a	n/a	n/a	N/A	28.1	<0.7	N/A	92	165	<1
		12	3.65	n/a	n/a	n/a	N/A	26.4	<0.7	N/A	109	154	<1
		15	3.59	n/a	n/a	n/a	N/A	25.2	<0.7	N/A	125	142	<1
		30	3.26	n/a	n/a	n/a	N/A	24.0	16.7	N/A	217	86	16
	60	2.80	356	1480	n/a	N/A	29.3	22.3	N/A	364	<1	<1	
	S2+alk	0	7.23	280	890	n/a	22	248	<0.7	N/A	6	31	<1
		0.25	6.61	n/a	n/a	n/a	n/a	237	<0.7	N/A	24	19	<1
		3	4.17	n/a	n/a	n/a	N/A	236	16.9	N/A	34	18	<1
		6	3.95	n/a	n/a	n/a	N/A	231	20.6	N/A	40	14	<1
		9	3.81	n/a	n/a	n/a	N/A	223	24.4	N/A	43	10	<1
		12	3.71	n/a	n/a	n/a	N/A	223	29.1	N/A	50	<1	<1
		15	3.66	n/a	n/a	n/a	N/A	217	33.2	N/A	55	<1	<1
		30	3.36	n/a	n/a	n/a	N/A	207	57.7	N/A	77	<1	<1
	60	3.43	717	1123	n/a	N/A	179	105.3	N/A	78	<1	<1	
	S3+alk	0	8.20	479	567	n/a	45	191	<0.7	N/A	<1	N/A	N/A
		0.25	6.69	n/a	n/a	n/a	n/a	184	<0.7	N/A	32	N/A	N/A
		3	6.65	n/a	n/a	n/a	n/a	180	17.1	N/A	24	N/A	N/A
		6	6.83	n/a	n/a	n/a	n/a	177	21.1	N/A	25	N/A	N/A
		9	6.99	n/a	n/a	n/a	n/a	173	25.6	N/A	26	N/A	N/A
		12	7.05	n/a	n/a	n/a	n/a	173	29.9	N/A	24	N/A	N/A
15		7.70	n/a	n/a	n/a	n/a	169	36.8	N/A	25	N/A	N/A	
30	8.09	n/a	n/a	n/a	n/a	154	60.5	N/A	25	N/A	N/A		

Step (refer to Fig. 3.2)	Effluent code	Sampling time (min)	pH	Eh (mV)	EC ($\mu\text{S}/\text{cm}$)	Acidity (mg CaCO_3/L)	Alkalinity (mg CaCO_3/L)	Cl ⁻ (mg/L)	Br ⁻ (mg/L)	NO ₃ ⁻ (mg/L)	SO ₄ ²⁻ (mg/L)	S ₂ O ₃ ²⁻ (mg/L)	S ₄ O ₆ ²⁻ (mg/L)	
	S3+alk (cont.)	60	8.11	273	652	n/a	20	127	108.5	N/A	26	N/A	N/A	
1e	E1+2CaCl ₂ at pH 3	0	3.06	448	5030	111	N/A	1033	9.4	75.2	684	190	n/a	
		0.25	2.92	n/a	n/a	n/a	n/a	N/A	1003	8.9	73.7	667	177	n/a
		3	2.97	n/a	n/a	n/a	n/a	N/A	986	10.4	66.3	691	141	n/a
		6	2.88	n/a	n/a	n/a	n/a	N/A	981	11.0	73.1	759	146	n/a
		9	2.92	n/a	n/a	n/a	n/a	N/A	996	12.5	72.2	715	110	n/a
		12	2.88	n/a	n/a	n/a	n/a	N/A	943	15.8	75.2	760	119	n/a
		15	2.84	n/a	n/a	n/a	n/a	N/A	960	17.5	72.5	746	95	n/a
		30	2.77	n/a	n/a	n/a	n/a	N/A	937	31.1	71.6	811	42	n/a
		60	2.69	681	5950	276	N/A	922	65.1	73.9	916	<1	n/a	
	E1+4CaCl ₂ at pH 3	0	2.82	409	8640	113	N/A	2226	4.0	70.9	724	191	n/a	
		0.25	2.90	n/a	n/a	n/a	N/A	2246	8.2	69.4	695	160	n/a	
		3	2.85	n/a	n/a	n/a	N/A	2205	9.2	68.8	717	143	n/a	
		6	2.83	n/a	n/a	n/a	N/A	2223	10.2	66.2	760	126	n/a	
		9	2.85	n/a	n/a	n/a	N/A	2226	12.2	71.1	782	118	n/a	
		12	2.77	n/a	n/a	n/a	N/A	2226	12.3	62.2	707	91	n/a	
		15	2.79	n/a	n/a	n/a	N/A	2218	14.7	65.7	768	90	n/a	
		30	2.69	n/a	n/a	n/a	N/A	2210	27.4	71.2	909	34	n/a	
		60	2.59	667	9730	276	N/A	2202	52.5	71.9	980	<1	n/a	
	E1+2CaCl ₂ at pH 5	0	5.27	401	4780	19	4	1055	14.9	75.5	840	190	n/a	
		0.25	3.42	n/a	n/a	n/a	N/A	993	17.1	75.4	1011	159	n/a	
		3	3.26	n/a	n/a	n/a	N/A	1074	19.2	76.8	948	139	n/a	
		6	3.15	n/a	n/a	n/a	N/A	1056	21.8	72.2	962	126	n/a	
		9	3.09	n/a	n/a	n/a	N/A	948	22.5	83.6	877	104	n/a	
		12	3.03	n/a	n/a	n/a	N/A	953	24.8	83.5	922	94	n/a	
		15	2.98	n/a	n/a	n/a	N/A	949	27.4	83.3	1030	82	n/a	
		30	2.83	n/a	n/a	n/a	N/A	921	41.8	84.5	1076	24	n/a	
		60	2.70	722	5610	163	N/A	921	76.7	88.4	1264	<1	n/a	
	E1+4CaCl ₂ at pH 5	0	5.17	414	7890	19	4	2321	12.8	79.2	869	199	n/a	
		0.25	3.53	n/a	n/a	n/a	N/A	2322	13.9	69.0	907	183	n/a	
		3	3.33	n/a	n/a	n/a	N/A	2322	15.0	79.6	967	153	n/a	
		6	3.19	n/a	n/a	n/a	N/A	2320	15.9	78.4	986	150	n/a	
		9	3.11	n/a	n/a	n/a	N/A	2324	16.9	70.6	976	133	n/a	
		12	3.12	n/a	n/a	n/a	N/A	2329	18.2	71.0	917	114	n/a	
		15	3.05	n/a	n/a	n/a	N/A	2317	19.9	71.2	1019	78	n/a	
		30	2.86	n/a	n/a	n/a	N/A	2316	30.1	72.1	1155	<1	n/a	

Step (refer to Fig. 3.2)	Effluent code	Sampling time (min)	pH	Eh (mV)	EC ($\mu\text{S}/\text{cm}$)	Acidity (mg CaCO_3/L)	Alkalinity (mg CaCO_3/L)	Cl^- (mg/L)	Br^- (mg/L)	NO_3^- (mg/L)	SO_4^{2-} (mg/L)	$\text{S}_2\text{O}_3^{2-}$ (mg/L)	$\text{S}_4\text{O}_6^{2-}$ (mg/L)
	E1+4 CaCl_2 at pH 5 (cont.)	60	2.78	736	8750	172	N/A	2303	58.7	74.2	1226	<1	n/a

Legend: n/a = not analyzed; N/A = not applicable

** Acidity was only measured once, prior to testing in triplicates.

4.2.2 Evolution of pH and S species during treatment

4.2.2.1 E1 vs. S1

The trends of $S_2O_3^{2-}$ removal were comparable for S1 and E1: 29% $S_2O_3^{2-}$ was removed from E1 in 15 min, whereas 48% $S_2O_3^{2-}$ was removed from S1. After 30 min, 66% and 78% $S_2O_3^{2-}$ removal was achieved in E1 and S1, respectively. The slight differences at 15 and 30 min could be attributable to the differences in the composition of both solutions, the real effluent containing species which could slow down $S_2O_3^{2-}$ oxidation kinetics. In addition, E1 was the first of the 4 effluents to be treated and the differences could be explained by the fact that the manipulations were improved as the project progressed and experience was acquired. Complete $S_2O_3^{2-}$ oxidation was reached, in both effluents, after 60 minutes of treatment, in agreement with increasing SO_4^{2-} concentrations (Fig. 4.2, Table 4.2).

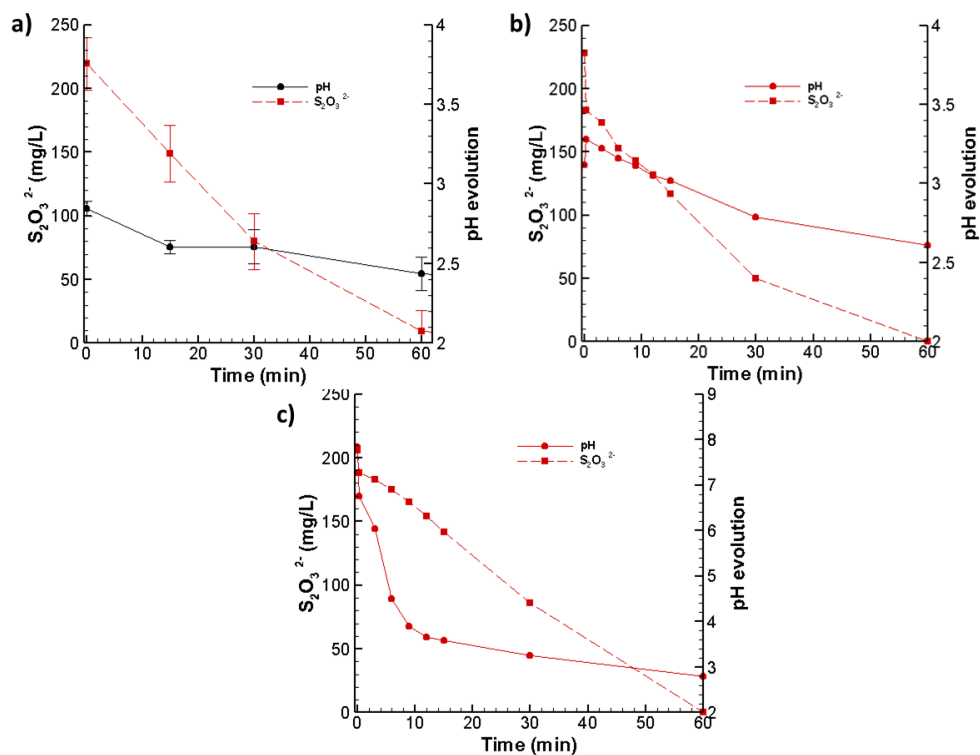


Figure 4.2 pH and $S_2O_3^{2-}$ evolution during EF treatment of (a) E1, (b) S1 and (c) S1+alk.

The percentage of S recovered in the form of SO_4^{2-} for E1 and S1 were of 93% and 97%, respectively, highlighting the outstanding potential of EF for fast, efficient, and complete thiosalts oxidation, compared to other AOPs. The high oxidation capacity of EF is, in part, attributable to the two pathways through which $\cdot\text{OH}$ can be generated: (1) directly at the anode surface via oxidation of H_2O and (2) indirectly via the reaction between Fe^{2+} and H_2O_2 , known as the Fenton reaction, which dominates $\text{S}_2\text{O}_3^{2-}$ oxidation pathways, according to a recent study (Olvera-Vargas et al., 2021). As a basis of comparison, treatment by H_2O_2 resulted in the incomplete oxidation of thiosalts after several days, as shown by the discrepancies in recovered S during the preliminary work (Gervais et al., 2021). The pH evolution during treatment was also comparable, only slightly decreasing and reaching a final value of ~ 2.5 , for both the synthetic and real effluent (**Fig. 4.2, Table 4.2**).

4.2.2.2 E2 vs. S2

During the treatment of E2, the pH was monitored at several times between 0 and 15 min using pH paper to avoid stopping the electrochemical reaction too often to insert the pH probe in the electrochemical cell (**Fig. 4.3**). The aim was to determine if a major pH variation would occur before 15 min, since the effluent contained very low amounts of $\text{S}_2\text{O}_3^{2-}$. The pH dropped from mildly basic to acidic within only 15 seconds. As a result, during the treatment of S2, 5 mL of the solution were sampled at 15 seconds and the pH was measured using a pH probe. Findings were consistent with the observations for E2, with the pH dropping by 3.69 units (from 7.62 to 3.93) in only 15 seconds. This rapid drop could be explained by the accumulation of H_2O_2 inside the cell, during the first 5 minutes of electrolysis, before the addition of Fe^{2+} (not shown in **Fig. 4.4**). When Fe^{2+} was added, its reaction with the H_2O_2 would have been instantaneous, producing a maximum $\text{HO}\cdot$ available to react with the $\text{S}_2\text{O}_3^{2-}$, resulting in a drastic pH drop. Complete $\text{S}_2\text{O}_3^{2-}$ removal ($> 99\%$) was achieved after 15 sec of treatment, in both waters (**Fig. 4.4, Table 4.2**). S recovered as SO_4^{2-} was of 90% for E2 and 102% for S2, most likely attributable to the measurement error in IC ($\pm 15\%$).

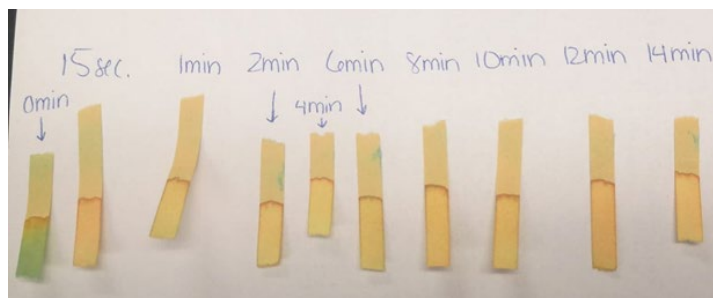


Figure 4.3 pH evolution of E2, between 0 and 15 min, during EF treatment.

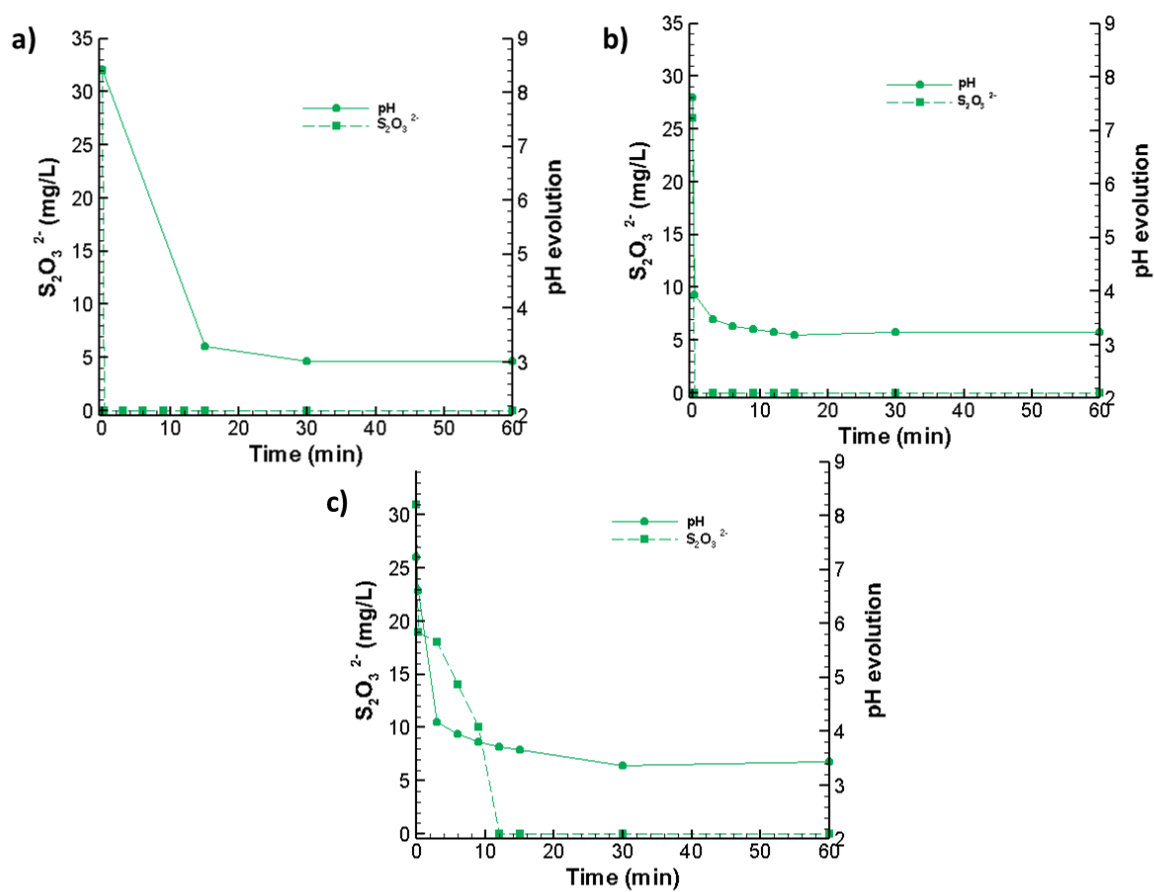


Figure 4.4 pH and $S_2O_3^{2-}$ evolution during EF treatment of (a) E2, (b) S2 and (c) S2+alk.

4.2.2.3 E3 vs. S3

During the treatment of E3, the pH went from 8.15 initially to 4.36 after 120 min of reaction, representing a drop of ~ 4 units, despite the absence of $\text{S}_2\text{O}_3^{2-}$ (**Fig. 4.5**, **Table 4.2**). This observation could potentially be attributed to the oxidation of Cl^- , which was, according to the physicochemical characterization, the only major oxidizable constituent of the matrix identified.

Several studies have reported that the oxidation of Cl^- by free radicals is very likely to occur in EAOPs, forming more reactive Cl^- species through a series of successive and simultaneous reactions, such as chlorates (ClO_3^-), chlorites (ClO_2^-), and perchlorates (ClO_4^-). This process, presented in detail in **Chapter 5**, produces acidity and could explain the pH drop (Bergmann et al., 2014; Olvera-Vargas et al., 2021). This hypothesis was confirmed by decreasing Cl^- concentrations (from 57.7 initially to 12.0 mg/L after 120 min; **Table 4.2**) during treatment, accompanied by increasing Br^- concentrations (from <0.7 mg/L initially to 33.3 mg/L after 120 min; **Table 4.2**). Studies using different mobile phases (KOH gradient and 9.0 mM Na_2CO_3), during IC analysis of inorganic ions, have shown that Br^- and ClO_3^- are eluted one after the other, with peaks separated by a small distance (Ronkart, 2016; Thomas and Rohrer, 2016). Several factors can influence retention times during analysis in IC and the increase of Br^- concentrations during treatment, despite its absence in the initial solution, could be attributed to the formation of ClO_3^- . The method used during this project was not adapted to quantify ClO_3^- and could have been identified as Br^- by the software. As a result, Br^- concentrations were used as an indicator of ClO_3^- formation thereafter.

To verify this hypothesis, EF treatability tests were performed on S3, which was essentially saline water, in which Cl^- was also the only oxidizable constituent of the matrix (**Table 4.2**). Results showed that the pH dropped by ~ 4 units after only 15 sec of treatment compared to 120 min for E3 (**Fig. 4.5**). Initially, it was thought that the lower alkalinity of S3 compared to E3 could explain why the pH drop occurred more rapidly in S3. Theoretically, results should have been the same as those for E3 when alkalinity was added to S3 (S3+alk). Results shown in **Fig. 4.5** suggest that another component of the matrix was responsible for the pH decrease in E3, since there was no net pH variation in S3+alk. Further details on the influence of alkalinity during treatment are presented in **Section 4.3**.

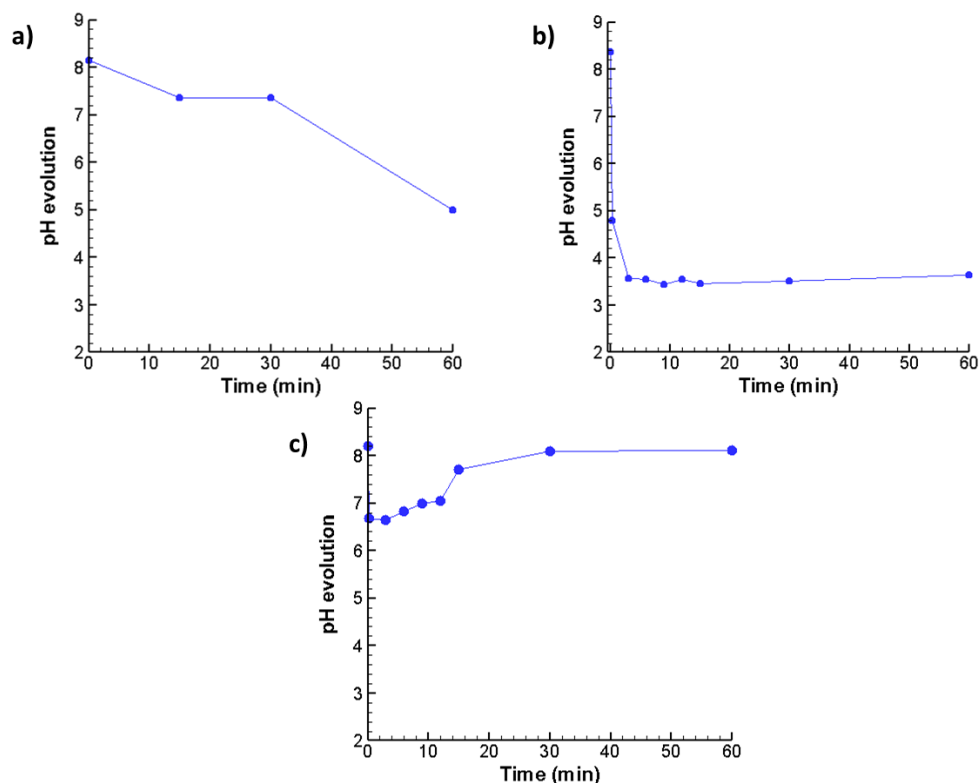


Figure 4.5 pH evolution during EF treatment of (a) E3, (b) S3 and (c) S3+alk.

4.3 Effect of alkalinity

To evaluate the impact of alkalinity on the performance of EF for thiosalts removal in S1, the alkalinity and the pH of the solution had to be fixed at the same values as the ones of E1 upon reception, in 2018, due to the oxidation of thiosalts during its preservation (from 653 in 2018 to 219 ± 21 mg/L in 2020; **Table 4.2**), which resulted in the depletion of alkalinity by 2020. The target $S_2O_3^{2-}$ concentration remained that of E1 in 2020 for comparison purposes. Results showed that the pH after treatment is acidic, independent of the initial pH (**Fig. 4.2**). After 15 min of treatment, $S_2O_3^{2-}$ concentrations in E1, S1 and S1+alk were of 149 ± 22 mg/L, 117 mg/L and 142 mg/L, respectively (**Table 4.2**). After 30 min of treatment, $S_2O_3^{2-}$ concentrations in E1, S1 and

S1+alk were of 80 ± 22 mg/L, 50 mg/L and 86 mg/L, respectively, highlighting the faster thiosalts oxidation kinetics in S1 without alkalinity in the first 30 min of treatment (**Table 4.2**). Regardless of the presence or absence of alkalinity, 60 min of treatment was sufficient for complete $S_2O_3^{2-}$ removal ($> 99\%$) in E1, S1 and S1+alk (**Table 4.2; Fig. 4.2**). The faster $S_2O_3^{2-}$ removal in S1 could be attributed to the absence of $\cdot OH$ -consuming species (other than $S_2O_3^{2-}$) in the solution matrix of S1, compared to E1 and S1+alk. For instance, E1 contained 497 ± 24 mg/L Cl^- (**Table 4.2**) which consume $\cdot OH$ radicals during EF, forming oxidative Cl^\cdot species (Olvera-Vargas et al., 2021). Further details on the impact of chlorinated salinity are presented in **Section 4.4**. Thiosalts oxidation kinetics in S1+alk, for the first 30 minutes, were comparable to that of E1 potentially due to the presence of CO_3^{2-} in both solutions, which are known to be free radical scavengers. A recent study stated that the carbonate-radical-anion ($CO_3^{\cdot-}$), resulting from the reaction of CO_3^{2-} with $\cdot OH$, is the active oxidizing product in neutral solutions containing HCO_3^- even at very low concentrations (Illés et al., 2018). In basic media, the redox potentials of $CO_3^{\cdot-}$ and $\cdot OH$ are of 1.57 V (Patra et al., 2020) and 1.89 V (Sharma, 2011), respectively. Considering that the initial pH of S1+alk was of 7.84 (**Table 4.2**), $S_2O_3^{2-}$ oxidation would have been governed by $CO_3^{\cdot-}$, until the pH became acidic (between 3 and 6 min), explaining the lower thiosalts concentration in S1+alk compared to S1 at 30 min.

Results obtained for the treatment of E2 and its corresponding synthetic effluents S2 and S2+alk confirm the above observations for E1, S1 and S1+alk. As shown in **Fig. 4.4c**, complete $S_2O_3^{2-}$ removal ($> 99\%$) was achieved after 12 min of treatment in S2+alk, compared to 15 sec for S1, indicating that CO_3^{2-} alkalinity increases treatment time during EF.

Considering the absence of thiosalts in E3, the effect of alkalinity on the pH variation during treatment was evaluated. For E3, a pH drop of ~ 3 units was observed after 60 min of treatment (**Fig. 4.5a**), whereas the same pH drop was observed in S3 after only 15 sec (**Table 4.2; Fig. 4.5b**). Initially, the buffering capacity of E3 attributed to the presence of alkalinity could explain the difference in pH drops between E3 and S3, but no net pH variation after 60 min of treatment when alkalinity was added to S3 was found (**Fig. 4.5c**). Since S3 contained 70% more Cl^- than E3, and Cl^- oxidation produces acidity following a series of reactions (detailed in **Chapter 5**), Cl^\cdot were also considered as a possible explanation for the inconsistent pH trends

observed between E3 and S3. In this context, E3 seems to contain an unidentified acidity-producing species, other than Cl^- and $\text{S}_2\text{O}_3^{2-}$, which could potentially be xanthates.

4.4 Effect of chlorinated salinity

The effect of chlorinated salinity on the performance of EF for thiosalts removal was also evaluated. The Cl^- concentration in effluent E1 was spiked at 2 and 4 g/L CaCl_2 , at pH 3 and pH 5, and the resulting solutions were treated as per usual. Results showed that $\text{S}_2\text{O}_3^{2-}$ removal was faster at pH 5 than pH 3 (**Fig. 4.6a**). In addition, $\text{S}_2\text{O}_3^{2-}$ oxidation also seemed to occur more rapidly at 4 g/L CaCl_2 than at 2 g/L CaCl_2 , with unmodified E1 showing the lowest $\text{S}_2\text{O}_3^{2-}$ oxidation kinetics (**Fig. 4.6a**). Faster oxidation kinetics at higher Cl^- concentrations was independent of the formation of oxidative Cl^- species, since Cl^- concentrations remained stable, overall, throughout the entire treatment, for all tests performed (**Fig. 4.6c**). Results based on the direct oxidation of $\text{S}_2\text{O}_3^{2-}$ at the anode surface vs indirect oxidation via the Fenton reaction could not be discussed since H_2O_2 concentrations were not measured in the present study. Interestingly, it was concluded in the preliminary work that that the main oxidants implicated during EF, when BDD anodes are used, are homogeneous $\cdot\text{OH}$ (generated via the Fenton reaction) and heterogeneous BDD($\cdot\text{OH}$), were both equally efficient and both participate indistinctively in the oxidation of $\text{S}_2\text{O}_3^{2-}$ (Olvera-Vargas et al., 2021).

In a recent study, a mixture of 6 organic contaminants was treated by photo-Fenton, at pH 3.0 and 5.0, in water containing 0, 1 and 30 g/L NaCl (Vallés et al., 2021). Consistently, oxidation kinetics were faster at 1 g/L relative to 0 g/L NaCl, and at pH 5.0 vs pH 3.0. Yet, the treatment was slower at extreme concentrations of Cl^- (30 g/L NaCl). These findings could be explained by the availability of Fe^{2+} ions in the Fenton reaction and produced hydroxyl radicals, which decrease at acidic pH in the presence of Cl^- . In the absence of Cl^- , the Fenton reaction is optimal at pH 2.8–3.0 as dissolved Fe^{2+} concentration is maximum (Brillas et al., 2009). In the presence of Cl^- , when the Cl^- concentration exceeds the OH^- , Fe-Cl complexation is favored (Vallés et al., 2021) and the Fe^{2+} becomes unavailable. Since OH^- ions have more affinity for Fe^{2+} than Cl^- , increasing the pH

favors the decomplexation of Fe-Cl complexes. Dissolved Fe^{2+} concentrations would be higher at pH 5 than at pH 3, explaining the tendencies observed in Fig. 4.6.

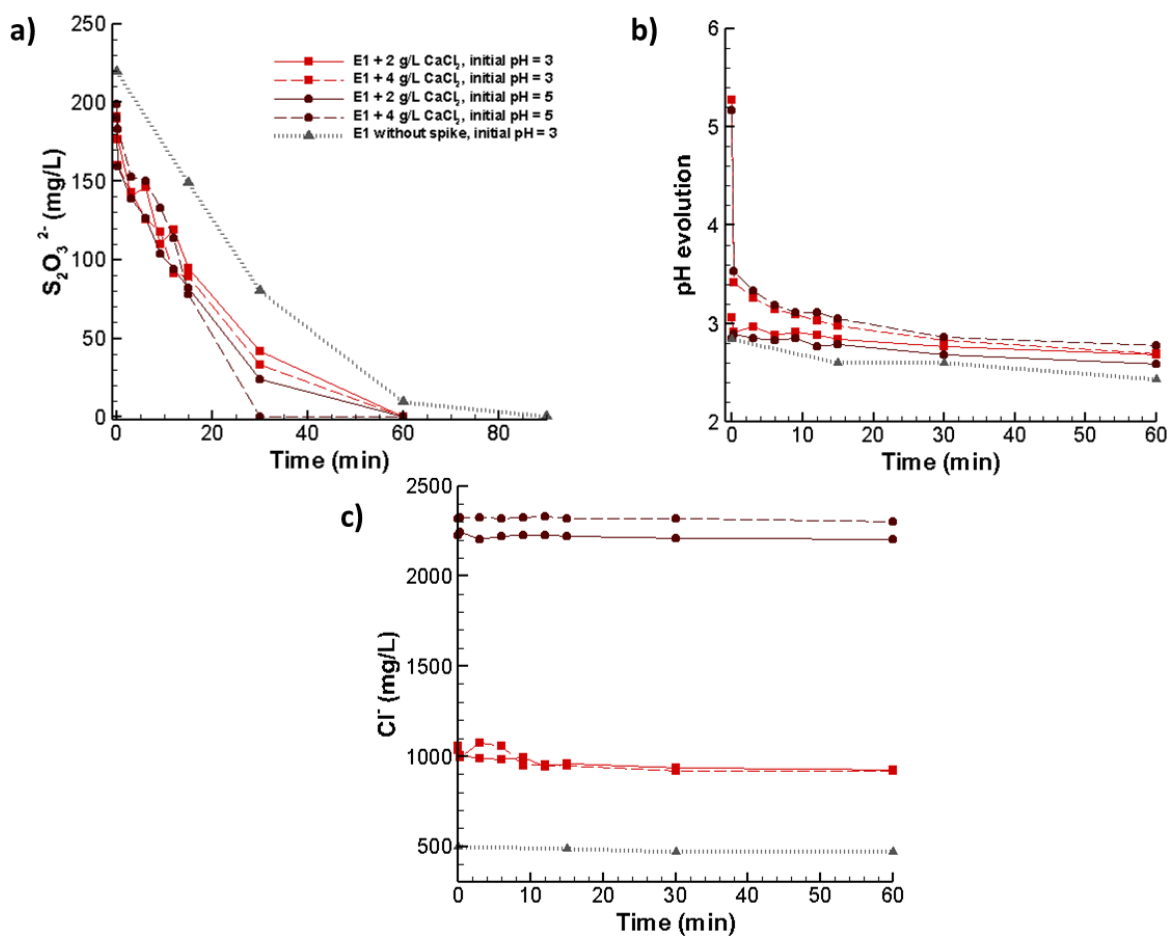


Figure 4.6 Effect of chlorinated salinity, at 2 g/L and 4 g/L CaCl_2 , on EF treatment in effluent E1, at pH 3 and 5. (a) $\text{S}_2\text{O}_3^{2-}$ removal, (b) pH evolution and (c) Cl^- concentration.

**CHAPTER 5 ARTICLE 1 ELECTRO-FENTON TREATMENT OF
CONTAMINATED MINE WATER TO DECREASE THIOSALTS
TOXICITY TO *DAPHNIA MAGNA***

Jennifer Dubuc ^a, Lucie Coudert ^a, Olivier Lefebvre ^b, Carmen M. Neculita ^{a*}

^a Research Institute on Mines and Environment (RIME), University of Québec in Abitibi-Témiscamingue (UQAT), Rouyn-Noranda, QC, Canada. Email: jennifer.dubuc@uqat.ca;
lucie.coudert@uqat.ca; carmen-mihaela.neculita@uqat.ca

^b Centre for Water Research, Department of Civil and Environmental Engineering, National University of Singapore (NUS), Singapore. Email: ceelop@nus.edu.sg

* Corresponding author: Tel.: +1 (819) 762-0971, Ext.: 2278; Fax: +1 (819) 797-4727;

Email: carmen-mihaela.neculita@uqat.ca

Abstract. Treatment of organic contaminants using the electro-Fenton (EF) process is efficient but generates toxic by-products. The aim of the present study was to assess the residual toxicity associated to the treatment of real mine effluents using EF and to perform a preliminary techno-economic analysis to compare the costs of different techniques. Two mine effluents from northern Quebec with different concentrations of thiosalts (ME_{low} and ME_{high}) were tested for acute toxicity to *Daphnia magna*, before and after EF treatment. The higher toxicity of untreated ME_{low} compared to ME_{high}, despite its lower thiosalts content (58 vs 199 mg/L), suggests the presence of an unidentified toxic species, which was removed during EF treatment, or that higher thiosalts concentrations mitigate the toxicity of other toxicants. EF treatment of ME_{high}, initially non-acutely toxic (50% mortality), resulted in the elimination of *D. magna* mortality. A preliminary techno-economic analysis conducted for northern Quebec vs the rest of Canada and the USA showed that energy consumption was the main contributor (52–95%) to the total costs. Electricity-related operating costs nearly doubled (55%) for northern Quebec relative to the rest of Canada. These findings provide new insights for the potential application of the EF for the treatment of thiosalts in mine water, for operations in central jurisdictions and in remote northern areas.

Keywords: thiosalts, advanced oxidation processes, toxicity, mine effluent, operating costs

5.1 Introduction

Thiosalts are metastable and partially oxidized sulfur (S) intermediates formed during ore flotation by the oxidation of sulfidic minerals to sulfate (SO_4^{2-}) in the presence of water and dissolved oxygen (DO) (Miranda-Trevino et al., 2013; Range and Hawboldt, 2019). A case study at Boliden AB (Sweden) revealed that thiosulfate ($\text{S}_2\text{O}_3^{2-}$) was the major thiosalt in mine waters (575 tons discharged per year), followed by tetrathionate ($\text{S}_4\text{O}_6^{2-}$, 135 tons discharged per year) (Forsberg, 2011). Mine operators in northern regions, where cold climate conditions (low temperature, freeze/thaw cycles, strong winds) prevail, also face the impact of seasonal changes on water flow rates and contamination levels (Neculita et al., 2019). As a result, accelerated S oxidation kinetics resulting from freeze/thaw cycles may lead to higher concentrations of thiosalts in mine water (Schudel et al., 2019). Oxidation of thiosalts is a slow, naturally occurring process that may even be halted in cold water ($\leq 4^\circ\text{C}$) (Range and Hawboldt, 2019). The environmental risks of thiosalts are often not directly due to their presence, but indirectly due to the residual acidity generated by the production of H_2SO_4 as the final oxidation product (Miranda-Trevino et al., 2013; Range and Hawboldt, 2019).

Electro-Fenton (EF) has recently emerged as a promising alternative to conventional thiosalts management practices, such as natural attenuation in tailings impoundment facilities, which are not adapted for northern regions (Kuyucak, 2014; Olvera-Vargas et al., 2021). In mine-impacted water, EF recently demonstrated thiosalts removal efficiencies $> 95\%$ after 60 min and $> 99\%$ after 90 min (Olvera-Vargas et al., 2021), an improvement over the performance of other advanced oxidation processes (AOPs) such as H_2O_2 , microbubble ozonation, and ferrates $[\text{Fe}(\text{VI})]$ (Gervais et al., 2020). Moreover, EF efficiency is independent of the water temperature (4 vs 20°C), making

this process relevant to northern climates. The operating costs (OCs) of EF, in terms of reagents and energy consumption (E_{consum}), are also lower than the above-mentioned AOPs (Gervais et al., 2020; Olvera-Vargas et al., 2021).

In general, AOPs can lead to the generation of by-products with higher toxicity than the original contaminants, depending upon the initial wastewater composition (Rueda-Marquez et al., 2020). Therefore, a toxicity assessment of the treated effluent is essential. The few studies that have evaluated the potential of EF treatment at optimal conditions for contaminant removal focused on organic contaminants. The consensus is a lack of correlation between optimal contaminant removal and detoxification (Rueda-Marquez et al., 2020). For example, total chemical oxygen demand (COD) removal from textile industry wastewater led to complete elimination of toxicity to *Aplocheilus panchax* (Kaur et al., 2018), but only a partial decrease in toxicity to *Daphnia magna* (*D. magna*) in another study on azo dyes (Zhuang et al., 2017). Similarly, EF treatment of coking wastewater led to a 60% decrease in toxicity to *Vibrio qinghaiensis* after 50% COD removal (Li et al., 2011), but another study observed a 57% increase in mortality of *Oryzias latipes* after 69% COD removal (Zhu et al., 2013). Therefore, new studies are needed to fill the knowledge gap on the toxicity and potential adverse effects of by-products resulting from EF treatment, especially in mine-impacted water.

In this context, the main objective of the present study was to assess the toxicity of two mine effluents, at low and high concentration (ME_{low} and ME_{high}) to *D. magna*, both before and after EF treatment, under optimal conditions as previously determined (Olvera-Vargas et al., 2021). A preliminary techno-economic analysis was also conducted to estimate OCs in terms of E_{consum} and reagent consumption

5.2 Materials and methods

5.2.1 Mine effluent sampling and characterization

Two mine effluents with different concentrations of thiosalts were collected from operating mine sites in northern Quebec, Canada. Flotation process effluent ME_{high} was sampled in the fall of 2018, for another purpose. Since the effluent was stored and preserved in a closed-lid container at 4°C, thiosalts were not completely oxidized and the effluent was used again for this study. Effluent ME_{low} was sampled in mid-summer 2021, specifically for this study, and was characterized and tested within one week of reception at the laboratory.

All samples were filtered (0.45 µm) and stored at 4°C prior to characterization and testing. The physicochemical characterization consisted of measuring the following parameters: pH, redox potential (ORP), electrical conductivity (EC), acidity, alkalinity, DO, N-NH₃, and anionic species (Cl⁻, Br⁻, NO₃⁻, SO₄²⁻, and S₂O₃²⁻). As the dominant thiosalt species in mine water, S₂O₃²⁻ was selected as the intermediate S species to be monitored ([Miranda-Trevino et al., 2013](#); [Range and Hawboldt, 2019](#)).

The pH was measured with an Orion GD9156BNWP double junction Ag/AgCl electrode (Thermo Fisher Scientific, Canada) connected to a VWR Symphony[®] multi-meter (Canada). The quality of measurements was ensured using a pH 8 standard buffer solution (Thermo Fisher Scientific). Eh (ORP corrected to standard hydrogen electrode) was measured with a VWR double junction Ag/AgCl electrode equipped with a platinum sensor (VWR, Canada). The quality control consisted of a 220 mV ORP Standard (Thermo Fisher Scientific, Canada). EC was measured with a VWR Traceable[®] Expanded Range Conductivity Meter (VWR, Canada) equipped with an epoxy probe. The quality control was a 1413 µS/cm conductivity standard (VWR, Canada). DO was measured

with an HQ40D portable multi-meter (Hach, Canada) equipped with an IntelliCA[®] LDO101 luminescence probe (Hach, Canada). Acidity and alkalinity were measured by titration using an 848 Titrino Plus titrator (Metrohm, Canada). N-NH₃ was measured with an Orion 9512HPBNWP ion selective electrode (Thermo Fisher Scientific, Canada). The quality control was a 10 mg/L ammonia nitrogen solution prepared, in laboratory, using a 1000 mg/L standard concentrate (Thermo Fisher Scientific). The monitoring of all anionic species was carried out by ion chromatography (IC) with an 881 Compact IC Pro instrument (Metrohm, Riverview, FL, USA) equipped with a conductivity detector, an 863 Compact IC Autosampler (Metrohm, Riverview, FL, USA), and a Supp 5 (150 x 4.0 mm) separation column (Metrohm, Riverview, FL, USA). Anions were eluted with a carbonate buffer (1.0 mM NaHCO₃, 3.2 mM Na₂CO₃) at 0.7 mL/min. Quality controls consisted of 6 and 15 mg/L solutions containing all anionic species and prepared from 1000 mg/L standard concentrates (SCP Science, Canada) to ensure the quality of the results.

5.2.2 EF treatment

EF tests were performed in an undivided electrolytic cell containing 0.5 L of ME_{high} or ME_{low}. The operating conditions were optimized in a previous study using synthetic effluents: carbon fiber brush cathode with stainless steel as current collector (3 cm diameter x 8 cm length, 48 cm² of geometric area), single-side coated Nb/boron-doped diamond (BDD) plate anode (100 x 50 x 2 mm; Condias, Germany), current intensity of 0.3 A, and initial Fe²⁺ concentration of 0.2 mM (using FeSO₄•7H₂O). Iron(II) was added ~5 min after the initiation of electrolysis to allow the formation of H₂O₂. The reaction time was started once Fe²⁺ was added to the solution ([Olvera-Vargas et al., 2021](#)). According to this last study, the oxidation of thiosalts by EF proceeds via the accumulation of H₂O₂ inside the cell, produced at the cathode (eq 5.1), followed by its reaction with Fe²⁺ to

produce a maximum of $\cdot\text{OH}$ which are available to oxidize the thiosalts (eq 5.2) or directly with $\text{S}_2\text{O}_3^{2-}$ to produce SO_4^{2-} (eq 5.3). All experiments were conducted at room temperature with continuous stirring and oxygenation using an aquarium pump. Both effluents were treated for 60 min. More details on the mounting of the electrochemical cell are available elsewhere (Olvera-Vargas et al., 2021).



All experiments were conducted at room temperature with continuous stirring and oxygenation using an aquarium pump. Both effluents were treated for 60 min. More details on the mounting of the electrochemical cell are available elsewhere (Olvera-Vargas et al., 2021).

5.2.3 Sample preparation for toxicity tests

Effluents ME_{high} and ME_{low} were treated in triplicate (**Fig. 5.1** – step 1) and mixed into a composite sample (**Fig. 5.1** – step 2) to ensure sufficient volume for the toxicity tests (**Fig. 5.1** – step 4). The pH of the composite sample, which was acidic following oxidation of thiosalts, was adjusted to ~ 7 using soda ash (Na_2CO_3) to comply with effluent discharge requirements according to provincial and federal legislation (JUS, 2002; MELCC, 2012) and to eliminate pH as a factor of toxicity to *D. magna*. Soda ash, which is a common chemical used in mining, was selected as the neutralizing agent to increase both pH and alkalinity. Following pH adjustment, the composite sample was filtered to remove precipitates (**Fig. 5.1** – step 3).

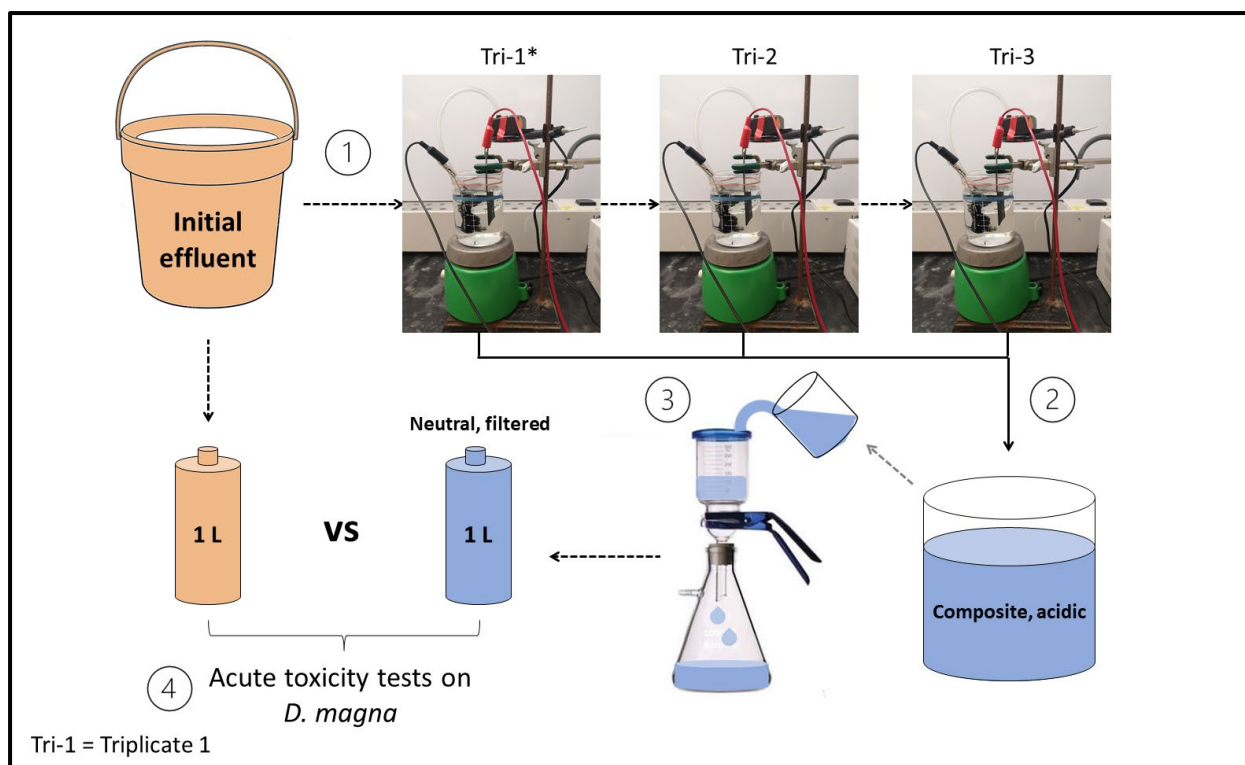


Fig. 5.1 Preparation of effluents for acute toxicity testing on *D. magna*. Step 1 – EF treatment (ME_{high} or ME_{low}), in triplicate. Step 2 – homogenization of triplicates to produce a composite sample. Step 3 – pH adjustment/filtration of the composite sample. Step 4 – pH adjustment/filtration of the initial effluent (ME_{high} only) and acute toxicity testing on *D. magna* using (un-)treated effluents (ME_{high} or ME_{low}).

Acidity, alkalinity, and $N-NH_3$ were only measured for the composite samples to conserve enough volume for toxicity testing. In the case of ME_{high} , the pH of the initial effluent was also adjusted to ~ 7 with Na_2CO_3 and then filtered. ME_{low} was not modified prior to the toxicity tests due to its near-neutral initial pH and the absence of visible mineral precipitates. The relative residual toxicity of both effluents was assessed both before and after treatment following the method described in **Section 5.2.4**.

5.2.4 Toxicity tests

Toxicity tests with *D. magna* were conducted according to the standard analysis method (SPE1/RM/14 – 2nd edition) of the Environmental Technology Centre of Environment Canada (Environment Canada, 2000). Treated and untreated samples were refrigerated immediately upon reception. The next day, the samples were brought to room temperature; pH, temperature, DO, EC, and hardness were measured prior to the start of the tests. The toxicity test consisted of mixing the effluent with dilution water in different proportions (0, 6.25, 12.5, 25, 50, 100% - v/v), with a final volume of 150 mL per container; the diluent was composed of hard water reconstituted in the laboratory to a hardness of 180 mg/L CaCO₃ for *D. magna* viability. The organisms selected for the toxicity tests were neonates (< 24 h old) from a culture of *D. magna* raised in the laboratories of Bureau Veritas (Sainte-Foy, QC, Canada). Ten neonates were added to each container to obtain a density of 15.0 mL/neonate. As per the standard method, the organisms were then exposed to a photoperiod of 16 h in the light and 8 h in the darkness, for 48 h at 20 ± 2 °C (Environment Canada, 2000). After 48 h of incubation, immobile (determined by the inability to swim for 15 sec after a slight agitation of the solution) and dead (determined by the absence of movement of the appendages and antennas, and by the absence of heartbeats) organisms were counted. A positive control was conducted with potassium dichromate as the toxicant. Immediately after counting, the pH, temperature, DO, and EC were measured again for all dilutions, including the control (dilution water). Effluent mixtures causing the mortality of > 50% (LC₅₀) of the *D. magna* population after 48 h of exposure were considered acutely toxic, as defined by Directive 019 (D019) under the Quebec provincial law on the quality of the environment (LQE) and the Metal and Diamond Mining Effluent Regulations (MMER) under the Canadian Fisheries Act (JUS, 2021; MELCC,

2012). Inversely, effluent mixtures causing the mortality of $\leq 50\%$ of the population were considered non-acutely toxic.

5.2.5 Cost calculations

Operating costs (OCs) were estimated in terms of E_{consum} and reagents ($\text{FeSO}_4 \cdot 7\text{H}_2\text{O}$ and Na_2CO_3) for effluents ME_{high} and ME_{low} . The values of all variables used in the model are presented in **Table 5.1**. Results were expressed in CAD\$ and US\$ per m^3 of treated effluent ($\$/\text{m}^3$). Total OCs were also expressed in \$ per kg of thiosalts removed ($\$/\text{kg}$ -thiosalts; eq 5.4) to facilitate the comparison of OCs for effluents containing different initial concentrations of thiosalts, and per order of magnitude of thiosalts removed ($\$/\text{m}^3/\text{order}$; eq 5.5):

$$\text{Total OCs } (\$/\text{kg-thiosalts}) = \frac{(E_{\text{consum}} \text{ cost in } \$/\text{m}^3 + \text{Reagent cost in } \$/\text{m}^3)}{\Delta C_{\text{thiosalts}}} * 1000 \quad (5.4)$$

where $\Delta C_{\text{thiosalts}}$ is the amount of thiosalts removed in mg/L, and

$$\text{Total OCs } (\$/\text{m}^3/\text{order}) = \frac{(E_{\text{consum}} \text{ cost in } \$/\text{m}^3 + \text{Reagent cost in } \$/\text{m}^3)}{\log(C_i/C_f)} \quad (5.5)$$

where C_i and C_f are the initial and final concentrations of thiosalts (mg/L), respectively.

5.2.5.1 Energy consumption

Costs for E_{consum} were calculated by accounting for energy costs for hydroelectric (central jurisdictions of Canada and USA) and diesel (northern QC) power generation, following eqs 5.6–5.7:

$$E_{\text{consum}} \text{ (kWh/m}^3\text{)} = E_{\text{cell}} * I * \text{HRT} / (V * 1000) \quad (5.6)$$

$$E_{\text{consum}} \text{ cost in } \$/\text{m}^3 = E_{\text{consum}} * \text{PPU} \quad (5.7)$$

where E_{cell} is the cell potential in V, I is the current in A, HRT is the hydraulic retention time in h, V is the treated volume in m^3 , and PPU is the price per unit for electricity in $\$/kWh$.

Table 5.1 Variable values in the techno-economic model.

Variable	Value		Ref.
<i>Fixed variables</i>			
Q (m^3/day)	100		--
V (L)	0.5		--
I (A)	0.3		--
$m_{FeSO_4 \cdot 7H_2O}$ (g)	0.03		--
PPU for electricity (CAD\$/kWh)	0.03 ¹		1
PPU for electricity (CAD\$/kWh) in northern QC	0.30 ²		2
PPU for electricity (US\$/kWh)	0.0633 ³		3
PPU for Na_2CO_3 (CAD\$/kWh)	0.21 ⁴		4
PPU for $FeSO_4 \cdot 7H_2O$ (CAD\$/kWh)	0.14 ⁵		5
Currency rate (CAD\$ \rightarrow US\$)	0.7878 ⁶		6
<i>Effluent-dependent variables</i>			
	ME_{high}	ME_{low}	
E_{cell} (V)	6	7.5	--
t (h)	1	0.5	--
C_i (mg/L)	219	58	--
C_f (mg/L)	0.9	0.9	--
$m_{Na_2CO_3}$ (g)	0.221	0.075	--

Legend: N/A = not applicable, Q = flow rate.

- 1) <https://www.hydroquebec.com/business/customer-space/rates/rate-l-industrial-rate-large-power-customers.html> (Accessed September 27, 2021)
- 2) Caron et al. (2021)
- 3) https://www.eia.gov/electricity/sales_revenue_price/pdf/table5_c.pdf (Accessed September 27, 2021)
- 4) https://www.alibaba.com/product-detail/Na2CO3-Na2CO3-99-2-Sodium-Carbonate_1600164656560.html (Accessed September 27, 2021)
- 5) https://www.alibaba.com/product-detail/High-content-factory-sells-98-ferrous_1600310662429.html (Accessed September 27, 2021)
- 6) <https://www.bankofcanada.ca/rates/exchange/currency-converter/> (mean value for 2021; Accessed August 20, 2021)

5.2.5.2 Reagents

Reagent costs ($\text{FeSO}_4 \cdot 7\text{H}_2\text{O}$ as initial Fe(II) source and Na_2CO_3 for post-treatment neutralization) were calculated following eqs 5.8–5.9:

$$C_{\text{reagent}} = m_{\text{reagent}}/V \quad (5.8)$$

$$\text{Reagent cost in } \$/\text{m}^3 = C_{\text{reagent}} * \text{PPU} \quad (5.9)$$

where C_{reagent} is the concentration of reagent in kg/m^3 , m_{reagent} is the mass of reagent in kg, V is the treated volume in m^3 , and PPU is the price per unit of $\text{FeSO}_4 \cdot 7\text{H}_2\text{O}$ or Na_2CO_3 in $\$/\text{kg}$.

5.3 Results and discussion

5.3.1 EF treatment of mine effluents

5.3.1.1 Physicochemical characterization of mine effluents ME_{high} and ME_{low}

Results of the initial physicochemical characterization showed that effluent ME_{low} contained less of all contaminants that were identified than ME_{high} . Effluent ME_{low} contained 58 mg/L $\text{S}_2\text{O}_3^{2-}$ and 595 mg/L SO_4^{2-} , and had an initial pH of 7.3 (**Table 5.2**). In contrast, effluent ME_{high} had initial concentrations of 199 mg/L $\text{S}_2\text{O}_3^{2-}$, 851 mg/L SO_4^{2-} , and a pH of 3.0 (**Table 5.2**). Initial Cl^- and Br^- concentrations were 72% and 34% higher, respectively, in ME_{high} as compared to ME_{low} . The physicochemical characteristics of the effluent matrix seemed to play an important role in $\text{S}_2\text{O}_3^{2-}$ removal mechanisms and kinetics, as discussed **Sections 5.3.1.2 – 5.3.1.4**.

5.3.1.2 Oxidation kinetics of thiosalts

Faster oxidation kinetics (calculated according to eq 5.10) were observed for lower initial $\text{S}_2\text{O}_3^{2-}$ concentrations (0.088/min vs 0.108/min for ME_{high} and ME_{low} , respectively). This observation

could be a consequence of $\cdot\text{OH}$ -consuming intermediates, which are more abundant at higher $\text{S}_2\text{O}_3^{2-}$ concentrations (Olvera-Vargas et al., 2021).

$$k_{\text{app}} t = \ln ([\text{S}_2\text{O}_3^{2-}]_0 / [\text{S}_2\text{O}_3^{2-}]) \quad (5.10)$$

where k_{app} is the kinetic constant and t is time in min.

The evolution of $\text{S}_2\text{O}_3^{2-}$, SO_4^{2-} , and pH during the treatment of ME_{low} is presented in **Figure 5.2a**. In the first 15 s (not visible in **Fig. 5.2a**), $\text{S}_2\text{O}_3^{2-}$ underwent a $14\% \pm 3\%$ decrease and the pH dropped to 4.7 ± 0.2 (SD). The rapid pH and $\text{S}_2\text{O}_3^{2-}$ decrease could be explained by the accumulation of H_2O_2 inside the cell, produced at the cathode (eq 5.1), during the 5 min of electrolysis prior to the addition of Fe^{2+} . The H_2O_2 in excess was then available to react with the Fe^{2+} to produce a maximum of $\cdot\text{OH}$ (eq 5.2) or directly with $\text{S}_2\text{O}_3^{2-}$ (eq 5.3; Gervais et al., 2020), resulting in fast $\text{S}_2\text{O}_3^{2-}$ removal and pH decrease.

Thiosulfate was completely removed from ME_{low} after 30 minutes of treatment (< 1 mg/L) and stoichiometrically converted to SO_4^{2-} , reaching 791 ± 45 mg/L after 30 minutes, indicating that $\text{S}_2\text{O}_3^{2-}$ oxidation was complete.

The initial and final physicochemical characterization of ME_{high} showed that $\text{S}_2\text{O}_3^{2-}$ was completely removed after 60 min of treatment (< 1 mg/L), which agrees with SO_4^{2-} concentrations increasing by 35% over the course of the treatment. Details of the physicochemical evolution of ME_{high} during treatment are reported elsewhere (Olvera-Vargas et al., 2021). The S (92%) was recovered in the form of SO_4^{2-} , likely due to the error on IC measurements (approx. 15% error). The pH decrease during the treatment of both effluents confirmed oxidation of thiosalts and subsequent formation of H_2SO_4 .

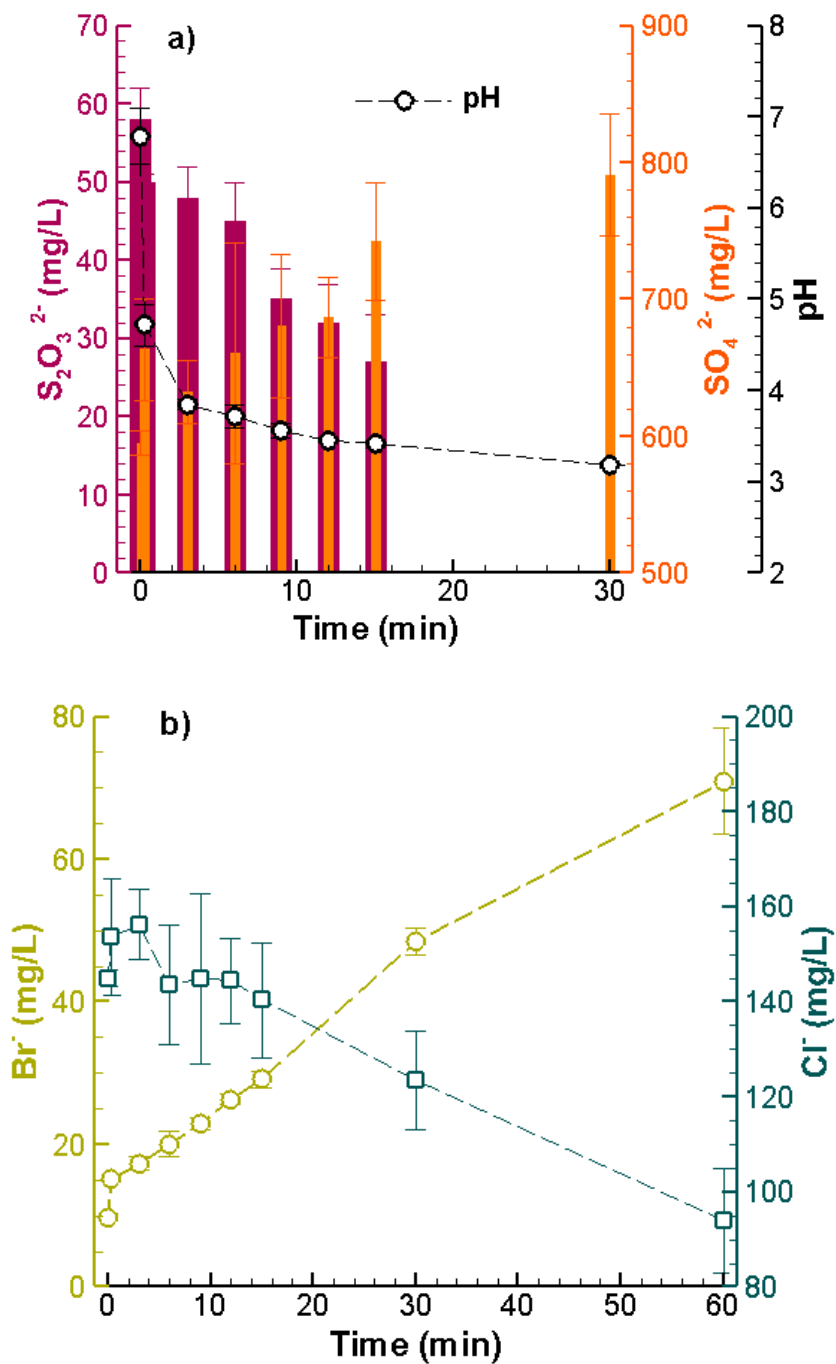


Fig. 5.2 Evolution of various parameters during EF treatment of effluent ME_{low}: (a) $S_2O_3^{2-}$, SO_4^{2-} , pH; (b) Br^- and Cl^- . Evolution of these parameters during EF treatment of effluent ME_{high} are presented elsewhere (Olvera-Vargas et al., 2021)

5.3.1.3 Effect of pH

The acidic pH of ME_{high} (3.0) favored FeSO₄ dissolution from the start, triggering the Fenton reaction, whereas the circumneutral pH of ME_{low} (7.3) was not optimal for FeSO₄ dissolution. Hence, S₂O₃²⁻ treatment may not have been governed by the Fenton reaction in the first seconds, but rather by a combination of direct electron transfer at the anode (eq 5.11) and indirect oxidation via surface-absorbed [•]OH produced at the BDD anode surface (BDD([•]OH); eq 5.12). The BDD([•]OH) oxidation pathway involves a series of complex reactions with the formation of several intermediates, yielding the overall reaction in eq 5.11 (Olvera-Vargas et al., 2021). The S₂O₃²⁻ could also have been oxidized by H₂O₂ produced at the cathode (eq 5.10). A series of disproportionation reactions occurring in acidic media could have also contributed to thiosalts oxidation to a lesser extent (Fig 5.3; Miranda-Trevino et al., 2013; Olvera-Vargas et al., 2021).

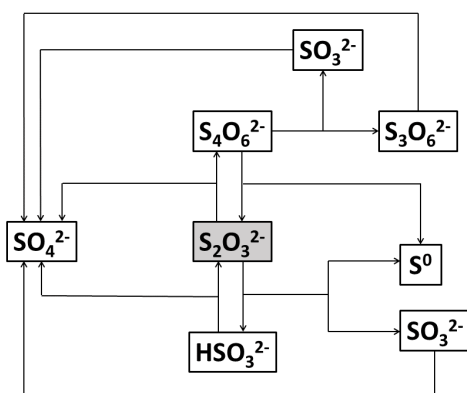


Fig. 5.3 S₂O₃²⁻ disproportionation pathways in acidic media (adapted from Miranda-Trevino et al., 2013)

5.3.1.4 Effect of salinity

After EF treatment, Cl⁻ concentrations decreased by 32 mg/L (6%) and 22 mg/L (15%) for ME_{high} and ME_{low}, respectively. These trends, presented in **Figure 5.2b**, could potentially be attributed to the formation of oxidative Cl⁻ species (HClO, ClO⁻, ClO₂⁻, ClO₃⁻, and/or ClO₄⁻) via Cl⁻ oxidation at the BDD anode, based on eqs 5.13–5.17 (Olvera-Vargas et al., 2021).



Following pH adjustment to neutral, the Cl⁻ concentration in ME_{low} decreased (from 123 ± 10 mg/L to 91.3 mg/L; **Table 5.2**). Initial solutions were treated in triplicates to create the composite sample, which is why the initial concentrations have SDs, whereas the final concentration does not have a SD since measurements were only taken once in the composite sample. These results seem to indicate that ClO₃⁻ was still forming after treatment. The pH evolution of the sample during its transportation (pH = 7.6 and 6.9, before expedition to the external laboratory and immediately before toxicity tests, respectively) also suggests that ClO₃⁻ continued to form after the electrochemical reaction stopped.

Overall, salinity plays a key role in S₂O₃²⁻ oxidation pathways and kinetics. Specifically, Cl⁻ ions can interfere with EF treatment in many ways, which could explain the faster S₂O₃²⁻ oxidation

Table 5.2 Physicochemical parameters of untreated and treated effluents ME_{high} and ME_{low}

Parameter	ME _{high}				ME _{low}		
	Untreated	Untreated, pH adjusted	Treated (n=3)	Treated, pH adjusted (composite sample)	Untreated	Treated (n=3)	Treated, pH adjusted (composite sample)
pH	3.03	7.80	2.68 ± 0.04	7.61	7.33	3.21 ± 0.01	7.62
Eh (mV)	547	197	714 ± 11	221	423	735 ± 5	440
EC (µS/cm)	3230	3010	3957 ± 15	3390	1424	1924 ± 14	1752
DO (mg/L)	9.00	6.00	8.02 ± 0.12	4.86	8.72	7.41 ± 0.72	5.39
Acidity (mg CaCO₃/L)	111	9	n.a.	12	6	n.a.	10
Alkalinity (mg CaCO₃/L)	N/A	60	N/A	137	16	N/A	n.a.
N-NH₃ (mg/L)	<0.15	<0.15	<0.15	<0.15	1.15	<0.15	<0.15
Cl⁻ (mg/L)	510	516	478 ± 2	478	145	123 ± 10	91.3
Br⁻ (mg/L)	14.8	15.4	77.1 ± 0.3	75.0	9.8	48.5 ± 1.9	76.1
NO₃⁻ (mg/L)	83.9	84.8	85.9 ± 0.5	86.0	34.5	35.0 ± 0.7	34.4
SO₄²⁻ (mg/L)	851	862	1313 ± 13	1258	595	791 ± 45	770
S₂O₃²⁻ (mg/L)	199	189	<1	<1	58	<1	<1

Legend: n.a. = not analysed, N/A = not applicable.

Note: metals could not be measured during this study due to the unavailability of the measuring device.

kinetics observed in ME_{low} (0.108/min) compared to that of ME_{high} (0.088/min), which initially contained 145 mg/L and 510 mg/L Cl⁻, respectively. For example, the [•]OH-scavenging effect of Cl⁻ to produce Cl[•] or Cl₂^{•-} (eq 5.18) is known to decrease the efficiency of Fenton-based processes (Vallès et al., 2021).



However, HClO produced via anodic oxidation of Cl⁻ (eqs 5.13–5.17) could participate in S₂O₃²⁻ oxidation and accelerate the process (eq 5.19; Varga et al., 2006).



Cl⁻ oxidation at the BDD anode can also result in the production of BDD(Cl[•]) (eq 5.20) with a redox potential comparable to that of H₂O₂ in acidic media (1.36 vs 1.78 V/SHE for BDD(Cl[•]) and H₂O₂, respectively) (Sharma, 2011; Lan et al., 2017). In this sense, BDD(Cl[•]) can also be involved in oxidation of contaminants.



Moreover, the presence of Cl⁻ at low pH promotes Fe-Cl complexation, decreasing the Fe²⁺ concentration available to participate in the Fenton reaction. With increasing pH, the OH⁻ concentration also increases and Fe-Cl complexation is less favored because OH⁻ ions have more affinity for Fe than Cl⁻ (Brillas et al., 2009; Vallès et al., 2021). Therefore, a higher concentration of Fe²⁺ remains available to catalyze the Fenton reaction. Accordingly, the treatment of ME_{high}, with an initial Cl⁻ concentration approximately 72% higher and an initial pH value 4.3 units lower than that of ME_{low}, was faster from 0 to 15 min (70 mg/L S₂O₃²⁻ removed in ME_{high} vs. 31 mg/L S₂O₃²⁻ removed in ME_{low}). Further research is deemed necessary for a better understanding of the impact of chlorinated salinity on the efficiency of the EF process for S₂O₃²⁻ oxidation.

5.3.2 Toxicity assessment

5.3.2.1 Effect of EF treatment on the mortality of *D. magna* in (un-)treated ME_{high} and ME_{low}

The pH of all acidic samples was adjusted to neutral using Na₂CO₃; these samples were subsequently filtered (0.45 μm). The physicochemical parameters of ME_{high} and ME_{low}, both before and after treatment, prior to their expedition to the external laboratory for toxicity testing, are presented in **Table 5.2**. The pH and EC measurements prior to toxicity testing showed negligible variation of water parameters during transportation. The only exception was the pH of effluent ME_{low}, as discussed in **section 5.3.1.4**.

Results showed that the mortality of *D. magna* decreased after EF treatment for both effluents (**Fig. 5.4**). Indeed, prior to treatment ME_{high} showed 10% *D. magna* mortality at a dilution of 25% (v/v), reaching 50% mortality in the undiluted effluent (100% - v/v). In the case of untreated ME_{low}, mortality spiked from 0 to 70% when the effluent dilution increased from 25 to 50% (v/v). Mortality reached its peak at 90% in the undiluted effluent (100% - v/v). Remarkably, there was a total absence of mortality in ME_{high} and ME_{low} after treatment for all effluent concentrations tested. Because the pH was eliminated as a factor of toxicity to *D. magna* following neutralization, it can be concluded that toxic by-products were not generated during EF treatment for either effluent.

5.3.2.2 Acute toxicity of (un-)treated ME_{high} and ME_{low} to *D. magna*

Effluent ME_{high} (**Fig. 5.4a**) showed an LC₅₀ > 100% (v/v), which is equivalent to < 1 acute toxic units (TUa; defined as 100/LC₅₀; [MMER, 2012](#)). As such, despite showing increasing mortality with increasing effluent concentration, ME_{high} was not acutely toxic before treatment. In contrast, with an LC₅₀ of 48% (v/v) (equivalent to 2.07 TUa), ME_{low} was acutely toxic before treatment

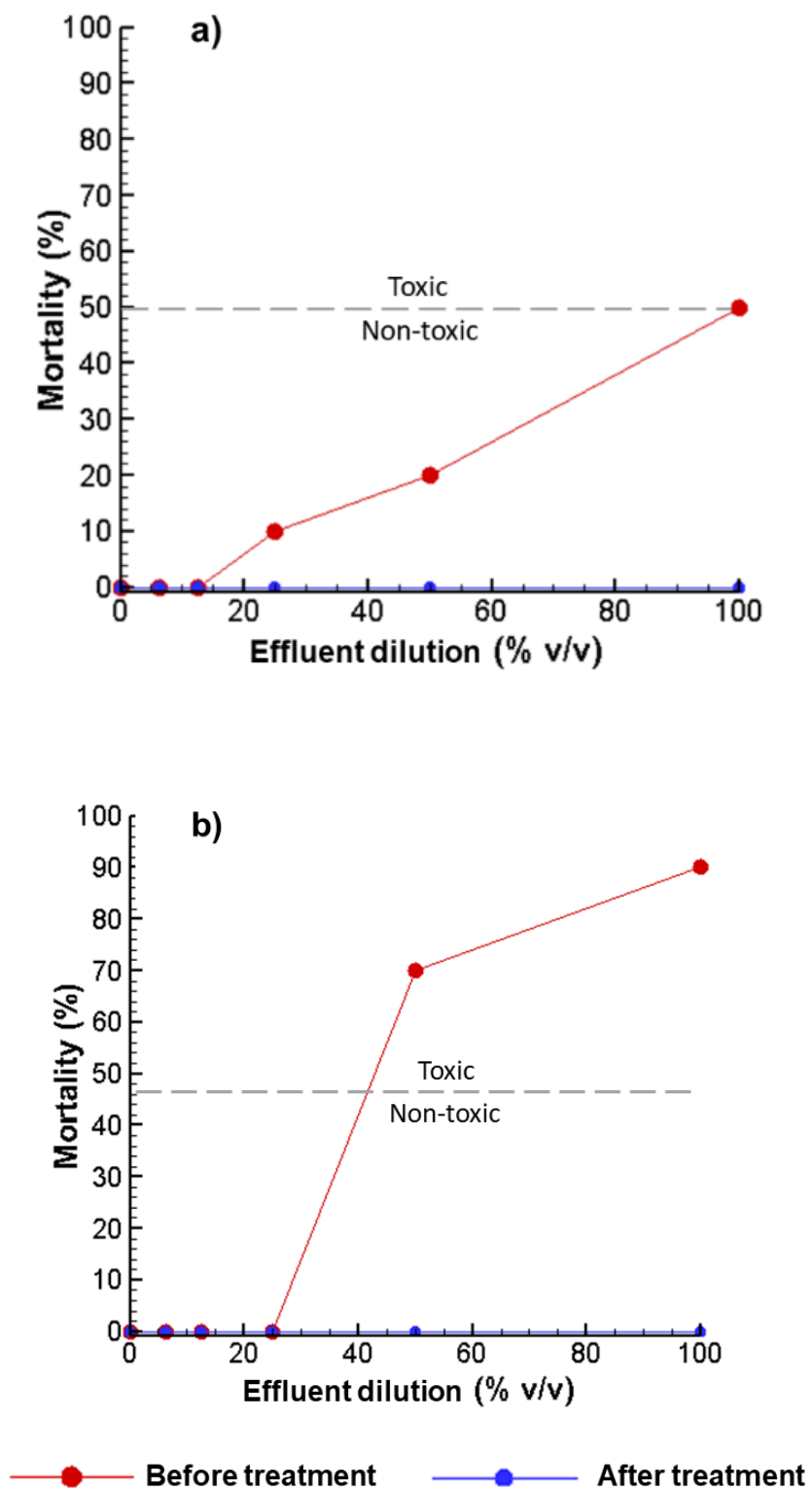


Fig 5.4 Mortality evolution of *D. magna* for (un-)treated effluents (a) ME_{high} and (b) ME_{low} .

(Fig. 5.4b). The physicochemical characterization of ME_{high} (with adjusted pH) and ME_{low} before toxicity tests indicated that ME_{high} was more contaminated than ME_{low} (Table 5.2).

For instance, EC, acidity, Cl⁻, NO₃⁻, SO₄²⁻, and S₂O₃²⁻ concentrations were 53%, 95%, 72%, 59%, 31%, and 69% higher in ME_{high}, respectively. These observations suggest that the toxicity of untreated ME_{low} was due to the presence of an unidentified toxic species, absent, or present in a lower concentration in ME_{high}. Another explanation could be that other matrix constituents mitigate the toxic species toxicity. One possibility could be xanthates, common flotation reagents used for preconcentration of base metal-bearing minerals, known to be highly toxic to aquatic organisms even at low concentrations (Na-ethyl xanthate EC₅₀ to *D. magna* = 0.35 mg/L; Bach et al., 2016). Xanthates were not measured prior to toxicity tests and their presence could not be confirmed in the original effluents, once toxicity results had been received, due to their high degree of instability in acidic media (Bach et al., 2016). Toxicity elimination in ME_{low} could potentially be attributed to the breakdown of xanthates by the Fenton reaction, yielding non-toxic CO₃²⁻ and SO₄²⁻ (García-Leiva et al., 2019). Initial S (from S₂O₃²⁻ and SO₄²⁻) in ME_{low} was 36.1*10⁻⁴ moles, whereas S recovered in the form of SO₄²⁻ was 41.2*10⁻⁴ moles, corresponding to 114% S recovery, further supporting this hypothesis. Yet, regardless of the initial composition and toxicity of the effluent, EF treatment followed by final pH neutralization resulted in the elimination of toxicity to *D. magna*, in agreement with one of the studies on the toxicity assessment of EF-treated industrial wastewater (>99% COD removal was correlated with toxicity elimination; Kaur et al., 2018). In contrast, other studies reported a decrease in the toxic inhibition ratio without complete contaminant removal (Zhuang et al., 2017; Li et al., 2011), or increased mortality at > 90% COD and ammonia nitrogen removal (Zhu et al., 2013). These inconsistencies are in accordance with

the literature, stating that the effluent toxicity after EF treatment is dependent on the initial nature of the effluent (Rueda-Marquez et al., 2021). Nevertheless, the findings of the present study highlight the outstanding potential of EF to provide a sustainable solution to the long-term toxicity risks imposed by thiosalts via delayed acidification of natural waterways.

5.3.3 Preliminary evaluation of EF operating costs

The results of the preliminary techno-economic analysis of EF treatment of thiosalts in ME_{high} and ME_{low} are presented in Table 5.3 and Fig. 5.5, in $\$/m^3$ and as a proportion (expressed in %) of total OCs, respectively. Calculations were made for a prospective plant with a treatment capacity of $100 m^3/day$. Total OCs (in $\$/m^3$, $\$/kg$ -thiosalts, and $\$/m^3/order$) were calculated in terms of E_{consum} , $FeSO_4 \cdot 7H_2O$ (as Fe(II) source), and Na_2CO_3 (as post-treatment neutralizing agent).

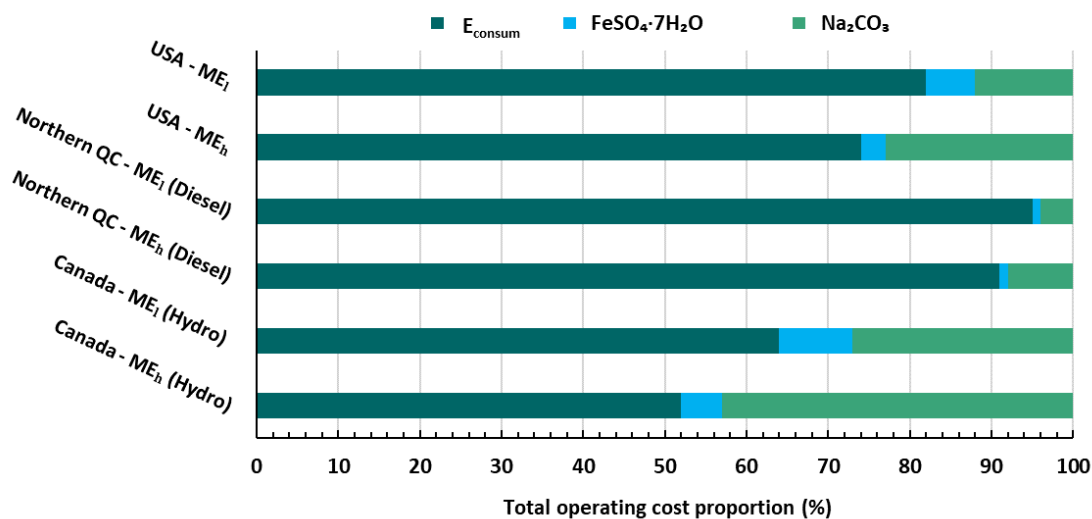


Fig 5.5 EF operating cost proportions of E_{consum} , $FeSO_4 \cdot 7H_2O$, and Na_2CO_3 for Canada, northern QC, and the USA, for effluents ME_{high} (ME_h) and ME_{low} (ME_l).

5.3.3.1 Energy consumption costs

The reality of mining activities in northern remote areas and central jurisdictions of Canada present two very distinct situations. Northern remote mines typically rely on fossil fuel combustion for self-sufficiency and power generation due to the unavailability of hydroelectricity, entailing higher energy production costs (Caron et al., 2021). Recently, a PPU of 0.28 CAD\$/kWh for electricity production was reported for a North Canadian mine relying on a diesel-powered generator (Caron et al., 2021). Consistently, the average PPU for on-site electricity production was estimated to be 0.30 CAD\$/kWh, based on official discussions with representatives of the mining company involved in the present study. This PPU was used as a conservative value to simulate the worst-case scenario of electricity production costs in remote areas of Canada. Moreover, hydroelectric power generation costs in the USA are twice those in Canada (Table 5.1). In this context, separate calculations were made for E_{consum} costs in central jurisdictions of Canada, northern QC, and the USA.

E_{consum} for the treatment of ME_{high} and ME_{low} were 3.60 kWh/m³ and 2.25 kWh/m³, respectively (Table 5.3). As expected, the E_{consum} of ME_{low} was lower than that of ME_{high} because the treatment time was half as long (30 min for ME_{low} vs. 60 min for ME_{high}), due to the lower $S_2O_3^{2-}$ content in ME_{low} (Table 5.2). For EF treatment powered by fossil fuel combustion (northern QC), E_{consum} represents a much greater proportion of total OCs (91% for ME_{high} and 95% for ME_{low}) than for activities utilizing hydroelectricity in central jurisdictions of Canada and the USA (52% for ME_{high} and 64% for ME_{low} in Canada, 74% for ME_{high} and 82% for ME_{low} in the USA) (Fig. 5.5). E_{consum} costs, in \$/kg-thiosalts, are higher for ME_{low} than for ME_{high} , which is attributable to the lower electrical conductivity (higher resistance) and lower amount of $S_2O_3^{2-}$ removed in ME_{low} (Table 5.2). Consequently, 1 kg of thiosalts requires more energy and is more expensive to treat in ME_{low} than ME_{high} (Table 5.3).

5.3.3.2 Reagent costs

Reagent costs represent the lowest proportion of the overall costs as compared to E_{consum} , with Na_2CO_3 representing a greater proportion than $\text{FeSO}_4 \cdot 7\text{H}_2\text{O}$ (**Fig. 5.5**). The proportional cost of Na_2CO_3 was the highest for central jurisdictions of Canada, due to the lower E_{consum} costs in these areas. The proportional cost of $\text{FeSO}_4 \cdot 7\text{H}_2\text{O}$ was minor in all cases. In fact, the low reagent requirement to drive EF is one of the main advantages of this process ([Olvera-Vargas et al., 2021](#)). Neutralization costs, in \$/kg-thiosalts, were less for ME_{high} than for ME_{low} (23% difference, for all geographical locations). As mentioned previously, both effluents had an acidic final pH, but ME_{high} initially contained 71% more $\text{S}_2\text{O}_3^{2-}$ than ME_{low} (**Table 5.2**). This inconsistency could be due to the lack of correlation between total initial thiosalts and acidity generated during oxidation ([Range and Hawboldt, 2019](#)), explaining the higher neutralization costs for every kg of thiosalts removed in ME_{low} despite the lower $\text{S}_2\text{O}_3^{2-}$ content. Reagent costs could be further reduced if they are replaced with recycled materials directly available on-site. For instance, Na_2CO_3 could be replaced by wood ash to increase the post-treatment pH ([Neculita et al., 2019](#)), and acid mine drainage could be an interesting alternative to $\text{FeSO}_4 \cdot 7\text{H}_2\text{O}$ for Fe^{2+} as the Fenton catalyst. However, further research is necessary to evaluate the feasibility of such alternatives.

5.3.3.3 BDD electrode

Electrode costs were not included as a contributor to total OCs because they are mainly limited by the high price of BDD electrodes ([Garcia-Rodriguez et al., 2021](#)). Previous work has shown that more affordable electrodes, such as dimensionally stable anodes (DSA), could provide an alternative to BDD electrodes while only affecting $\text{S}_2\text{O}_3^{2-}$ oxidation efficiency by 11.1% ([Olvera-Vargas et al., 2021](#)). Further research focusing on alternative, more economical electrode materials is needed.

Table 5.3 Preliminary OCs evaluation for the treatment of effluents ME_{high} and ME_{low} by EF.

<i>Effluent-dependent requirements</i>		<i>ME_{high}</i>		<i>ME_{low}</i>		
E _{consum} (kWh/m ³)		3.60		2.25		
FeSO ₄ •7H ₂ O required (kg/m ³)		0.06		0.06		
Neutralizing agent required (kg/m ³)		0.44		0.15		
<i>Costs – E_{consum} and reagents</i>						
	<i>CAD\$</i>	<i>CAD\$</i> <i>(Northern QC)</i>	<i>US\$</i>	<i>CAD\$</i>	<i>CAD\$</i> <i>(Northern QC)</i>	<i>US\$</i>
Cost for E_{consum} (\$/m³)	0.11	1.08	0.23	0.07	0.68	0.14
Cost for FeSO₄•7H₂O (\$/m³)		0.01	0.01		0.01	0.01
Cost for neutralization (\$/m³)		0.09	0.07		0.03	0.02
<i>Total OCs for thiosalts treatment</i>						
OC (\$/m³)	0.21	1.18	0.31	0.11	0.72	0.17
OC (\$/kg-thiosalts)	0.96	5.41	1.42	1.93	12.61	2.98
OC (\$/m ³ /order)	8.63*10 ⁻⁴	4.85*10 ⁻³	1.27*10 ⁻³	1.71*10 ⁻³	1.00*10 ⁻²	2.64*10 ⁻³

5.3.3.4 Total operating costs

Overall, results indicate that EF is more effective for effluents with higher thiosalt contamination levels. Yet, the treatment of less contaminated effluents is less expensive per volume treated. Total OCs were estimated to be, on average, 55% higher for both effluents when the EF process was powered by fossil fuel combustion (northern QC) as compared to hydroelectricity in the central jurisdictions of Canada (**Table 5.3**).

Treatment processes with total OCs around 1.00 CAD\$/m³ are considered feasible, based on discussions with Canadian mining representatives. Although EF treatment costs in northern QC are higher than those for Fe(VI) treatment, elimination of toxicity to *D. magna* was nonetheless achieved regardless of the initial chemistry and toxicity of the effluent; in contrast, high residual salinity resulting in potential toxicity is the main drawback of Fe(VI) (Gervais et al., 2020; Olvera-Vargas et al., 2021). Hydrogen peroxide oxidation is less expensive than EF treatment in northern QC, but the electro-generation of H₂O₂ during EF treatment eliminates concerns related to its transportation, handling, and storage (Gervais et al., 2020; Olvera-Vargas et al., 2021). Ozonation of 287 mg/L of thiosalts consumes 11.3 kWh/m³ (Gervais et al., 2020; Olvera-Vargas et al., 2021),

representing costs of 3.39 CAD\$/m³ for E_{consum} alone, greatly exceeding the total OCs for EF treatment. Thus, EF is a promising technology to remove thiosalts quickly and efficiently, thus eliminating the toxicity of mine water at a reasonable price compared to other AOPs (Fe(VI), H₂O₂, and ozonation).

5.4 Conclusion

The toxicity of two EF-treated mine waters was assessed. A preliminary techno-economic analysis was also conducted to determine costs related to E_{consum} and reagent requirements to estimate OCs for three geographical locations (Canada, northern QC, and the USA). Before treatment, ME_{high} was more contaminated than ME_{low}; however, toxicity tests showed that ME_{low} was toxic while ME_{high} was non-toxic (< 50% mortality), suggesting the presence of an unidentified S-bearing toxic species in ME_{low}, a hypothesis that was reinforced by > 100% S recovery in the form of SO₄²⁻. Complete removal of thiosalts from ME_{low} after 30 min of treatment resulted in elimination of the toxicity to *D. magna*. Elimination of *D. magna* mortality and complete oxidation of thiosalts was achieved after 60 min of treatment for ME_{high}. The initial matrix had no impact on the final toxicity for either effluent, but Cl⁻ ions seemed to have an impact on thiosalts oxidation kinetics and pathways. The results of the preliminary techno-economic analysis showed that EF is generally more effective for high concentrations of thiosalts, but the treatment of effluents with low levels of contamination is less expensive per volume treated. E_{consum} costs represented the highest proportion of total OCs in all cases. Reagent costs were lowest compared to all other expenditures for all geographical regions. Forthcoming studies will have to focus on EF performance for the removal of oxidizable contaminants, including high chlorinated salinity and its impact on the process efficiency, final effluent toxicity, and E_{consum} requirements.

Credit authorship contribution statement

Jennifer Dubuc: Conceptualization, Methodology, Visualization, Formal analysis, Investigation, Writing - original draft. **Lucie Coudert:** Conceptualization, Methodology, Visualization, Supervision, Writing - review & editing. **Olivier Lefebvre:** Formal analysis, Writing – review & editing. **Carmen M. Neculita:** Conceptualization, Visualization, Supervision, Writing - review & editing, Project administration, Funding acquisition.

Declaration of Competing Interest

The authors declare that there is no conflict of interest.

Acknowledgements

This study was funded by the FRQNT (Fonds de Recherche du Québec – Nature et Technologies; Québec’s Research Funds - Nature and Technology), Natural Sciences and Engineering Research Council of Canada (NSERC), Canada Research Chairs Program, and the industrial partners of the Research Institute on Mines and Environment (RIME) - University of Québec in Abitibi-Témiscamingue (UQAT) - Polytechnique Montréal, including Agnico Eagle, Iamgold, Canadian Malartic Mine, Newmont Éléonore, Raglan Mine - Glencore and Rio Tinto.

5.5 References

- Bach, L., Nørregaard, R.D., Hansen, V., Gustavson, K., 2016. Review on environmental risk assessment of mining chemicals used for mineral separation in the mineral resources industry and recommendations for Greenland. Danish Centre for Environment and Energy, Aarhus, Denmark. <https://dce2.au.dk/pub/sr203.pdf>
- Brillas, E., Sirés, I., Oturan, M.A., 2009. Electro-Fenton process and related electrochemical technologies based on Fenton’s reaction chemistry. *Chem. Rev.*, 109, 6570–6631. <https://doi.org/10.1021/cr900136g>

- Caron, F., Zephyr, L., Moore, M., Sanongboon, P., Zekveld, D., 2021. Small modular reactor (SMR) economic feasibility and cost-benefit study for remote mining in the Canadian North: A case study. Ontario Power Generation, Canadian Laboratories, Miraco Mining Innovation.
- Environment Canada, 2000. Reference test method for determining acute lethality of effluents to *Daphnia magna*. SPE1/RM/14 – 2nd edition. Environmental Technology Centre, Ottawa, Ontario, Canada, 34p.
- Forsberg, E., 2011. Study on thiosalts formation in alkaline sulphidic ore slurries under anaerobic conditions and methods for minimizing treatment cost in the mining industry. A case study at Boliden Mineral AB. MSc thesis, Engineering Technology, Industrial and Management Engineering, Lulea University of Technology, Sweden, 113p.
- Foudhaili, T., Jaidi, R., Neculita, C.M., Rosa, E., Triffault-Bouchet, G., Veilleux, E., Coudert, L., Lefebvre, O., 2019. Effect of the electrocoagulation process on the toxicity of gold mine effluents: A comparative assessment of *Daphnia magna* and *Daphnia pulex*. Sci. Total Environ., 708, 134739. <https://doi.org/10.1016/j.scitotenv.2019.134739>
- García-Leiva, B., Texeria, L.A.C., Torem, M.L., 2019. Degradation of xanthate in waters by hydrogen peroxide, Fenton and simulated solar photo-Fenton processes. J. Mater. Res. Technol., 8(6), 5698–5706. <https://doi.org/10.1016/j.jmrt.2019.09.037>
- Gervais, M., Dubuc, J., Paquin, M., Gonzalez-Merchan, C., Neculita, C.M., Genty, T., 2020. Comparative efficiency of three advanced oxidation processes for thiosalts treatment in mine impacted water. Miner. Eng., 153, 160349. <https://doi.org/10.1016/j.mineng.2020.106349>
- Kaur, P., Kushwaha, J.P., Sangal, V.K., 2018. Transformation products and degradation pathway of textile industry wastewater pollutants in Electro-Fenton process. Chemosphere, 207, 690–698. <https://doi.org/10.1016/j.chemosphere.2018.05.114>
- Kuyucak, N., 2014. Management of thiosalts in mill effluents by chemical oxidation or buffering in the lime neutralization process. Miner. Eng., 60, 41–50. <http://dx.doi.org/10.1016/j.mineng.2014.02.007>
- Lan, Y., Coetsier, C., Causserand, C., Serrano, K.G., 2017. On the role of salts for the treatment of wastewaters containing pharmaceuticals by electrochemical oxidation using a boron doped diamond anode. Electrochim. Acta, 231, 309–318. <https://doi.org/10.1016/j.electacta.2017.01.160>

- Li, H., Li, Y., Cao, H., Li, X., Zhang, Y., 2011. Advanced electro-Fenton degradation of biologically treated coking wastewater using anthraquinone cathode and Fe-Y catalyst. *Water. Sci. Technol.*, 64(1), 63–69. <https://doi.org/10.2166/wst.2011.570>
- Ministry of Justice, Canada (JUS), 2002. Metal and diamond mining effluent regulations. <https://laws-lois.justice.gc.ca/PDF/SOR-2002-222.pdf>
- Ministère de l'environnement et de la lutte contre les changements climatiques (MELCC), 2012. Directive 019 sur l'industrie minière. http://www.mddefp.gouv.qc.ca/milieu_ind/directive019/directive019.pdf
- Mousset, E., Loh, W.H., Lim, W.S., Jarry, L., Wang, Z., Lefebvre, O., 2021. Cost comparison of advanced oxidation processes for wastewater treatment using accumulated oxygen-equivalent criteria. *Water Res.*, 200, 117234. <https://doi.org/10.1016/j.watres.2021.117234>
- Neculita, C.M., Coudert, L., Rosa, E., 2019. Challenges and opportunities in mine water treatment in cold climate. In: *Proc. of Geo-Environmental Engineering*, 2019, Montreal, Quebec, Canada.
- Olvera-Vargas, H., Dubuc, J., Wang, Z., Coudert, L., Neculita, C.M., Lefebvre, O., 2021. Electro-Fenton beyond the degradation of organics: treatment of thiosalts in contaminated mine water. *Environ. Sci. Technol.*, 55(4): 2564-2574. <https://dx.doi.org/10.1021/acs.est.0c06006>
- Range, B.M.K., Hawboldt, K.A., 2019. Review: removal of thiosalt/sulfate from mining effluents by adsorption and ion exchange. *Min. Proc. Ext. Met. Rev.*, 79–86. <https://doi.org/10.1080/08827508.2018.1481062>
- Rueda-Marquez, J.J., Levchuk, I., Manzano, M., Sillanpää, M., 2020. Toxicity reduction of industrial and municipal wastewater by advanced oxidation processes (photo-Fenton, UVC/H₂O₂, e-Fenton and galvanic Fenton): A review. *Catalysts*, 10(2), 612–640. <https://doi.org/10.3390/catal10060612>
- Schudel, G., Plante, B., Bussière, B., Mcbeth, J., Dufour, G., 2019. The effect of arctic conditions on the geochemical behavior of sulfidic tailings. In: *Proc. of Tailings and Mine Waste*, 2019, Vancouver, British Columbia, Canada.
- Sharma, V.K., 2011. Oxidation of inorganic contaminants by ferrates (VI, V, and IV) - kinetics and mechanisms: a review. *J. Environ. Manage.* 92, 1051–1073. <https://doi.org/10.1016/j.jenvman.2010.11.026>

- Vallès, I., Santos-Juanes, L., Amat, A.M., Moreno-Andrés, J., Arques, A., 2021. Effect of salinity on UVA-VIS light driven photo-Fenton process at acidic and circumneutral pH. *Water*, 13, 1315–1325. <https://doi.org/10.3390/w13091315>
- Varga, D., Horváth, A. K., Nagypál, I., 2006. Unexpected formation of higher polythionates in the oxidation of thiosulfate by hypochlorous acid in a slightly acidic medium. *J. Phys. Chem. B*, 110, 2467–2470. <https://doi.org/10.1021/jp0567873>
- Zhu, X., Chen, L., Liu, R., Liu, C., Pan, Z., 2013. Biototoxicity evaluation of coking wastewater treated with different technologies using Japanese medaka (*Oryzias latipes*). *Environ. Sci.: Process. Impacts*, 25, 1391–1396. <https://doi.org/10.1039/C3EM00064H>
- Zhuang, H., Shan, S., Guo, J., Han, Y., Fang, C., 2017. Waste rice straw and coal fly ash composite as a novel sustainable catalytic particle electrode for strengthening oxidation of azo dyes containing wastewater in electro-Fenton process. *Environ. Sci. Pollut. Res.*, 24, 27136–27144. <https://doi.org/10.1007/s11356-017-0319-1>

Web references

- Alibaba. 99.2% Sodium carbonate soda ash bake soda powder dense Na_2CO_3 . Last access: September 27, 2021. https://www.alibaba.com/product-detail/Na2CO3-Na2CO3-99-2-Sodium-Carbonate_1600164656560.html
- Alibaba. High-content factory sells 98% ferrous sulfate heptahydrate. Last access: September 27, 2021. https://www.alibaba.com/product-detail/High-content-factory-sells-98-ferrous_1600310662429.html
- Bank of Canada. Currency converter. Last access: August 20, 2021. <https://www.bankofcanada.ca/rates/exchange/currency-converter/>
- Hydro Quebec. Rate L – Industrial rate for large power customers. Last access: September 27, 2021. <https://www.hydroquebec.com/business/customer-space/rates/rate-l-industrial-rate-large-power-customers.html>
- U.S. Energy information administration, 2020. 2019 Average monthly bill - industrial. Last access: September 27, 2021. https://www.eia.gov/electricity/sales_revenue_price/pdf/table5_c.pdf

CHAPTER 6 GENERAL DISCUSSION

The objective of this chapter is to highlight and link together the main findings of **Chapter 4** and **Chapter 5**. A preliminary techno-economic analysis including BDD electrode costs is also presented herein, with the aim to complement the study of OCs of the EF process developed in this project and presented in **Chapter 5**.

6.1 Impact of chlorides on the overall performance of thiosalts treatment by EF

EF oxidation « boosts » of 1, 15 and 30 min were insufficient to allow for complete thiosalts oxidation in S0 (0 mg/L $S_2O_3^{2-}$), even after several days (**Table 4.1**), most likely attributable to the absence of other oxidizable contaminants in the effluent. These results also suggest that the likelihood of generating residual H_2O_2 inside the electrochemical cell is low, since the remaining H_2O_2 would have reacted with $S_2O_3^{2-}$ within the 7-day post- “boost” observation period. Although residual H_2O_2 would have provided an advantage for reducing the electrochemical reaction time, and E_{consum} costs, its absence is an advantage over the chemical Fenton process, where the toxicity of the final effluent is often linked to the presence of unconsumed H_2O_2 (Zhang et al., 2005).

Results of EF treatment tests on E1, E2 and E4 showed that the composition of the effluent matrix plays a major role in thiosalts oxidation mechanisms by EF. Precisely, Cl^- were identified as important contributors to thiosalts oxidation mechanisms mainly via the formation of oxidative Cl^- species ($HClO$, ClO^- , ClO_3^- , and/or ClO_4^-), resulting from their oxidation at the BDD anode. When samples were prepared for toxicity tests, the Cl^- concentration in E4 decreased from 123 ± 10 to 91.3 mg/L, while the Br^- concentration increased from 48.5 ± 1.9 to 76.1 mg/L (**Table 5.2**), following pH adjustment to neutral. These results seem to indicate that ClO_3^- were still forming after treatment. The pH evolution of the sample during its transportation (pH = 7.6 and 6.9, before expedition to the external laboratory and immediately before toxicity tests, respectively) also suggested that ClO_3^- continued to form after the electrochemical reaction stopped. Considering these findings, oxidation “boosts” could potentially allow for complete thiosalts removal in mine effluents contaminated by chlorinated salinity, in which case total OCs could be considerably reduced. This advantage could be particularly interesting for northern

remote mines, where, contrary to temperate climate, water treatment could benefit from the high salinity of mine effluents (Neculita et al., 2019). Indeed, the techno-economic analysis presented in **Chapter 5** suggest that OCs would be over the 1.00 \$/m³ feasibility limit in northern QC due to fossil fuel combustion powered energy production costs (Caron et al., 2021), which are 10x higher than hydroelectricity².

In addition, results of the toxicity assessment revealed that initial Cl⁻ concentrations of ≤ 497 mg/L did not induce toxicity towards *D. magna*, following treatment by EF. Precisely, E1 and E4 contained initially 497 mg/L and 145 mg/L of Cl⁻, and both effluents were non-acutely toxic, according to the official definitions stated in D019 and the MMER (JUS, 2021; MELCC, 2012), after 60 min of treatment. In agreement, the technical background report for the ambient water quality guidelines for ClO₃⁻ in British Columbia states that the 48-hour LC₅₀ for *D. magna* is estimated at 3162 mg/L (Ministry of Environment of British Columbia, 2002). Since Cl⁻ were far below this concentration in both effluents, ClO₃⁻ toxicity towards *D. magna* would have been theoretically impossible. Nonetheless, Cl⁻ concentrations in spiked E1 would likely have resulted in *D. magna* toxicity due to the presence of ClO₃⁻.

Further studies focusing on the impact of chlorinated salinity on EF performance, including contaminant removal efficiency, residual toxicity and OCs, are crucial for the industry.

6.2 Techno-economic evaluation: BDD electrode costs

Lastly, a preliminary techno-economic evaluation excluding BDD electrode costs was conducted (**Chapter 5**) considering that BDD electrodes are expensive and not essential in the EF process. Previous work has shown that more affordable electrodes, such as DSA, could provide an alternative to BDD electrodes. Yet, BDD electrodes are classified as the most effective anodes due to their exceptional properties including their high O₂ evolution overpotential, wide potential window, low background current, chemical inertness, long term stability and durability in aggressive media as well as weak adsorption on their surface (Garcia-Rodriguez et al., 2020;

² <https://www.hydroquebec.com/business/customer-space/rates/rate-l-industrial-rate-large-power-customers.html>

Oturan, 2021). A preliminary techno-economic analysis including BDD electrode costs was deemed necessary.

The costs associated to the BDD electrode were determined using 2 scenarios. Scenario 1 considered that the plant would operate 90% of the year, and the remaining 10% would account for interruptions related to breakdowns and/or regular maintenance. In that case, the estimated lifetime of the electrode was 10 years (Serrano et al., 2015; **Table 3.3**). For central jurisdictions of Canada, electrode costs represent 77% of total OCs for E1 and 76% for E4. In the USA, electrode costs amount to 64% of total OCs for E1 and 61% for E4. In northern QC, E_{consum} costs surpass all other expenditures, due to the higher cost of producing electricity (**Fig. 6.1**).

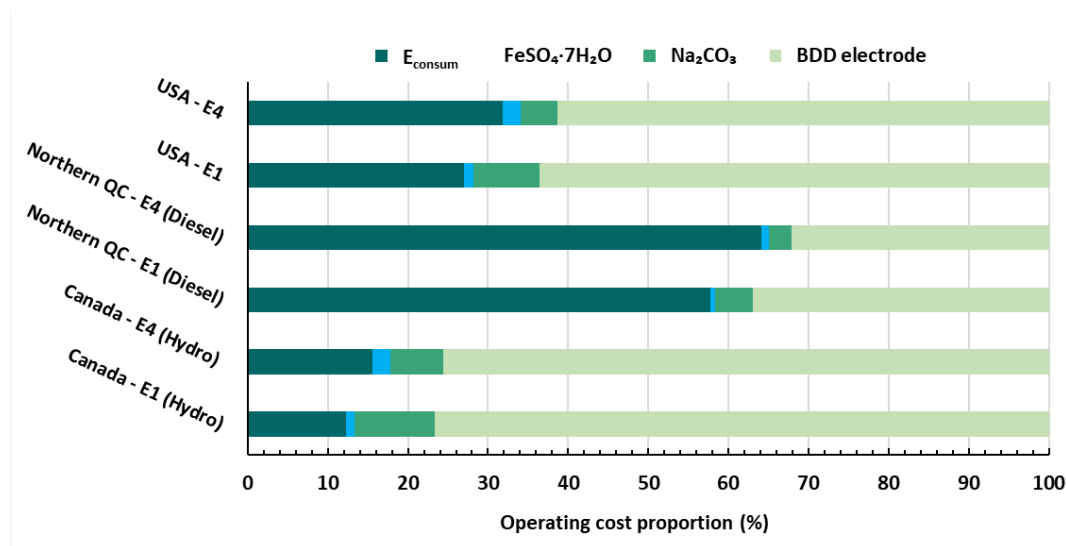


Figure 6.1 EF operating cost proportions of E_{consum} , $\text{FeSO}_4 \cdot 7\text{H}_2\text{O}$, Na_2CO_3 and BDD electrodes for Canada, northern QC, and the USA, for effluents E1 and E4.

Scenario 2 was used to simulate a realistic context that remote mines face in periods of extreme cold. It was supposed that the period of free water flow to the plant and the frost period lasted 6 months each. Considering that the electrochemical cell would be inoperative for half the year, the estimated lifetime of the BDD electrode was twice as that of the electrode in Scenario 1 (20 years, **Table 3.2**). Results listed in **Table 6.1** show that the difference in electrode costs for Scenario 1 vs. Scenario 2 are minimal (no more than $0.07 \text{ \$/m}^3$, for all geographical locations).

The only advantage of halting water treatment during the frost period, in terms of electrode costs, is an investment period spread over 20 years, rather than 10 years. Since the available information concerning the long-term durability of BDD electrodes in different media is very scarce, the service life of the electrode estimated in Scenario 2 is arguable. Oxidative damage of the electrode surface, during its inactivity, could occur and reduce its service life. Considering a hypothetical Scenario 3, in which the treatment plant operates 6 months/year, but the service life of the electrode is 10 years, electrode costs would amount to 1.23 and 0.67 CAD\$/m³, for E1 and E4, respectively.

Based on discussions with Canadian mining representatives, treatment processes with total OCs below 1.00 CAD\$/m³ are considered feasible. When BDD electrode costs were included, total OCs in northern QC were 0.87 and 0.06 CAD\$/m³ higher than the feasibility limit for E1 and E4 respectively, but remained below the limit, for the other geographical locations (**Table 6.1**). Considering these findings, and although EF has repetitively proven its remarkable oxidation capacity, further research focused on alternative anode materials in EF treatment is imperative.

In summary, E_{consum} costs for activities related to fossil fuel combustion (northern QC) represented the highest proportion of total OCs. BDD electrode cost proportions of total OCs were the highest, when power was produced by hydroelectricity (Canada and USA). Reagent costs were the lowest compared to all other expenditures, for all geographical regions.

Table 6.1. Preliminary OCs evaluation for the treatment of effluents E1 and E4 by EF. Simulation for a treatment plant with influent flow rate of 100 m³/d.

<i>Effluent-dependent requirements</i>	<i>E1</i>		<i>E4</i>			
E_{cons} (kWh/m ³)	3.6		2.25			
FeSO ₄ •7H ₂ O required (kg/m ³)	0.06		0.06			
Neutralizing agent required (kg/m ³)	0.44		0.15			
BDD electrode surface area required (m ²)	4.17		2.08			
<i>Costs – EC</i>						
	<i>\$ CAD</i>	<i>\$ CAD (Northern QC)</i>	<i>\$ US</i>	<i>\$ CAD</i>	<i>\$ CAD (Northern QC)</i>	<i>\$ US</i>
Cost for E_{cons} (\$/m³ treated effluent)	0.11	1.08	0.23	0.07	0.68	0.14
Cost for E_{cons} (\$/kg thiosalts treated)	0.50	5.16	1.04	1.18	11.91	2.48
<i>Costs – FeSO₄•7H₂O</i>						
Cost for FeSO₄•7H₂O (\$/m³ treated effluent)	0.01		0.01	0.01		0.01
Cost for FeSO₄•7H₂O (\$/kg thiosalts treated)	0.04		0.03	0.12		0.15
<i>Costs – Neutralization</i>						
Cost for neutralization (\$/m³ treated effluent)	0.09		0.07	0.03		0.02
Cost for neutralization (\$/kg thiosalts treated)	0.42		0.33	0.55		0.43
<i>Costs – BDD electrode</i>						
Cost for electrode, Scenario 1 (\$/m³ treated effluent)	0.69		0.54	0.34		0.27
Cost for electrode, Scenario 1 (\$/kg thiosalts treated)	3.14		2.48	6.00		4.73
Cost for electrode, Scenario 2 (\$/m ³ treated effluent)	0.62		0.49	0.31		0.24
Cost for electrode, Scenario 2 (\$/kg thiosalts treated)	2.84		2.25	5.43		4.20
<i>Total OC for thiosalts treatment (Scenario 1)</i>						
OC (\$/m³ treated effluent)	0.90	1.87	0.85	0.45	1.06	0.44
OC (\$/kg thiosalts treated)	4.10	8.76	3.88	7.85	18.58	7.79
OC (\$/m ³ /order)	0.37	0.79	0.35	0.25	0.59	0.24
<i>Total OC for thiosalts treatment (Scenario 2)</i>						
OC (\$/m³ treated effluent)	0.83	1.80	0.80	0.42	1.03	0.41
OC (\$/kg thiosalts treated)	3.80	8.46	3.65	7.28	18.01	7.26
OC (\$/m ³ /order)	0.35	0.76	0.34	0.23	0.57	0.23

CHAPTER 7 CONCLUSION AND RECOMMENDATIONS

Thiosalts are commonly found in contaminated mine effluents, especially in flotation process effluents, where conditions favor their formation. Precisely, thiosalts are metastable and partially oxidized intermediate S species. They are the result of the intermediate reactions that eventually lead to the formation of AMD, when sulfidic minerals contact with water and oxygen, engaging the oxidation process of the rock particles. Although thiosalts are not likely to be a direct source of toxicity to aquatic organisms at concentrations typically found in mine water, they represent a non-negligible source of environmental toxicity via the production of delayed acidity, especially with reported concentrations on the rise in the past years.

The current preferred thiosalts management method, which uses a chemical neutralizer (lime or carbonates), has important limitations including its ability to increase the buffering capacity of the effluent only temporarily. For example, quantifying the appropriate dosage is complex and difficult to predict, due to a lack of correlation between the total thiosalts concentration and the amount of generated delayed acidity. Several innovative approaches have been investigated with aim to develop AOPs for fast and efficient thiosalts oxidation, overcoming the biggest limitations of thiosalts management by neutralization. Among these emerging technologies, EF was recently identified as having a promising potential for thiosalts oxidation in synthetic mine effluents.

Acknowledging the need for new and efficient thiosalts treatment technologies, especially in northern climate, as well as the recent advancements in EF studies pertaining to the treatment of inorganic contaminants in synthetic mine effluents, the main objective of this project was to evaluate the performance of EF in complex, real mine effluents under optimal operating conditions predetermined on synthetic effluents (Olvera-Vargas et al., 2021). The specific objectives of this Master's project were elaborated by defining EF "performance" as the assessment of : (1) contaminant removal efficiency, (2) residual toxicity on *D. magna* and (3) OCs in terms of E_{consum} , reagents and BDD electrode costs.

First, the evaluation of EF efficiency for thiosalts removal in real mine water, treatability tests were conducted on a synthetic effluent containing 1 g/L $S_2O_3^{2-}$ by applying oxidation "boosts" of 1, 15 and 30 min with the aim to investigate the possibility of reducing electrochemical treatment time. After the boosts, the electrochemical reaction was stopped, and the effluents' physicochemical parameters were evaluated over a period of 7 days post-"boost". Results showed

that the “boosts” were ineffective at oxidizing thiosalts when the power source was turned off, indicating that they cannot reduce the electrochemical reaction time in the sole presence of $S_2O_3^{2-}$, in synthetic effluents.

Then, 4 different effluents and their corresponding, simplified synthetic effluents were treated using EF. Tests on synthetic effluents were performed in an attempt to explain the different phenomena occurring during the treatment of real effluents, without the influence of the effluent matrix. Results indicated that $S_2O_3^{2-}$ removal in E1 was comparable to that of S1 and complete $S_2O_3^{2-}$ oxidation was reached, in both effluents, after 60 minutes of treatment. Thiosalts treatment in S2 and E2 was also comparable and confirmed the remarkable oxidation capacity of EF. Precisely, complete $S_2O_3^{2-}$ oxidation was achieved in only 15 sec, supported by a pH drop of approximately 4 units in the same time. Effluent E3, which initially contained no thiosalts, was treated to better evaluate the impact of the EF process on pH evolution during treatment, in the absence of thiosalts. Results showed that the pH evolution of E3 was different than that of S3, where a drop of approximately 3 units was observed after 60 min of treatment for E3, and the same pH drop was observed after 15 sec in the case of S3. Two hypotheses were emitted considering these observations: 1) Cl^- , present at a higher concentration in S3 vs. E3, could be responsible for the faster pH drop in S3, considering that their oxidation (at the BDD anode surface or via HO^\bullet consumption) generates acidity, or 2) the alkalinity of E3 could have given it a buffering capacity, which was not the case for S3.

Treatability tests were then performed on S1, S2 and S3, to which alkalinity was added at a concentration matching that of the corresponding real mine effluent. Results allowed to refute the above-mentioned hypotheses: 1) the alkalinity of E3 was not the reason of the faster pH drop observed in S3 because the net pH variation of S3+alk after treatment was null and 2) the higher Cl^- concentration in S3 was not the reason of the faster pH drop observed in S3 compared to E3 because S3 and S3+alk contained similar Cl^- concentrations, yet their pH evolution was not comparable. It was concluded that E3 contained an unidentified acidity-producing species, other than thiosalts and other than Cl^- . In the case of E2, S2 and S2+alk, it was observed that alkalinity considerably elongated treatment time (> 99% removal attained after 15 sec for S2 vs. 12 min for S2+alk), potentially due to the HO^\bullet -scavenging effect of CO_3^{2-} .

Overall, results of the contaminant removal efficiency component of the project also indicated that the final pH of EF-treated mine effluents was always acidic, independent of the initial pH and the initial effluent composition (i.e. $\text{S}_2\text{O}_3^{2-}$ and Cl^- concentration and alkalinity). These findings highlight the need for an additional post-treatment neutralization step and provide crucial information to the industry by suggesting that chemical neutralization of the effluent should be performed after thiosalts treatment, rather than before, as per current management practices. This suggestion is further reinforced when considering that alkalinity extends thiosalts treatment time.

Considering the impact that Cl^- seemed to have on treatment mechanisms and process performance, treatability tests were then conducted by spiking the Cl^- concentration in effluent E1 at 2 and 4 g/L CaCl_2 , at pH 3 and pH 5, and the resulting solutions were treated as per usual. Briefly, it was observed that $\text{S}_2\text{O}_3^{2-}$ removal was faster at pH 5 than pH 3, and faster at 4 g/L CaCl_2 than at 2 g/L CaCl_2 , with unmodified E1 showing the slowest $\text{S}_2\text{O}_3^{2-}$ oxidation kinetics. The monitoring of Cl^- concentrations during treatment indicated that chlorates were not responsible for faster $\text{S}_2\text{O}_3^{2-}$ removal when the Cl^- concentration was higher since Cl^- concentrations remained stable overall. These observations agreed with the literature because, according to a recent study, Cl^- interfere with the Fenton reaction by governing the dissolved Fe^{2+} concentration. At the typical optimal working pH of the Fenton reaction (pH 2–3), Fe-Cl complexes are favored and the reaction of Fe^{2+} with H_2O_2 to form the HO^\bullet is hindered. When the pH increases, Fe-Cl decomplexation is favored, resulting in higher dissolved Fe^{2+} concentrations.

Results of the toxicity assessment on effluents E1 and E4 revealed that regardless of the initial composition and initial toxicity of the effluent, EF treatment followed by final pH neutralization resulted in the elimination of toxicity to *D. magna*. The EF toxicity assessment results available in the literature are scarce and tendencies observed are inconsistent. Considering that the aquatic toxicity data collected as part of this project are limited to two effluents whose compositions are relatively similar, identifying concordances with the literature would be difficult. Nonetheless, the common conclusion in EF toxicity studies is that inconsistencies are related to the fact that the effluent toxicity after EF treatment is dependent on the initial nature of the effluent. The knowledge pertaining to the toxicity of EF-treated effluents should be broadened in future studies.

Lastly, a techno-economic analysis in terms of E_{consum} , reagents and BDD electrode costs, for 3 geographical locations including central jurisdictions of Canada, northern remote regions of Canada, and the USA, was performed. Results revealed that electrode costs were the main limitation in central jurisdictions of Canada and the USA, whereas E_{consum} was the main drawback for northern QC. Yet, the optimization of electrode materials could result in total OCs that respect the common 1.00 $\$/\text{m}^3$ feasibility limit established in the mining industry for water treatment, hence the need to carry out studies that aim to identify electrode materials that are efficient for fast thiosalts oxidation, durable and more cost-effective than BDD electrodes.

The performance of EF in terms of contaminant removal, residual toxicity and OCs was evaluated. Crucial information was acquired during the execution of this master's project, providing a starting point in the field of applied research and development of the EF process as a new, effective, and ecologically sustainable mine water treatment technology. Further research deepening current knowledge of the technology is imperative. As such, a list of the main research needs identified is presented below, as a recommendation of follow-up research paths.

- Evaluation of oxidation "boosts" to reduce treatment time in the presence of Cl^- , in synthetic and real mine effluents;
- Evaluation of the impact of F/T cycles on thiosalts treatment following oxidation "boosts" to decrease treatment time;
- Evaluation of EF efficiency for the treatment of other oxidizable contaminants and subsequent toxicity assessment of treated effluents;
- Identification of alternative anode materials to reduce total OCs;
- Evaluation of the impact of chlorinated salinity on the EF process:
 - Testing on effluents with various Cl^- concentrations to deepen the knowledge acquired in this project;
 - Identification of the optimal working pH of the Fenton reaction at different Cl^- concentrations;

- Toxicity assessment of treated effluents. Oxidative Cl⁻ species including HClO, ClO⁻, ClO₃⁻ and ClO₄⁻ should be monitored to link toxicity results with effluent composition at different treatment times;
- Assessment of the impact of chlorinated salinity on E_{consum} requirements and total OCs.

REFERENCES

- Bach, L., Nørregaard, R.D., Hansen, V., Gustavson, K., 2016. Review on environmental risk assessment of mining chemicals used for mineral separation in the mineral resources industry and recommendations for Greenland. *Danish Centre for Environment and Energy*, 203: 38 pp.
- Bejan. D., Bunce, N.J., 2015 Acid mine drainage: electrochemical approaches to prevention and remediation of acidity and toxic metals. *J. Appl. Electrochem.*, 45: 1239–1254.
- Bergmann, M.E.H., Koparal, A.S., Iourtchouk, T., 2014. Electrochemical advanced oxidation processes, formation of halogenate and perhalogenate species - a critical review. *Crit. Rev. Environ. Sci. Technol.*, 44(4): 348–390.
- Boulanger-Martel, V., 2015. Performance d'une couverture avec effets de barrière capillaire faite de mélanges gravier-bentonite contrôler la migration d'oxygène en conditions nordiques. (Master's thesis) University of Québec in Abitibi-Témiscamingue (UQAT).
- Brillas, E., Sirés, I., Oturan, M.A., 2009. Electro-Fenton process and related electrochemical technologies based on Fenton's reaction chemistry. *Chem. Rev.*, 109: 6570–6631.
- Brito, C.N., Ferreira, M.B., de O. Marcionilio, S.M.L., de Moura Santos, E.C.M., Léon, J.J.L., Ganiyu, S.O., Martínez-Huitle, C.A., 2018. Electrochemical oxidation of acid violet 7 dye by using Si/BDD and Nb/BDD electrodes. *J. Electrochem. Soc.*, 165(5): E250–E255.
- Bussière, B., Aubertin, M., Zagury, G.J., Potvin, R., Benzaazoua, M., 2005. Principaux défis et pistes de solution pour la restauration des aires d'entreposage de rejets miniers abandonnées. *Symposium sur l'Environnement et les Mines*, 15-18 mai, 2005, Rouyn-Noranda, Québec, Canada, 29 pp.
- Carvalho, F.P., 2017. Mining industry and sustainable development: time for change. *Food Energy Secur.*, 6(2): 61–77.
- Clary, R., DiNuzzo, P., Hunter, T., Varghese, S., 2018. Treatment of refractory gold concentrates. *Proc. Extr.* 2018, 1327–1338.

- Deluna, M.D.G., Veciana, M.L., Su, C-C., Lu, M-C., 2012. Acetaminophen degradation by electro-Fenton and photoelectro-Fenton using a double cathode electrochemical cell. *J. Hazard. Mater.*, 217–218: 200–207.
- Dieter, C.A., Maupin, M.A., Caldwell, R.R., Harris, M.A., Ivahnenko, T.I., Lovelace, J.K., Barber, N.L., Linsey, K.S., 2018. Estimated use of water in the United States in 2015: U.S. Geological Survey Circular 1441, 65 pp.
- Drogui, P., Blais, J-F., Mercier, G., 2007. Review of Electrochemical Technologies for Environmental Applications. *Recent Pat. Eng.*, 1(3), 257–272.
- Environment Canada, 2000. Biological test method: Reference method for determining acute lethality of effluents to *Daphnia magna*. SPE1/RM/14 – Second edition. 34 pp.
- Éthier, M.P., 2011. Évaluation du comportement géochimique en conditions normale et froides de différents stériles présents sur le site de la mine Raglan. (Master's thesis) UQAT.
- Éthier, M.P., Bussière, B., Benzaazoua, M., Garneau, P., 2012. Effect of temperature on the weathering of various waste rock types from the Raglan Mine. In: *Proc. of Cold Regions Engineering 2012*, August 19-22, 2012, Quebec City, Canada.
- Fahd, F., 2014. Ecological risk assessment of thiosalts. (Master's thesis) Memorial University of Newfoundland, St-John's, Newfoundland, Canada.
- Forsberg, E., 2011. Study on thiosalts formation in alkaline sulphidic ore slurries under anaerobic conditions and methods for minimizing treatment cost in the mining industry. A case study at Boliden Mineral AB (Master's thesis) Luleå University of Technology, Luleå, Sweden.
- Foudhaili, T., 2019. Traitement de la salinité sulfatée et de la toxicité associée des effluents miniers au moyen de l'électrocoagulation. (Thèse de doctorat), UQAT.
- Foudhaili, T., Jaidi, R., Neculita, C.M., Rosa, E., Triffault-Bouchet, G., Veilleux, E., Coudert, L., Lefebvre, O., 2019. Effect of the electrocoagulation process on the toxicity of gold mine effluents: A comparative assessment of *Daphnia magna* and *Daphnia pulex*. *Sci. Total Environ.*, 708 : 134739.

- Garcia-Rodriguez, O., Mousset, E., Olvera-Vargas, H., Lefebvre, O., 2020. Electrochemical treatment of highly concentrated wastewater: A review of experimental and modeling approaches from lab- to full-scale. *Crit. Rev. Environ. Sci. Technol.*, 52 : 240-309.
- Gervais, M., Dubuc, J., Paquin, M., Gonzalez-Merchan, C., Neculita, C.M., Genty, T., 2020. Comparative efficiency of three advanced oxidation processes for thiosalts treatment in mine impacted water. *Miner. Eng.*, 153: 160349.
- Ghoneim, M.M., El-Desoky, H.S., Zidan, N.M., 2011. Electro-Fenton oxidation of sunset yellow FCF azo-dye in aqueous solutions. *Desalination*, 274: 22–30.
- Gonzalez-Merchan, C., Genty, T., Bussière, B., Potvin, R., Paquin, M., Benhammadi, M., Neculita, C.M., 2016. Ferrates performance in thiocyanates and ammonia degradation in gold mine effluents. *Miner. Eng.*, 95: 124–130.
- Illés, E., Mizrahi A., Marks, V., Meyerstein, D., 2018. Carbonate-radical-anions, and not hydroxyl radicals, are the products of the Fenton reaction in neutral solutions containing bicarbonate. *Free Radic. Biol. Med.*, 131, 1–6.
- Justice Canada, Ministère de la (JUS), 2002. Règlement sur les effluents des mines de métaux et des mines de diamants. <https://laws-lois.justice.gc.ca/PDF/SOR-2002-222.pdf>
- Kaur, P., Kushwaha, J.P., Sangal, V.K., 2018. Transformation products and degradation pathway of textile industry wastewater pollutants in Electro-Fenton process. *Chemosphere*, 207: 690–698.
- Kaushal, S.S., Groffman, P.M., Likens, G.E., Belt, K.T., Stack, W.P., Kelly, V.R., Band, L.E., Fisher, G.T., 2005. Increased salinization of fresh water in the northeastern United States. *Proc. Natl. Acad. Sci.* 102(38): 13517–13520.
- Kuyucak, N., 2014. Management of thiosalts in mill effluents by chemical oxidation or buffering in the lime neutralization process. *Miner. Eng.*, 60: 41–50.
- Lessard, F., 2018. Évaluation de couvertures isolantes avec effets de barrière capillaire faites de résidus désulfurés afin de contrôler le drainage minier acide en condition nordique. (Master's thesis) UQAT.

- Li, H., Li, Y., Cao, H., Li, X., Zhang, Y., 2011. Advanced electro-Fenton degradation of biologically treated coking wastewater using anthraquinone cathode and Fe-Y catalyst. *Water Sci. Technol.*, 64(1): 63–69.
- Majzlan, J., Plášil, J., Škoda, R., Gescher, J., Kögler, F., Rusznyak, A., Küsel, K., Neu, T.R., Mangold, S., Rothe, J., 2014. Arsenic-rich acid mine water with extreme arsenic concentration: mineralogy, geochemistry, microbiology and environmental implications. *Environ. Sci. Technol.*, 48: 13685–13693.
- Medeiros de Araújo, D., Cañizares, P., Martínez-Huitle, C.A., Rodrigo, M.A., 2014. Electrochemical conversion/combustion of a model organic pollutant on BDD anode: Role of sp³/sp² ratio. *Electrochem. Commun.*, 47: 37–40.
- Meijide, J., Dunlop, P. S. M., Pazos, M., & Sanromán, M. A., 2021. Heterogeneous electro-Fenton as “green” technology for pharmaceutical removal: A review. *Catalysts*, 11(1), 85 pp.
- Ministère de l’environnement et de la lutte contre les changements climatiques (MELCC), 2012. Directive 019 sur l’industrie minière. http://www.mddefp.gouv.qc.ca/milieu_ind/directive019/directive019.pdf
- Ministry of Environment of British Columbia, 2002. Technical background report - Ambient water quality guidelines for chlorate. [chlorate-tr.pdf \(gov.bc.ca\)](#)
- Miranda-Trevino, J.C., Pappoe, M., Hawboldt, K., Bottaro, C., 2013. The importance of thiosalts speciation: review of analytical methods, kinetics, and treatment. *Crit. Rev. Environ. Sci. Technol.*, 43: 2014–2070.
- Mount, D.R., Gulley, D.D., Hockett, J.R., Garrison, T.D., Evans, J.M., 1997. Statistical models to predict the toxicity of major ions to *Ceriodaphnia dubia*, *Daphnia magna* and *Pimephales promelas* (fathead minnows). *Environ. Toxicol. Chem.* 16(10): 2009–2019.
- Nair, K.M., Kumaravel, V., Pillai, S.C., 2021. Carbonaceous cathode materials for electro-Fenton technology: Mechanism, kinetics, recent advances, opportunities and challenges. *Chemosphere*, 269: 129325.
- Neculita, C. M., Rosa, E. 2019. A review of the implications and challenges of manganese removal from mine drainage. *Chemosphere*, 214: 491-510.


- Neculita, C. M., Coudert, L., Rosa, E., Mulligan, C. N., 2020. Future prospects for treating contaminants of emerging concern in water and soils/sediments. In: *Advanced Nano-Bio Technologies for Water and Soil Treatment*; Filip, J., Cajthaml, T., Najmanová, P., Černík, M., Zbořil, R., Eds.; Springer, Cham, 589–605.
- Negeri, T., Paktunc, A.D., Boisclair, M, Kingston. D.M., 1999. Characterization of thiosalts generation during milling of sulphide ores. CANMET Mining and Mineral Sciences Laboratories (CANMET-MMSL), Report presented for Thiosalts Consortium, Project: 601838, Report CANMET-MMSL 99-055 (CR), 125 pp.
- Neyens, E., Baeyens, J., 2003. A review of classic Fenton's peroxidation as an advanced oxidation technique. *J. Hazard. Mater.*, B98: 33–50.
- Nidheesh, P.V., Ganhimathi, R., 2012. Trends in electro-Fenton process for water and wastewater treatment: An overview. *Desalination*, 299: 1–15.
- Nordstrom, D.K., Alpers, C.N., Ptacek, C.J., 2015. Hydrogeochemistry and microbiology of mine drainage: an update. *J. Appl. Geochem.*, 57: 3–16.
- Nordstrom, D.K., Alpers, C.N., Ptacek, C.J., Blowes, D.W., 2000. Negative pH and extremely acidic mine waters from Iron Mountain, California. *Environ. Sci. Technol.*, 34: 254–258.
- Novak, L., Holtze, K., 2010. Toxicity investigations: Case study with metal mining effluent. AquaTox testing and consulting Inc., 26 pp.
- Olvera-Vargas, H., Dubuc, J. Wang, Z., Coudert, L., Neculita, C.M., Lefebvre, O., 2021. Electro-Fenton beyond the degradation of organics: treatment of thiosalts in contaminated mine water. *Environ. Sci. Technol.*, 55(4): 2564-2574.
- Oturan, M.A., 2021. Outstanding performances of the BDD film anode in electro-Fenton process: Applications and comparative performance. *Curr. Opin. Solid St. M.*, 25: 100925.
- Özcan, A., Sahin, Y., Koparal, A.S., Oturan, M.A., 2008. Degradation of picloram by the electro-Fenton process. *J. Hazard. Mater.*, 153: 718–727.
- Patra, S.G., Mizrahi, A., Meyerstein, D., 2020. The role of carbonate in catalytic oxidations. *Acc. Chem. Res.*, 53(10), 2189–2200.

- Range, B.M.K., Hawboldt, K.A., 2019. Review: removal of thiosalt/sulfate from mining effluents by adsorption and ion exchange. *Min. Proc. Ext. Met. Rev.*, 79–86.
- Read, J.F., Bewick, S.A., Donaher, S.C., Eelman, M.D., Oakey, J., Shaubel, C., Tam, N.C., Theriault, A., Watson, K.J., 2005b. The kinetics and mechanism of the oxidation of inorganic oxysulfur compounds by potassium ferrate, Part III –trithionate and pentathionate ions. *Inorg. React. Mech.*, 5: 281–304.
- Read, J.F., Bewick, S.A., Oikle, S.E., Shaubel, C., Nichole, S.N., Theriault, A., Watson, K.J., 2005a. The kinetics and mechanism of the oxidation of inorganic oxysulfur compounds by potassium ferrate, Part II – tetrathionate ions. *Inorg. React. Mech.*, 5: 265–280.
- Read, J.F., John, J., MacPherson, J., Shaubel, C., Theriault, A., 2001. The kinetics and mechanism of the oxidation of inorganic oxysulfur compounds by potassium ferrate, Part I - sulfite, thiosulfate and dithionite ions. *Inorg. Chim. Acta*, 315: 96–100.
- Ronkart, S.N., 2016. Quantification of trace and major anions in water by ion chromatography in a high-throughput laboratory. Application note: 114. Thermo Fisher Scientific Inc., 8 pp.
- Rosales, E., Pazos, M., Longo, M.A., Sanromán, M.A., 2009. Electro-Fenton decoloration of dyes in a continuous reactor: a promising technology in colored wastewater treatment. *Chem. Eng. J.*, 155: 62–67.
- Rueda-Marquez, J.J., Levchuk, I., Manzano, M., Sillanpää, M., 2020. Toxicity reduction of industrial and municipal wastewater by advanced oxidation processes (photo-Fenton, UVC/H₂O₂, e-Fenton and galvanic Fenton): A review. *Catalysts*, 10(2): 612–640.
- Ryskie, S., Gonzalez-Merchan, C., Neculita, C.M., Genty, T., 2020. Efficiency of ozone microbubbles for ammonia removal from mine effluents. *Miner. Eng.*, 145 : 106071.
- Ryskie, S., Neculita, C.M., Rosa, E., Coudert, L., Couture, P., 2021. Active treatment of contaminants of emerging concern in cold mine water using advanced oxidation and membrane-related processes: A review. *Minerals*, 11(3): 259.
- Sato, K., Furuya, S., Takenaka, N., Bandow, H., Maeda, Y., Furukawa, Y., 2003. Oxidative reaction of thiosulfate with hydrogen peroxide by freezing. *Bull. Chem. Soc. Jpn.*, 76: 1139–1144.

- Schudel, G., Plante, B., Bussière, B., Mcbeth, J., Dufour, G., 2019. The effect of arctic conditions on the geochemical behavior of sulfidic tailings. In: Proc. of Tailings and Mine Waste, 2019, Vancouver, Canada.
- Schwartz, M., Vigneault, B., McGeer, J., 2006. Evaluating the potential for thiosalts to contribute to toxicity in mine effluents. CANMET-MMSL, Project: 602591, 101 pp.
- Serrano, K.G., Savail, A., Latapie, L., Racaud, C., Rondet, P., Bertrand, N., 2015. Performance of Ti/Pt and Nb/BDD anodes for dichlorination of nitric acid and regeneration of silver(II) in a tubular reactor for the treatment of solid wastes in nuclear industry. *J. Appl. Electrochem.*, 45, 779–786.
- Skousen, J., Zipper, C.E., Rose, A., Ziemkiewicz, P.F., Nairn, R., McDonald, L.M., Kleinmann, R.L., 2017. Review of passive systems for acid mine drainage treatment. *Mine Water Environ.*, 36: 133–153.
- Sulonen, M.L.K., Kokko, M.E., Lakaniemi, A.M., Puhakka, J.A., 2018. Simultaneous removal of tetrathionate and copper from simulated acidic mining water in bioelectrochemical and electrochemical systems. *Hydrometallurgy*, 176: 129–138.
- Sun, Z., Forsling, W., 1997. The degradation kinetics of ethyl-xanthate as a function of pH in aqueous solution, *Miner. Eng.*, 10(4): 389–400
- Takenaka, N., Ueda, A., Daimon, T., Bandow, H., Dohmaru, Maeda, Y., 1996. Acceleration mechanism of chemical reaction by freezing: The reaction of nitrous acid with dissolved oxygen. *J. Phys. Chem.*, 100: 13874–13884.
- Tan, K.G., Rolia, E., 1985. Chemical oxidation methods for the treatment of thiosalts-containing mill effluents. *Can. Metall. Q.*, 24: 303–310.
- Taušová, M., Čulková, K., Domaracká, L., Drebenstedt, C., Muchová, S.M., Koščo, J., Annamária, B., Drevková, M., Benčöová, B., 2017. The importance of mining for socio-economic growth of the country. *Acta Montan. Slovaca.*, 22(4): 359–367.
- Thomas, D., Rohrer, J., 2016. Determination of chlorite, bromate, bromide, and chlorate in drinking water by ion chromatography with an on-line-generated postcolumn reagent for sub- $\mu\text{g/L}$ bromate analysis. Application note: 149. Thermo Fisher Scientific Inc., 9 pp.

- Vallès, I., Santos-Juanes, L., Amat, A.M., Moreno-Andrés, J., Arques, A., 2021. Effect of salinity on UVA-Vis light driven photo-Fenton process at acidic and circumneutral pH. *Water*, 13: 1315–1325.
- Vongporm, Y., 2008. Thiosalt behaviour in aqueous media. (Master's thesis) Memorial University of Newfoundland, 171 pp.
- Whaley-Martin, K., Marshall, S., Colenbrander-Nelson, T.E., Twible, L., Jarolimek, C.V., King, J.J., Apte, S.C., Warren, L.A., 2020. A mass-balance tool for monitoring potential dissolved sulfur oxidation risks in mining impacted waters. *Mine Water Environ.*, 39: 291–307.
- Wahlström, M. et al. (15 authors), 2017. Water Conscious Mining (WASCIOUS), Report, Northern Council of Ministers, Denmark, 171 pp.
- Wang, X-Q., Chuan-Ping, L., Yuan, Y., Li, F-B., 2014. Arsenite oxidation and removal driven by a bio-electro-Fenton process under neutral pH conditions. *J. Hazard. Mater.*, 275: 200–209.
- Zhang, H., Choi, H.C., Huang, C-P., 2005. Optimization of Fenton process for the treatment of landfill leachate. *J. Hazard. Mater.*, B125: 166–174.
- Zhu., X., Chen, L., Liu, R., Liu, C., Pan, Z., 2013. Biototoxicity evaluation of coking wastewater treated with different technologies using Japanese medaka (*Oryzias latipes*). *Environ. Sci.: Process. Impacts*, 25: 1391–1396.
- Zhuang, H., Shan, S., Guo, J., Han, Y., Fang, C., 2017. Waste rice straw and coal fly ash composite as a novel sustainable catalytic particle electrode for strengthening oxidation of azo dyes containing wastewater in electro-Fenton process. *Environ. Sci. Pollut. Res.* 24: 27136–27144.

APPENDIX A EXPERIMENTAL PROTOCOL

 <p style="font-size: small; margin-top: 5px;">Unité de recherche et de service en technologie minérale de l'Abitibi-Témiscamingue</p>	PROTOCOLE EXPERIMENTAL						
Protocole 1	Nombres de pages : 15						
Version 3	Date : 26 mai 2021						
Auteur : Jennifer Dubuc							
Approuvé par : _____ _____	<table style="width: 100%; border: none;"> <tr> <td style="width: 50%;">Signatures :</td> <td style="width: 50%;">Date :</td> </tr> <tr> <td style="border: none;"> <input style="width: 20px; height: 20px; margin-right: 5px;" type="checkbox"/> _____ </td> <td style="border: none;"> _____ </td> </tr> <tr> <td style="border: none;"> <input style="width: 20px; height: 20px; margin-right: 5px;" type="checkbox"/> _____ </td> <td style="border: none;"> _____ </td> </tr> </table>	Signatures :	Date :	<input style="width: 20px; height: 20px; margin-right: 5px;" type="checkbox"/> _____	_____	<input style="width: 20px; height: 20px; margin-right: 5px;" type="checkbox"/> _____	_____
Signatures :	Date :						
<input style="width: 20px; height: 20px; margin-right: 5px;" type="checkbox"/> _____	_____						
<input style="width: 20px; height: 20px; margin-right: 5px;" type="checkbox"/> _____	_____						

Montage des essais de traitement des composés oxydables par électro-Fenton dans des effluents miniers

Institut de recherche Mines et Environnement (IRME)

Université du Québec en Abitibi-Témiscamingue (UQAT)

Mots clés: électro-Fenton, traitement des eaux, composés oxydables

TABLE DES MATIÈRES

TABLE DES MATIÈRES	129
LISTE DES TABLEAUX.....	129
LISTE DES FIGURES	129
MESURES DE SANTÉ, SÉCURITÉ ET HYGIÈNE AU LABORATOIRE	130
1. Contexte	131
2. Principe	131
3. Objectif de travail	132
4. Démarches du travail	132
5. Matériel et réactifs	133
6. Préparation des effluents synthétiques.....	134
7. Montage de la cellule électrolytique.....	135
8. Mode opératoire	136
9. Analyses et tests.....	137
10. Calculs.....	139
RÉFÉRENCES	141

LISTE DES TABLEAUX

Tableau A.1. Paramètres à analyser pour la caractérisation des effluents avant, pendant et après traitement.....	138
---	-----

LISTE DES FIGURES

Figure A.1 Représentation schématique de l'oxydation des thiosels par EF lorsque la cathode est une brosse en fibres de carbone et l'anode est une BDD (tiré de Olvera-Vargas et al., 2021)	132
Figure A.2 Montage de la cellule électrochimique	136

MESURES DE SANTÉ, SÉCURITÉ ET HYGIÈNE AU LABORATOIRE

Règlements et directives en bref (URSTM, 2010):

- **L'accès au laboratoire : Heure d'opération :** 8h à 17h, du lundi au vendredi
- **On ne doit pas travailler seul en laboratoire :** avertir de sa présence et de son départ aux personnes présentes au laboratoire. Signaler le 2911 en cas d'urgence ou d'accident.
- **Planification du travail de laboratoire :** Planifier l'utilisation de l'équipement de travail. Consulter la fiche signalétique avant utilisation de produits.
- **Tenue vestimentaire :** Utiliser l'équipement de protection prévue (obligatoire): gants, lunettes, sarrau. Port de lentilles cornéennes (verres de contact) interdites, bijoux, coiffures ou autres ornements encombrants. Les jambes et les pieds doivent être protégés.
- **S'abstenir de boire, de manger et de fumer dans le laboratoire.**
- **Laisser les objets personnels, y compris nourriture et boisson à l'extérieur.**
- **Les vêtements de protection doivent demeurer à l'intérieur du laboratoire.**
- **Signaler tout accident ou déversement (même) mineur au responsable le plus près.**
- **Les rebuts doivent être jetés dans les contenants à usage spécifique :** verre brisé irrécupérable dans le local de chimie D113.5 et près de hotte de chimie D-013. Les produits chimiques à éliminer doivent être versés dans les contenants appropriés. Ne pas laisser les produits chimiques dans la verrerie après utilisation ; rincer avec le solvant approprié et jeter les résidus dans les contenants appropriés.
- **Il est interdit de pipeter avec la bouche :** toujours utiliser des propipettes.
- **Les cylindres de gaz doivent toujours être bien fixés :** inspecter et fixer tous les cylindres de gaz comprimé.
- **Tout récipient contenant un produit chimique doit être identifié :** nom du produit, formule chimique, concentration, nom de l'utilisateur, mention appropriée (inflammable, acide toxique etc...), date de réception.
- **Les montages en opération laissés sans surveillance doivent être identifiés au nom de leur utilisateur.**
- **Ranger son poste de travail, éteindre les appareils et bien se laver les mains avant de quitter le laboratoire.**
- **Il est obligatoire d'avoir suivi une formation avant d'utiliser les instruments.**

1. Contexte

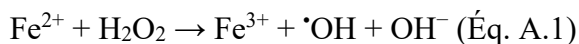
De nombreuses activités minières sont à l'origine de différents types d'effluents contaminés contenant une variété de composés oxydables sur les sites miniers. Par exemple, le forage et le dynamitage des roches requis pour atteindre le minerai d'intérêt génèrent de l'azote ammoniacal (N-NH₃) en solution (Bailey et al., 2012). D'autre part, le procédé de cyanuration utilisé par les mines d'or pour récupérer les métaux précieux génère des effluents contaminés avec des cyanures et dérivés des cyanures, dont certains sont oxydables comme les thiocyanates (SCN⁻) (Mudder et al., 2002). Ces composés oxydables sont toxiques pour le biote et doivent être traités afin de respecter les critères de toxicité selon la Directive 019 (MDDELCC, 2012) et le Règlement sur les effluents des mines de métaux et des mines de diamants (REMM; JUS, 2002).

D'autant plus, l'oxydation naturelle des minéraux sulfurés, en présence d'eau et d'oxygène dissous, mène éventuellement à la génération du drainage minier acide (DMA). Précisément, cette oxydation se produit en plusieurs étapes et génère des espèces intermédiaires du soufre partiellement oxydées, nommées thiosels (Range and Hawboldt, 2019). Les thiosels sont une source d'acidité latente car, étant métastables, ils s'oxydent très lentement, mais lorsqu'ils sont complètement oxydés, ils génèrent de l'acide sulfurique et provoquent un abaissement du pH (Miranda-Trevino et al., 2013; Gervais et al., 2020). Ainsi, les thiosels représentent un risque de toxicité pour les organismes aquatiques ainsi qu'une menace à l'intégrité de l'environnement et à la machinerie des usines (Olvera-Vargas et al., 2021).

Une étude récente a démontré l'excellente efficacité de l'électro-Fenton (EF) pour le traitement des thiosels dans des effluents synthétiques (Olvera-Vargas et al., 2021). Avant celle-ci, la majorité des études portant sur l'EF se concentraient sur la dégradation des composés organiques dans les eaux usées municipales et industrielles tels que les colorants et les composés pharmaceutiques (Özcan et al., 2008 ; Rosales et al., 2009 ; Ghoneim et al., 2011). Ainsi, considérant l'efficacité remarquable de l'EF pour l'enlèvement des thiosels dans les effluents synthétiques et le manque de connaissances sur l'application de cette technologie pour le traitement des composés inorganiques dans les eaux minières, l'évaluation de l'efficacité du traitement des composés oxydables par EF dans des effluents miniers réels devient d'un intérêt marqué.

2. Principe

Le principe de l'EF consiste à générer *in-situ* les réactifs de Fenton (fer ferreux ; Fe²⁺ et peroxyde ; H₂O₂) dans la cellule électrolytique (**Fig. A.1**) grâce à une différence de potentiel appliquée entre deux électrodes. Une fois générés, ils réagissent ensemble selon la réaction de Fenton chimique conventionnelle (Éq. A.1).



Ensuite, le radical hydroxyle ($\cdot\text{OH}$), étant très réactif et non-sélectif, peut réagir avec tout composé oxydable présent en solution. De plus, l'électrode de diamant dopé au bore (BDD) possède les capacités d'oxyder les composés oxydables via la production et l'adsorption de $\cdot\text{OH}$ directement à sa surface (BDD- $\cdot\text{OH}$) (Olvera-Vargas et al., 2021).

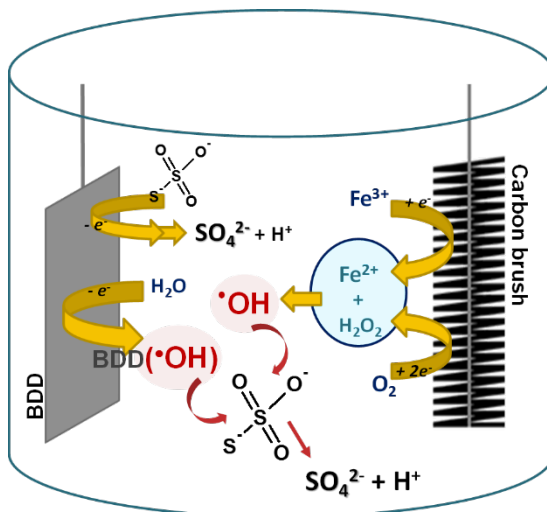


Figure A.1 Représentation schématique de l'oxydation des thiosels par EF lorsque la cathode est une brosse en fibres de carbone et l'anode est une BDD (tiré de Olvera-Vargas et al., 2021).

3. Objectif de travail

Ce protocole, adapté de Nidheesh et Ganhimathi (2012) et de Olvera-Vargas et al. (2021), est conçu pour mener une expérience à l'échelle laboratoire pour le traitement des composés oxydables, seuls ou en mélange, dans des effluents miniers réels ou synthétiques (correspondant à un effluent réel), par EF. L'objectif général est de déterminer le pourcentage d'enlèvement des contaminants oxydables par EF.

4. Démarches du travail

Le travail doit se dérouler selon les étapes de préparation et de réalisation suivantes :

Étape 1: Se procurer les matériaux et réactifs nécessaires (**Section 5**) et avoir lu les fiches signalétiques propres à chaque produit avant de les utiliser.

Étape 2: Étalonner les sondes de pH, de Eh et de conductivité électrique (CE) à l'aide de leurs solutions d'étalonnage respectives (la sonde de détection de N-NH_3 doit aussi être étalonnée si l'effluent en contient).

Étape 3: Préparer l'effluent synthétique (**Section 6**), le cas échéant, sinon procéder directement à l'étape 4.

Étape 4: Effectuer le montage de la cellule électrolytique (**Section 7**).

Étape 5: Effectuer l'essai de traitement (**Section 8**).

Étape 6: Mesurer les paramètres électrochimiques et chimiques (**Section 9**).

- *Caractérisation de l'effluent synthétique ou réel avant, pendant et après traitement selon le Tableau A.1.*

Étape 7: Calculer l'efficacité d'enlèvement des contaminants (**Section 10**).

5. Matériel et réactifs

<u>Matériel</u>	<u>Réactifs</u>	<u>Appareillage</u>
○ Bécher en pyrex de 500 mL	○ Eau désionisée	○ Balance analytique
○ Bécher en pyrex de 750 mL	○ Étalons de calibration pH 4, 7 et 10	○ pH-mètre multifonctions
○ Élastiques de caoutchouc (1 ou 2)	○ Étalon de CE	○ Conductimètre
○ Ruban adhésif	○ Étalon de Eh	○ Sonde de pH
○ Agitateur magnétique	○ Sulfate ferreux heptahydraté (FeSO ₄ •7H ₂ O)	○ Sonde de Eh
○ Barreau aimanté	○ Thiosulfate de sodium pentahydraté (Na ₂ S ₂ O ₃ •5H ₂ O)	○ Sonde de CE
○ Tige d'agitation	○ Standard liquide de N-NH ₃	○ Sonde de détection de N-NH ₃
○ Support vertical	○ Solution d'ajustement de pH	○ Chromatographie ionique à gradient d'éluant (940 Professional IC Vario – Metrohm)
○ Pince avec embouts de caoutchouc	○ Thiocyanate de potassium (KSCN)	
○ Support d'ampoule de décantation (ou équivalent)	○ Acide chlorhydrique (HCl) 1 N	
○ Digital DC power supply	○ Chlorure de sodium (NaCl)	
○ 2 pinces alligators	○ Carbonate de sodium (Na ₂ CO ₃)	
○ Minuteur		
○ Électrode de brosse de carbone (2 cm de diamètre, 8 cm de longueur)		
○ Électrode de BDD (10 cm de hauteur x 5 cm de largeur)		
○ Pompe d'aquarium		
○ Seringues (25 mL)		
○ Filtres (0,45 µm)		
○ Tubes ICP (15 mL)		
○ Effluents réels		

6. Préparation des effluents synthétiques

6.1 Préparation d'un effluent synthétique sans ajout d'alcalinité

1. Rincer la verrerie propre 3x à l'eau déionisée.
2. Remplir la fiole jaugée de 500 mL avec environ 250 mL d'eau déminéralisée.
3. Ajouter la masse ou le volume du contaminant afin d'obtenir la concentration désirée selon les calculs présentés à la **Section 10**.
4. Au besoin, ajuster le pH de la solution à l'aide de petits ajouts de HCl 1 N. Attention de ne pas dépasser le pH désiré.
5. Mélanger la solution à l'aide de la tige d'agitation jusqu'à ce qu'elle soit bien homogène et que tous les solides soient dissous.
6. Compléter à la jauge de 500 mL avec de l'eau déionisée.

6.2 Préparation d'un effluent synthétique avec ajout d'alcalinité

1. Rincer la verrerie propre 3x à l'eau déionisée.
2. Remplir la fiole jaugée de 750 mL avec environ la moitié d'eau déminéralisée (soit 500 mL environ).
3. Ajouter la masse ou le volume du contaminant afin d'obtenir la concentration désirée selon les calculs présentés à la **Section 10**.
4. Ajouter la masse de Na_2CO_3 afin d'obtenir l'alcalinité désirée selon les calculs présentés à la **Section 10**.
5. Compléter à la jauge de 750 mL avec de l'eau déionisée.
6. Mesurer le pH et noter la valeur.
7. Mesurer l'alcalinité et noter la valeur (APHA 2320, 2005).
8. Ajuster le pH de la solution à l'aide de petits ajouts de HCl 1 N. Attention de ne pas dépasser le pH désiré.
9. Mesurer de nouveau l'alcalinité (APHA 2320, 2005).
10. La valeur mesurée à l'étape 9 devrait se retrouver dans un intervalle de $\pm 15\%$ de la valeur d'alcalinité de l'effluent réel correspondant. Si c'est le cas, passer à l'étape 11. Sinon, disposer correctement de la solution et recommencer depuis l'étape 1.
11. Mélanger la solution à l'aide de la tige d'agitation jusqu'à ce qu'elle soit bien homogène et que tous les solides soient dissous.

7. Montage de la cellule électrolytique

Note : Se référer à la **Fig. A.2** pour un support visuel.

1. Effectuer le montage de la cellule électrolytique dans une hotte chimique (dégagement de H_2S et possibilité de volatilisation d'espèces toxiques comme les NO_x lors du traitement) (Olvera-Vargas et al., 2021).
2. Sur le support vertical, installer la pince avec embouts de caoutchouc.
3. Sur le support vertical, installer le support d'ampoule de décantation (ou équivalent) au-dessus de la pince avec embouts de caoutchouc.
4. Fixer la pompe d'aquarium sur le support d'ampoule de décantation à l'aide de ruban adhésif.
5. Placer l'électrode de BDD dans la pince avec embouts de caoutchouc, puis serrer la pince.
6. Remplir le bécher avec 500 mL d'effluent réel ou synthétique préalablement préparé.
7. Mettre le bécher sur une plaque agitatrice.
8. Déposer le barreau aimanté au fond du bécher.
9. Placer l'électrode de brosse de carbone directement dans la solution (à l'opposé de l'électrode de BDD) en déposant le côté plié du fil d'acier sur le rebord du bécher.
10. Placer les élastiques autour du bécher afin de positionner l'électrode de brosse de carbone et l'empêcher de flotter.
11. Repositionner la pince et le support d'ampoule de décantation afin que l'électrode de BDD et la pierre de diffusion d'air soient complètement submergés dans la solution.
12. S'assurer que les deux électrodes soient à une distance d'environ 2 cm l'une de l'autre.
13. Fixer la pince alligator rouge sur l'électrode de BDD et la pince alligator noire sur le fil d'acier de l'électrode en brosse de carbone.
14. Placer le Digital DC power supply à droite du montage puis brancher le fil rouge dans le cercle rouge et le fil noir dans le cercle noir de la source de courant.

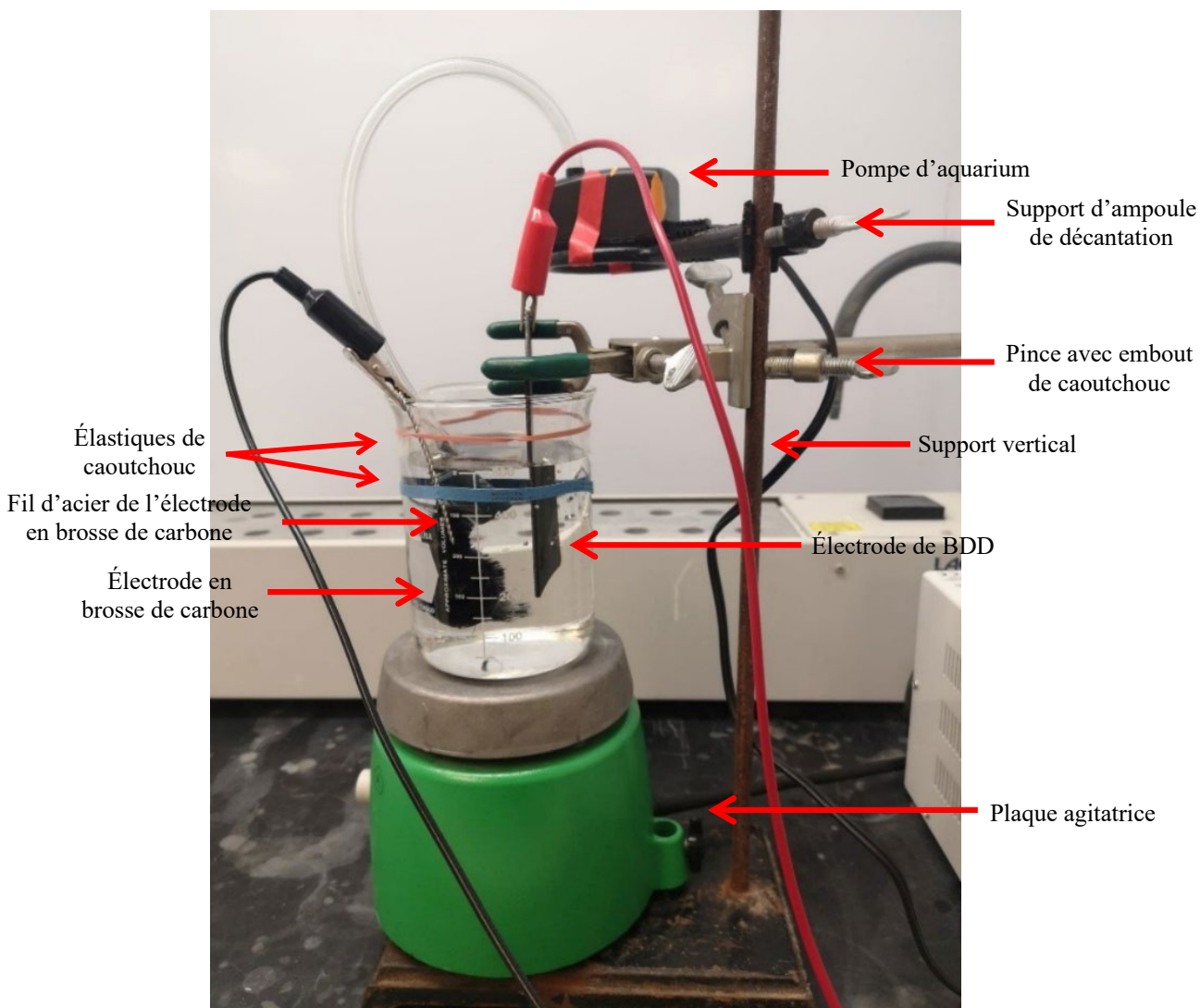


Figure A.2 Montage de la cellule électrochimique

8. Mode opératoire

1. Prendre les mesures électrochimiques et/ou chimiques selon le **Tableau A.1** à la **Section 9**.
2. Si la CE est $< 500 \mu\text{S}/\text{cm}$, ajouter du NaCl jusqu'à ce que la CE atteigne la même valeur que celle de l'effluent réel correspondant (dans un intervalle de $\pm 15\%$).
3. Noter la nouvelle valeur de CE.
4. Prélever 10 mL de la solution à traiter avec une seringue puis filtrer ($0,45 \mu\text{m}$) dans un tube de 50 mL (temps : 0 min).
5. Peser exactement environ 0,03 g de $\text{Fe}_2\text{SO}_4 \cdot 7\text{H}_2\text{O}$ (pour atteindre une concentration de 0,2 mM dans la solution).
6. Démarrer l'agitateur magnétique au niveau 6.

7. Brancher la source de courant puis la fixer en mode « courant constant » à 300 mA.
8. Démarrer le minuteur.
9. Après 5 minutes, réinitialiser le minuteur puis transférer quantitativement et d'un seul coup le $\text{Fe}_2\text{SO}_4 \cdot 7\text{H}_2\text{O}$.
10. Échantillonner 10 mL de solution avec une seringue et filtrer ($0,45 \mu\text{m}$) dans un tube de 50 mL aux temps souhaités pour les analyses chimiques selon le **Tableau A.1** à la **Section 9**.
11. À la fin de l'essai, arrêter la source de courant.
12. Arrêter l'agitateur magnétique.
13. Débrancher la pompe d'aquarium
14. Prendre les mesures électrochimiques et/ou chimiques selon le **Tableau A.1** à la **Section 9** directement dans les tubes de 50 mL.
15. Bien nettoyer et ranger l'équipement aux endroits appropriés.

9. Analyses et tests

Le **Tableau A.1** présente les principales analyses à réaliser, les méthodes utilisées, le matériel nécessaire, et le moment d'échantillonnage.

Tableau A.7.1 Paramètres à analyser pour la caractérisation des effluents avant, pendant et après traitement.

Type d'analyse	Paramètre	Méthode	Matériel	Moment de la mesure/d'échantillonnage
Électrochimique	pH	Mesure par électrode (ASTM E70-19, 2019)	pH-mètre, sonde de pH, étalons de calibration pH 4, 7, et 10, agitateur + barreau magnétique	Avant, pendant et après traitement
	Eh	Mesure par électrode (ASTM D1498-14, 2014)	pH-mètre, sonde de POR, étalon de calibration, agitateur + barreau magnétique	Avant et après traitement
	CE	Mesure par électrode (ASTM D1125-14, 2014)	Conductimètre, sonde de conductivité, étalon de calibration	Avant et après traitement
Chimique	N-NH₃	Mesure par électrode sélective d'ions (ASTM D1426-15, 2015)	Électrode sélective d'ions, solution standard de 1000 ppm, solution d'ajustement de pH	Avant et après traitement, le cas échéant
	Anions	Échange anionique (CEAEQ, 2014)	Chromatographie ionique	Avant, pendant et après traitement

10. Calculs

10.1 Calcul de la masse de $\text{Na}_2\text{S}_2\text{O}_3 \cdot 5\text{H}_2\text{O}$ à peser :

$$m = \frac{V * C_{\text{S}_2\text{O}_3^{2-}} * m.m_{\text{Na}_2\text{S}_2\text{O}_3 \cdot 5\text{H}_2\text{O}}}{m.m_{\text{S}_2\text{O}_3^{2-}}}$$

où :

m - masse de $\text{Na}_2\text{S}_2\text{O}_3 \cdot 5\text{H}_2\text{O}$ à peser (g)

V - volume de solution à traiter = 0,5 (L)

$C_{\text{S}_2\text{O}_3^{2-}}$ - concentration de $\text{S}_2\text{O}_3^{2-}$ désirée (g/L)

$m.m_{\text{Na}_2\text{S}_2\text{O}_3 \cdot 5\text{H}_2\text{O}}$ - masse molaire du $\text{Na}_2\text{S}_2\text{O}_3 \cdot 5\text{H}_2\text{O}$ = 248,18 (g/mol)

$m.m_{\text{S}_2\text{O}_3^{2-}}$ - masse molaire du $\text{S}_2\text{O}_3^{2-}$ = 112,13 (g/mol)

10.2 Calcul du volume de standard de 1000 ppm (1 g/L) N-NH₃ à prélever :

$$V_{std} = \frac{V * C_{\text{N-NH}_3}}{C_{std}}$$

où :

V_{std} - volume de standard à prélever

V - volume de solution à traiter = 0,5 (L)

$C_{\text{N-NH}_3}$ - concentration de N-NH₃ désirée (g/L)

C_{std} - concentration du standard = 1 (g/L)

10.3 Calcul de la masse de KSCN à peser :

$$m = \frac{V * C_{\text{SCN}^-} * m.m_{\text{KSCN}}}{m.m_{\text{SCN}^-}}$$

où :

m - masse de KSCN à peser (g)

V - volume de solution à traiter = 0,5 (L)

C_{SCN^-} - concentration de SCN^- désirée (g/L)

$m.m_{\text{KSCN}}$ - masse molaire du KSCN = 97,18 (g/mol)

$m.m_{\text{SCN}^-}$ - masse molaire du SCN^- = 58,08 (g/mol)

10.4 Calcul de la masse de Na_2CO_3 à peser :

Note : L'ajustement du pH par ajout de HCl consommera des carbonates (CO_3^{2-}) et diminuera donc l'alcalinité. Pour atteindre la valeur d'alcalinité de l'effluent réel correspondant (dans un intervalle maximal de $\pm 15\%$) après ajustement du pH, l'alcalinité visée doit être environ 2x celle de l'effluent réel.

a) Conversion de l'alcalinité carbonatée sous forme CaCO_3 en CO_3^{2-}

$$\text{Alc}_{\text{CO}_3^{2-}} = \frac{m.m_{\text{CO}_3^{2-}}}{m.m_{\text{CaCO}_3}} * \text{Alc}_{\text{CaCO}_3}$$

où :

$\text{Alc}_{\text{CO}_3^{2-}}$ - alcalinité carbonatée sous forme de CO_3^{2-} (mg/L)

$m.m_{\text{CO}_3^{2-}}$ - masse molaire du CO_3^{2-} (g/mol)

$m.m_{\text{CaCO}_3}$ - masse molaire du CaCO_3^{2-} (g/mol)

$\text{Alc}_{\text{CaCO}_3}$ - alcalinité carbonatée visée sous forme de CaCO_3^{2-} (mg/L)

b) Masse de Na_2CO_3 à peser :

$$m = \frac{V * \text{Alc}_{\text{CO}_3^{2-}} * m.m_{\text{Na}_2\text{CO}_3}}{1000 * m.m_{\text{CO}_3^{2-}}}$$

où :

m - masse de Na_2CO_3 à peser (g)

V - volume de solution à traiter = 0,75 (L)

$\text{Alc}_{\text{CO}_3^{2-}}$ - alcalinité carbonatée sous forme de CO_3^{2-} (mg/L), calculée à l'étape a)

$m.m_{\text{Na}_2\text{CO}_3}$ - masse molaire du Na_2CO_3 (g/mol)

$m.m_{\text{CaCO}_3}$ - masse molaire du CaCO_3^{2-} (g/mol)

10.5 Calcul du pourcentage d'enlèvement des contaminants :

$$\text{Enlèvement (\%)} = ((C_i - C_f) / C_i) * 100$$

où :

C_i - concentration initiale (avant traitement) du contaminant (g/L)

C_f - concentration finale (après traitement) du contaminant (g/L)

RÉFÉRENCES

- American Public Health Association (APHA 2320), 2005. Standard Methods for the Examination of Water and Wastewater in: Clesceri, L.S., Greenberg, A.E., Eaton, A.D. (Eds.), Washington, DC, pp. 1–12.
- American Society for Testing and Materials (ASTM E70-19), 2019. Standard test method for pH of aqueous solutions with the glass electrode, ASTM International, West Conshohocken, PA, www.astm.org.
- ASTM D1125-14, 2014. Standard test methods for electrical conductivity and resistivity of water, ASTM International, West Conshohocken, PA, www.astm.org.
- ASTM D1426-15, 2015. Standard Test Methods for Ammonia Nitrogen In Water, Sections 17-24, ASTM International, West Conshohocken, PA, www.astm.org.
- ASTM D1498-14, 2014. Standard test method for oxidation-reduction potential of water, ASTM International, West Conshohocken, PA, www.astm.org.
- Bailey, B.L., Smith, L.J.D., Blowes, D.W., Ptacek, C.J., Smith, L., Segó, D.C., 2012. The Diavik waste rock project: Persistence of contaminants from blasting agents in waste rock effluents. *Applied Geochemistry* 36, 256–270.
- Centre d'Expertise en Analyse Environnementale du Québec (CEAEQ), 2014. Détermination des anions: méthode par chromatographie ionique. MA. 300-Ions 1.3, Rév. 3. Ministère du Développement durable, de l'Environnement et de la Lutte contre les changements climatiques, QC, Canada.
- Gervais, M., Dubuc, J., Paquin, M., Gonzalez-Merchan, C., Neculita, C.M., Genty, T., 2020. Comparative efficiency of three advanced oxidation processes for thiosalts treatment in mine impacted water. *Miner. Eng.*, 153: 160349.
- Ghoneim, M.M., El-Desoky, H.S., Zidan, N.M., 2011. Electro-Fenton oxidation of sunset yellow FCF azo-dye in aqueous solutions. *Desalination*, 274: 22–30.
- Justice Canada, Ministère de la (JUS), 2002. Règlement sur les effluents des mines de métaux et des mines de diamants. <https://laws-lois.justice.gc.ca/PDF/SOR-2002-222.pdf>
- Mudder, T., Botz, M., Smith, A., 2002. The chemistry and treatment of cyanidation wastes. 2nd edition, London, Mining Journal Books.
- Nidheesh, P.V., Ganhimathi, R., 2012. Trends in electro-Fenton process for water and wastewater treatment: An overview. *Desalination*, 299: 1–15.
- Olvera-Vargas, H., Dubuc, J., Wang, Z., Coudert, L., Neculita, C.M., Lefebvre, O., 2021. Electro-Fenton beyond the degradation of organics: treatment of thiosalts in contaminated mine water. *Environ. Sci. Technol.*, 55(4): 2564-2574.

- Özcan, A., Sahin, Y., Koparal, A.S., Oturan, M.A., 2008. Degradation of picloram by the electro-Fenton process. *J. Hazard. Mater.*, 153: 718–727.
- Range, B.M.K., Hawboldt, K.A., 2019. Review: removal of thiosalt/sulfate from mining effluents by adsorption and ion exchange. *Min. Proc. Ext. Met. Rev.*, 79–86.
- Rosales, E., Pazos, M., Longo, M.A., Sanromán, M.A., 2009. Electro-Fenton decoloration of dyes in a continuous reactor: a promising technology in colored wastewater treatment. *Chem. Eng. J.*, 155: 62–67.
- Unité de recherche de et services en technologies minérales (URSTM), 2010. Document de synthèse de santé et sécurité au laboratoire de l'URSTM, Santé, Sécurité et Hygiène au Laboratoire.

**APPENDIX B TOXICITY ANALYSIS CERTIFICATE FOR EFFLUENT
E1 (UNTREATED)**

BUREAU
VERITAS

RÉSULTATS DE DAPHNIE - CL50 (AIGUE-48H)-FÉDÉRAL

144

Client : 6088 H2LAB

No. de dossier : C139940

Nom et no. de projet :

No. d'échantillon : JM4701-01

Résultats d'analyse:**48 hres CL50 %v/v (95% CL):** >100 (N/A) Méthode statistique: Visuelle**Unité toxique:** <1**48 hres CE50 %v/v (95% CL):** >100 (N/A) Méthode statistique: Visuelle**Commentaire:** non toxique**Nom de l'échantillon:** 317268 99473

Type d'échantillon: Eau usée

Apparence : Beige, translucide, pas de solides en suspension

Échantillon avant l'analyse:

Date/heure de prélèvement : 03 août 2021

Méthode d'échantillonnage : Instantanée

pH: 7.2

Prélevé par : JENNIFER DUBUC

Lieu de prélèvement : URSTM

Température : 21 °C

Échantillon reçu : 05 août 2021 09:45

Volume d'échantillon fourni : 1 L

Oxygène dissous : 88.0 %

Début de l'essai : 06 août 2021 12:20

Temp. Moy. 16 °C

Conductivité : 3244 µS/cm

Récep.:

Fin : 08 août 2021 13:00

Entreposage: 2-6°C

Dureté : 1052 mg CaCO₃/L

Concentration	Température (°C)	pH (pH)	Conductivité (µS/cm)	Oxygène dissous (mg/L)	Température (°C)	pH (pH)	Oxygène dissous (mg/L)	Immobilité (#)	Immobilité (%)	Mortalité (#)	Mortalité (%)
%v/v	0 hre	0 hre	0 hre	0 hre	48 hres	48 hres	48 hres	48 hres	48 hres	48 hres	48 hres
0	21	8.0	476	8.2	20	8.2	8.5	0	0	0	0
6.25	21	7.9	697	8.1	20	8.0	8.3	0	0	0	0
12.5	21	7.8	905	8.3	20	8.0	8.4	0	0	0	0
25	21	7.7	1284	8.3	20	7.9	8.4	0	0	1	10.0
50	21	7.6	1981	8.2	20	7.9	8.5	0	0	2	20.0
100	21	7.5	3374	7.8	20	7.8	8.3	0	0	5	50.0

Commentaires:**Eau de contrôle et dilution :**

Eau reconstituée pour Daphnia

Dureté:

180 mg/l CaCO₃

Autres paramètres disponibles sur demande.

Installations et conditions de l'essai

Concentrations effectuées : 0,6,25,12,5,25,50,100 (%v/v)

Nombre d'organismes par récipient : 10

Temps de pré aération : 0 min

Taux de pré aération : 40±5 mL/min/L

Nombre total d'organismes utilisés : 60

Température : 20 ± 2 °C

Ajustement de la dureté : Non

Volume dans les réservoirs d'essai : 150 mL

Volume de récipient : 200 ml

Ajustement du pH : Non

Densité de chargement :

15.0 mL/daphnie Photopériode : 16 heures de lumière: 8 heures d'obscurité

Organisme :*Daphnia magna*

Provenance : Culture de laboratoire BV

Âge des organismes au début de l'essai : <24 hres

Nombre moyen de néonates par couvée : 37.0

Photopériode :

16 heures de lumière: 8 heures d'obscurité

% de mortalité 7 jours avant lessai : 4.2

Température d'acclimatation :

20 ± 2 °C

Âge à la naissance de la première couvée : 11 jours

Régime alimentaire :

Nourrit 1 fois par jour.

Données relatives au contrôle de qualité:

Dichromate de potassium

Date d'analyse :

03 août 2021

Effet d'analyse 48 hres CL50 (intervalle de confiance 95%) : 0.18 (0.13, 0.25)mg/L

Méthode statistique:

Binomiale

Moyenne géométrique antérieure CL50 :

0.17 (0.11, 0.29) mg/L

Concentration : 0,0.0625,0.125,0.25,0.5,1 mg/L

Méthode d'analyseQUE SOP-00406. Méthode de référence pour la détermination de la létalité aiguë d'effluents chez *Daphnia magna*. SPE1/RM/14 - Deuxième édition. Environnement Canada. 2000.

Essentiellement, il s'agit d'un essai statique d'une durée de 48 heures. Dix individus sont soumis à différentes concentrations d'effluent pour en mesurer la CL50 dans des conditions de température, d'éclairage et de densité de chargement contrôlées.

Déviations de la méthode :

Aucune



BUREAU
VERITAS

RÉSULTATS DE DAPHNIE - CL50 (AIGUE-48H)-FÉDÉRAL

145

Client : 6088 H2LAB

No. de dossier : C139940

Nom et no. de projet :

No. d'échantillon : JM4701-01

Analyste : Anouar Guitouni, Chelsea Blake, Wael Ellamouchi

Validé par : Wael Ellamouchi, Analyste 2

Date: 19 août 2021 11:30

**APPENDIX C TOXICITY ANALYSIS CERTIFICATE FOR EFFLUENT
E1 (TREATED)**



RÉSULTATS DE DAPHNIE - CL50 (AIGUE-48H)-FÉDÉRAL

147

BUREAU
VERITAS

Client : 6088 H2LAB

No. de dossier : C139940

Nom et no. de projet :

No. d'échantillon : JM4702-01

Résultats d'analyse:

48 hres CL50 %v/v (95% CL): >100 (N/A) Méthode statistique: Visuelle

Unité toxique: <1

48 hres CE50 %v/v (95% CL): >100 (N/A) Méthode statistique: Visuelle

Commentaire: non toxique

Nom de l'échantillon: 317269 99478

Type d'échantillon: Eau usée

Apparence : Incolore, translucide, pas de solides en suspension

Échantillon avant l'analyse:

Date/heure de prélèvement : 03 août 2021

Méthode d'échantillonnage : Instantanée

pH: 7.4

Prélevé par : JENNIFER DUBUC

Lieu de prélèvement : URSTM

Température : 21 °C

Échantillon reçu : 05 août 2021 09:45

Volume d'échantillon fourni : 1 L

Oxygène dissous : 58.0 %

Début de l'essai : 06 août 2021 12:15

Temp. Moy. 16 °C

Conductivité : 3721 µS/cm

Récep.:

Fin : 08 août 2021 11:15

Entreposage: 2-6°C

Dureté : 1141 mg CaCO₃/L

Concentration	Température (°C)	pH (pH)	Conductivité (µS/cm)	Oxygène dissous (mg/L)	Température (°C)	pH (pH)	Oxygène dissous (mg/L)	Immobilité (#)	Immobilité (%)	Mortalité (#)	Mortalité (%)
%v/v	0 hre	0 hre	0 hre	0 hre	48 hres	48 hres	48 hres	48 hres	48 hres	48 hres	48 hres
0	21	7.8	479	8.3	22	7.7	8.4	0	0	0	0
6.25	21	7.8	726	8.2	22	7.7	8.2	1	10.0	0	0
12.5	21	7.8	955	8.2	22	7.7	8.1	0	0	0	0
25	21	7.8	1385	8.1	22	7.7	8.0	0	0	0	0
50	21	7.7	2230	7.8	22	7.7	7.7	0	0	0	0
100	20	7.6	3728	5.7	22	7.8	7.9	0	0	0	0

Commentaires:

Eau de contrôle et dilution :

Eau reconstituée pour Daphnia

Dureté:

180 mg/l CaCO₃

Autres paramètres disponibles sur demande.

Installations et conditions de l'essai

Concentrations effectuées : 0,6,25,12.5,25,50,100 (%v/v)

Nombre d'organismes par récipient : 10

Temps de pré aération : 0 min

Taux de pré aération : 40±5 mL/min/L

Nombre total d'organismes utilisés : 60

Température : 20 ± 2 °C

Ajustement de la dureté : Non

Volume dans les réservoirs d'essai : 150 mL

Volume de récipient : 200 ml

Ajustement du pH : Non

Densité de chargement :

15.0 mL/daphnie Photopériode : 16 heures de lumière: 8 heures d'obscurité

Organisme :

Daphnia magna

Provenance : Culture de laboratoire BV

Âge des organismes au début de l'essai : <24 hres

Nombre moyen de néonates par couvée : 37.0

Photopériode :

16 heures de lumière: 8 heures d'obscurité

% de mortalité 7 jours avant lessai : 4.2

Température d'acclimatation :

20 ± 2 °C

Âge à la naissance de la première couvée : 11 jours

Régime alimentaire :

Nourrit 1 fois par jour.

Données relatives au contrôle de qualité:

Dichromate de potassium

Date d'analyse :

03 août 2021

Effet d'analyse 48 hres CL50 (intervalle de confiance 95%) : 0.18 (0.13, 0.25)mg/L

Méthode statistique:

Binomiale

Moyenne géométrique antérieure CL50 :

0.17 (0.11, 0.29) mg/L

Concentration : 0,0.0625,0.125,0.25,0.5,1 mg/L

Méthode d'analyse

QUE SOP-00406. Méthode de référence pour la détermination de la létalité aiguë d'effluents chez *Daphnia magna*. SPE1/RM/14 - Deuxième édition. Environnement Canada. 2000.

Essentiellement, il s'agit d'un essai statique d'une durée de 48 heures. Dix individus sont soumis à différentes concentrations d'effluent pour en mesurer la CL50 dans des conditions de température, d'éclairage et de densité de chargement contrôlées.

Déviations de la méthode :

Aucune



BUREAU
VERITAS

RÉSULTATS DE DAPHNIE - CL50 (AIGUE-48H)-FÉDÉRAL

148

Client : 6088 H2LAB

No. de dossier : C139940

Nom et no. de projet :

No. d'échantillon : JM4702-01

Analyste : Anouar Guitouni, Chelsea Blake, Wael Ellamouchi

Validé par : Wael Ellamouchi, Analyste 2

Date: 19 août 2021 11:37

**APPENDIX D TOXICITY ANALYSIS CERTIFICATE FOR EFFLUENT
E4 (UNTREATED)**



RÉSULTATS DE DAPHNIE - CL50 (AIGUE-48H)-FÉDÉRAL

150

BUREAU
VERITAS

Client : 6088 H2LAB

No. de dossier : C138784

Nom et no. de projet :

No. d'échantillon : JL6945-01

Résultats d'analyse:

48 hres CL50 %v/v (95% CL): 48.1 (35.8-65.0) Méthode statistique: Probit

Unité toxique: 2.07

48 hres CE50 %v/v (95% CL): 48.1 (35.8-65.0) Méthode statistique: Probit

Commentaire: toxique

Nom de l'échantillon: 317049 99326

Type d'échantillon: Eau usée

Apparence : Incolore, translucide, pas de solides en suspension

Échantillon avant l'analyse:

Date/heure de prélèvement : 28 juil. 2021

Méthode d'échantillonnage : Instantanée

pH: 7.0

Prélevé par : JENNIFER DUBUC

Lieu de prélèvement : UQAT

Température : 19 °C

Échantillon reçu : 30 juil. 2021 10:00

Volume d'échantillon fourni : 1 L

Oxygène dissous : 65.0 %

Début de l'essai : 31 juil. 2021 11:33

Temp. Moy. 15 °C

Conductivité : 1609 µS/cm

Récep.:

Fin : 02 août 2021 12:54

Entreposage: 2-6°C

Dureté : 649 mg CaCO₃/L

Concentration	Température (°C)	pH (pH)	Conductivité (µS/cm)	Oxygène dissous (mg/L)	Température (°C)	pH (pH)	Oxygène dissous (mg/L)	Immobilité (#)	Immobilité (%)	Mortalité (#)	Mortalité (%)
%v/v	0 hre	0 hre	0 hre	0 hre	48 hres	48 hres	48 hres	48 hres	48 hres	48 hres	48 hres
0	21	7.8	470	8.4	20	7.9	8.9	0	0	0	0
6.25	21	7.8	556	8.3	19	7.8	8.9	0	0	0	0
12.5	21	7.7	636	8.2	19	7.8	8.7	0	0	0	0
25	21	7.7	794	8.0	19	7.7	8.2	0	0	0	0
50	21	7.6	1054	7.7	19	7.6	7.8	0	0	7	70.0
100	20	7.3	1600	6.4	19	7.5	8.1	0	0	9	90.0

Commentaires:

Eau de contrôle et dilution :

Eau reconstituée pour Daphnia

Dureté:

180 mg/l CaCO₃

Autres paramètres disponibles sur demande.

Installations et conditions de l'essai

Concentrations effectuées : 0,6,25,12,5,25,50,100 (%v/v)

Nombre d'organismes par récipient : 10

Temps de pré aération : 0 min

Taux de pré aération : 40±5 mL/min/L

Nombre total d'organismes utilisés : 60

Température : 20 ± 2 °C

Ajustement de la dureté : Non

Volume dans les réservoirs d'essai : 150 mL

Volume de récipient : 200 ml

Ajustement du pH : Non

Densité de chargement :

15.0 mL/daphnie Photopériode : 16 heures de lumière: 8 heures d'obscurité

Organisme :

Daphnia magna

Provenance : Culture de laboratoire BV

Âge des organismes au début de l'essai : <24 hres

Nombre moyen de néonates par couvée : 37.0

Photopériode :

16 heures de lumière: 8 heures d'obscurité

% de mortalité 7 jours avant lessai : 2.0

Température d'acclimatation :

20 ± 2 °C

Âge à la naissance de la première couvée : 11 jours

Régime alimentaire :

Nourrit 1 fois par jour.

Données relatives au contrôle de qualité:

Dichromate de potassium

Date d'analyse :

26 juil. 2021

Effet d'analyse 48 hres CL50 (intervalle de confiance 95%) : 0.20 (0.16, 0.24)mg/L

Méthode statistique:

Trimmed Spearman-Kärber

Moyenne géométrique antérieure CL50 :

0.18 (0.11, 0.30) mg/L

Concentration : 0,0.0625,0.125,0.25,0.5,1 mg/L

Méthode d'analyse

QUE SOP-00406. Méthode de référence pour la détermination de la létalité aiguë d'effluents chez *Daphnia magna*. SPE1/RM/14 - Deuxième édition. Environnement Canada. 2000.

Essentiellement, il s'agit d'un essai statique d'une durée de 48 heures. Dix individus sont soumis à différentes concentrations d'effluent pour en mesurer la CL50 dans des conditions de température, d'éclairage et de densité de chargement contrôlées.

Déviations de la méthode :

Aucune



BUREAU
VERITAS

RÉSULTATS DE DAPHNIE - CL50 (AIGUE-48H)-FÉDÉRAL

151

Client : 6088 H2LAB

No. de dossier : C138784

Nom et no. de projet :

No. d'échantillon : JL6945-01

Analyste : Aida Sley, Sean Le Brasseur

Validé par : Wael Ellamouchi, Analyste 2

Date: 13 août 2021 16:20

**APPENDIX E TOXICITY ANALYSIS CERTIFICATE FOR EFFLUENT
E4 (TREATED)**

BUREAU
VERITAS

RÉSULTATS DE DAPHNIE - CL50 (AIGUE-48H)-FÉDÉRAL

153

Client : 6088 H2LAB

No. de dossier : C138784

Nom et no. de projet :

No. d'échantillon : JL6946-01

Résultats d'analyse:**48 hres CL50 %v/v (95% CL):** >100 (N/A) Méthode statistique: Visuelle**Unité toxique:** <1**48 hres CE50 %v/v (95% CL):** >100 (N/A) Méthode statistique: Visuelle**Commentaire:** non toxique**Nom de l'échantillon:** 317050 99375

Type d'échantillon: Eau usée

Apparence : Incolore, translucide, pas de solides en suspension

Échantillon avant l'analyse:

Date/heure de prélèvement : 28 juil. 2021

Méthode d'échantillonnage : Instantanée

pH: 6.9

Prélevé par : JENNIFER DUBUC

Lieu de prélèvement : UQAT

Température : 20 °C

Échantillon reçu : 30 juil. 2021 10:00

Volume d'échantillon fourni : 1 L

Oxygène dissous : 92.0 %

Début de l'essai : 31 juil. 2021 11:40

Temp. Moy. 15 °C

Conductivité : 1819 µS/cm

Récep.:

Fin : 02 août 2021 12:58

Entreposage: 2-6°C

Dureté : 661 mg CaCO₃/L

Concentration	Température (°C)	pH (pH)	Conductivité (µS/cm)	Oxygène dissous (mg/L)	Température (°C)	pH (pH)	Oxygène dissous (mg/L)	Immobilité (#)	Immobilité (%)	Mortalité (#)	Mortalité (%)
%v/v	0 hre	0 hre	0 hre	0 hre	48 hres	48 hres	48 hres	48 hres	48 hres	48 hres	48 hres
0	21	7.5	471	8.3	20	7.7	8.7	0	0	0	0
6.25	21	7.6	572	8.3	20	7.7	8.9	0	0	0	0
12.5	21	7.7	651	8.3	19	7.7	8.9	0	0	0	0
25	21	7.7	852	8.3	19	7.7	9.1	0	0	0	0
50	21	7.7	1187	8.4	19	7.8	8.7	0	0	0	0
100	20	7.6	1818	8.7	19	7.7	8.9	0	0	0	0

Commentaires: Aucune anomalie observée durant l'essai.**Eau de contrôle et dilution :**

Eau reconstituée pour Daphnia

Dureté:

180 mg/l CaCO₃

Autres paramètres disponibles sur demande.

Installations et conditions de l'essai

Concentrations effectuées : 0,6,25,12,5,25,50,100 (%v/v)

Nombre d'organismes par récipient : 10

Temps de pré aération : 0 min

Taux de pré aération : 40±5 mL/min/L

Nombre total d'organismes utilisés : 60

Température : 20 ± 2 °C

Ajustement de la dureté : Non

Volume dans les réservoirs d'essai : 150 mL

Volume de récipient : 200 ml

Ajustement du pH : Non

Densité de chargement :

15.0 mL/daphnie Photopériode : 16 heures de lumière: 8 heures d'obscurité

Organisme :*Daphnia magna*

Provenance : Culture de laboratoire BV

Âge des organismes au début de l'essai : <24 hres

Nombre moyen de néonates par couvée : 37.0

Photopériode :

16 heures de lumière: 8 heures d'obscurité

% de mortalité 7 jours avant lessai : 2.0

Température d'acclimatation :

20 ± 2 °C

Âge à la naissance de la première couvée : 11 jours

Régime alimentaire :

Nourrit 1 fois par jour.

Données relatives au contrôle de qualité:

Dichromate de potassium

Date d'analyse :

26 juil. 2021

Effet d'analyse 48 hres CL50 (intervalle de confiance 95%) : 0.20 (0.16, 0.24)mg/L

Méthode statistique:

Trimmed Spearman-Kärber

Moyenne géométrique antérieure CL50 :

0.18 (0.11, 0.30) mg/L

Concentration : 0,0.0625,0.125,0.25,0.5,1 mg/L

Méthode d'analyseQUE SOP-00406. Méthode de référence pour la détermination de la létalité aiguë d'effluents chez *Daphnia magna*. SPE1/RM/14 - Deuxième édition. Environnement Canada. 2000.

Essentiellement, il s'agit d'un essai statique d'une durée de 48 heures. Dix individus sont soumis à différentes concentrations d'effluent pour en mesurer la CL50 dans des conditions de température, d'éclairage et de densité de chargement contrôlées.

Déviations de la méthode :

Aucune



BUREAU
VERITAS

RÉSULTATS DE DAPHNIE - CL50 (AIGUE-48H)-FÉDÉRAL

154

Client : 6088 H2LAB

No. de dossier : C138784

Nom et no. de projet :

No. d'échantillon : JL6946-01

Analyste : Aida Sley, Sean Le Brasseur

Validé par : Wael Ellamouchi, Analyste 2

Date: 13 août 2021 16:24